

PG&E
Geosciences Department
Departmental Calculation Procedure
Attachment 5.2

Number: GEO.001
Revision: 04
Page: 1 of 1

Title: Design Calculation Cover Sheet

PACIFIC GAS AND ELECTRIC COMPANY
GEOSCIENCES DEPARTMENT
CALCULATION DOCUMENT

Calc Number GEO.DCPP.01.17
Revision 2
Date 11/19/01
Calc Pages: 21
Verification Method: A
Verification Pages: 1

TITLE: Determination of mean and standard deviation of unconfined compression strengths for hard rock at DCPD ISFSI based on laboratory tests.

PREPARED BY: *Joseph I. Sun* DATE Nov. 19/01

Joseph I. Sun
Printed Name

Geosciences
Organization

VERIFIED BY: *Robert K. White* DATE 11/19/01

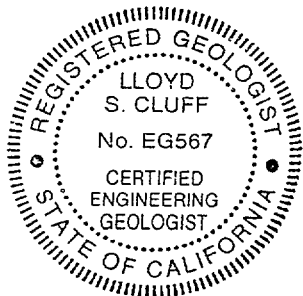
Robert K. White
Printed Name

Geosciences
Organization

APPROVED BY: *Lloyd S. Cluff* DATE 11/19/01

Lloyd S. Cluff
Printed Name

Geosciences
Organization



Expires 12/31/02

for hard rock at DCPD ISFSI based on laboratory tests.

Calc. Number GEO.DCIPP.01.17

Record of Revisions

[illegible]

DCPP ISFSI GEOTECHNICAL CALCULATION PACKAGE

Title: Determination of mean and standard deviation of unconfined compression strengths for hard rock at DCPD ISFSI based on laboratory tests

Calc Number: GEO.DCPP.01.17

Revision: Rev. 2

Date: November 19, 2001

Author: Joseph I. Sun

Verifier: Robert K. White

PURPOSE

As required by Geosciences Work Plan GEO 2001-03, Appendix M, this calculation package documents the evaluation and statistical analysis of the laboratory test results of unconfined compressive tests on hard (non-friable) dolomite and sandstone samples. The unconfined compressive strengths of the intact rock samples will be used in separate calculations GEO.DCPP.01.19 and GEO.DCPP.01.20, in conjunction with geological indices describing discontinuity properties of the rock mass, to develop the overall strength envelopes for jointed rock mass and rock discontinuities at DCPD ISFSI. The strength envelopes developed will then be reviewed in separate calculations for applicability to slope stability analyses and ISFSI pad analyses.

ASSUMPTIONS

1. Samples represent a wide range of in-situ rock encountered at the ISFSI site. This assumption is reasonable because the sample selection process was carefully designed and implemented to accomplish this as described in Sun (4/23/01).
2. Scattering of the test results reflects the natural variation of the in-situ intact rock strengths. This assumption is reasonable because the tests were conducted shortly after samples were obtained at the same laboratory using calibrated equipment as documented in Sun (5/23/01), so scatter can not be a result of sample deterioration, equipment failure or lab error.
3. The strengths of friable sandstone depend on the confining pressure. This assumption is reasonable because unconfined compression test results for this material were

found to be inappropriate to be used to characterize its strength as documented in Sun (5/23/01). For friable sandstone, its strength characterization should be based on triaxial tests as documented in Calculation package GEO.DCPP.01.16.

4. Unconfined compression tests that failed on existing joints do not reflect the strength of the intact rocks and thus will not be included in the statistical analyses of the intact rock strengths. This assumption is reasonable because the influence of joints on overall rock mass strength is determined elsewhere (GEO.DCPP.01.19 and GEO.DCPP.01.20).
5. Spatially unassociated very high unconfined compression strengths (close to mean plus three standard deviations of the remaining samples) will be conservatively discarded and not incorporated in the statistical analysis. This is a conservative assumption as the resulting mean strength will be lower.

INPUTS

1. Test results from Witter (11/5/01), Data Report I, Rock Laboratory Test Data.
2. Boring log summaries from Witter (11/5/01), Data Report B, Borings in ISFSI Site Area.

METHOD

1. Obtain laboratory test results for all December 2000 and May 2001 unconfined compression (UC) tests from Data Report I. A total of 28 unconfined compression tests were performed.
2. Review UC laboratory test sheets and results. Identify and mark samples that failed along existing joints or show any indication that the unconfined compression test results do not represent the strength of the in-place intact rock.
3. Classify each sample as sandstone, friable sandstone, or dolomite in accordance with boring log summaries from Data Report B.
4. Evaluate if sufficient lab test results for each rock type warrant separate statistical analyses.
5. Perform statistical analysis based on classified rock samples.

SOFTWARE

Standard statistical analyses were performed using Microsoft Excel 2000.

ANALYSIS

Out of the 28 UC tests, 9 were on sandstone, 13 were on dolomite, and 6 were on friable sandstone. The results for each type of rock are discussed below.

Sandstone

For the 9 sandstone samples tested, sample No. 6 from Boring 01-D, and sample No. 26 from Boring 01-E have strengths of 959 psi and 437 psi, respectively. These two unconfined strengths were discarded because they failed in shear on existing joints.

Sample No. 12 from Boring 01-H and sample No. 2-E from Boring 00BA-2 both have strengths in excess of 10,000 psi. These two values were significantly higher than the remaining group of sandstone samples (close to mean plus three standard deviations). Furthermore, the occurrence of these two high strength samples cannot be associated with any geological features, thus cannot be predicted spatially with certainty elsewhere at the ISFSI site area. Consequently, these two data points were conservatively ignored in the statistical analysis of sandstone strength. The remaining five samples are listed in Table 1.

Dolomite

Of the 13 dolomite samples tested, sample No. 1-13 from Boring 00BA-1 was discarded because the sample failed in shear along an existing joint. Therefore, its unconfined compression strength does not represent the strength of the intact dolomite and the measured strength from this test was not used in the statistical analysis for the dolomite. The remaining 12 samples are listed in Table 2.

Friable Sandstone

Four samples (Sample Nos. 19, 14, 4, and 10) from Borings 01-B, 01-D, 01-G, and 01-CTF-A were judged to be friable sandstone based on the boring log summaries. Sample No. 15 from Boring No. 01-CTF-A and sample No. 39A from Boring No. 01-I were borderline friable sandstone samples. They were not identified as friable sandstone in the boring logs summaries. However, based on the lab test results, it was concluded that these two samples would have engineering properties similar to friable sandstone based on their strengths and stress strain properties. Unconfined compression test results are not appropriate for characterizing the strength of friable sandstone. This weakly cemented material strength is better characterized with triaxial tests as documented in

GEO.DCPP.01.16. As a result, unconfined compression test results on friable sandstone are discarded.

RESULTS

Table 1 lists the statistical analysis results of the five sandstone samples that were judged to be representative of the unconfined compressive strength of the intact sandstone at the ISFSI site area. Four of the five samples were from the pad footprint area and the remaining sample was taken from Boring 01-F above the proposed cut slope. The unconfined compressive strengths vary from 1,113 psi to 4,778 psi with an average of 3,165 psi and a standard deviation of 1,506 psi.

Table 2 lists the statistical analysis results of the 12 dolomite samples that were judged to be representative of the unconfined compressive strength of the intact dolomite at the ISFSI site area. Samples were taken from Borings 01-I and 00BA-1 above the proposed ISFSI cut slope, Boring 01-H on the cut slope and Borings 01-E and 01-G under the pad. The unconfined compressive strengths vary from 1,834 psi to 8,649 psi with an average of 4,517 psi and a standard deviation of 2,086 psi.

The difference between the average unconfined compressive strengths of sandstone (3,165 psi) and dolomite (4,517 psi) is relatively small. The difference would be even smaller if the two very high strength test results for sandstone, which were conservatively discarded in the statistical analysis, were included. The similarities between the two types of rocks were also noted during the field program as documented in GEO.DCPP.01.21. On the above basis, and to increase the number of data points for a meaningful statistical analysis, the test results for sandstone and dolomite were combined to evaluate the overall unconfined compressive strength for the rock encountered at the ISFSI site area. Table 3 lists the statistical analysis results performed using the combined 17 test results (5 for sandstone and 12 for dolomite) and shows an average unconfined compressive strength of 4,120 psi with a standard deviation of 1,990 psi.

If the two high strength sandstone test results are included, the distribution of the unconfined strengths of all 19 samples would be skewed toward the high side, and a log normal distribution would be more appropriate to characterize such a distribution. The mean of the log-normally distributed 19 test results would then be 4,095 psi, which is very close to the average strength of 4,120 psi calculated without the 2 high strength

samples and assuming the strengths of the remaining 17 samples to be normally distributed.

Table 4 lists the discarded samples that were judged not to be representative of the intact rock strengths and samples that were classified as friable sandstone.

CONCLUSIONS

Table 5 summarizes the statistical analysis results for the intact rock unconfined compressive strength. The results can be used, in conjunction with associated geological properties, to develop the rock mass strength properties in calculations GEO.DCPP.01.19 and GEO.DCPP.01.20.

REFERENCES

1. Geosciences Work Plan GEO 2001-03, Development of Engineering Properties for ISFSI and CTF Foundation Design, ISFSI Slope Analyses, and ISFSI Cut and Fill Slope Reinforcement Design for The DCPD ISFSI Site, rev. 1.
2. Witter (11/5/01): letter from Rob Witter to Rob White, entitled "Completion of Data Reports," dated 11/5/01, and accompanying:
Data Report B, Borings in ISFSI Site Area, rev. 0
Data Report I, Rock Laboratory Test Data, rev. 0.
3. Geosciences Calculation GEO.DCPP.01.16, Development of strength envelopes for non-jointed rock at DCPD ISFSI based on laboratory data, rev. 1.
4. Geosciences Calculation GEO.DCPP.01.19, Development of strength envelopes for jointed rock mass at DCPD ISFSI using Hoek-Brown equations, rev. 1.
5. Geosciences Calculation GEO.DCPP.01.21, Analysis of Bedrock Stratigraphy and Geologic Structure at the DCPD ISFSI Site, rev. 1.
6. Geosciences Calculation GEO.DCPP.01.20, Development of strength envelopes for shallow discontinuities at DCPD ISFSI using Barton equations, rev. 1.
7. Sun (4/23/01): letter from Joseph Sun to Chris Hartz, Independent Reviewer Documentation Report of GeoTest Unlimited Sample Selection Procedures at DCPD, dated April 23, 2001.
8. Sun (5/23/01): letter from Joseph Sun to Chris Hartz, Independent Reviewer Documentation Report of GeoTest Unlimited Rock Testing Facility located in Nevada City, CA, dated May 23, 2001.

ATTACHMENTS

1. Witter (11/5/01): letter from Rob Witter to Rob White, entitled "Completion of Data Reports," dated 11/5/01 (without attachments).
2. Sun (4/23/01): letter from Joseph Sun to Chris Hartz, Independent Reviewer Documentation Report of GeoTest Unlimited Sample Selection Procedures at DCP, dated April 23, 2001 (without attachments).
3. Sun (5/23/01): letter from Joseph Sun to Chris Hartz, Independent Reviewer Documentation Report of GeoTest Unlimited Rock Testing Facility located in Nevada City, CA, dated May 23, 2001 (without attachments).

Table 1 Summary and Statistical Analysis of Sandstone Unconfined Compression Test Results

Boring No.	Sample No.	Depth (ft)	Feature in Sample	Unit Wt. (pcf)	Failure Mode	Strength (psi)
01-A	1	19.5	2 healed joint 27 deg to axis	161.4	axial splitting	2888
01-A	2	24.5	bedding at 69 deg to axis	146.6	axial splitting and crushing	1113
01-B	18	26.5	-	147.3	shear	4778
01-C	22	24.0	joint	155.0	axial splitting	4504
01-F	30	57.6	No apparent jointing	138.9	shear not on existing joint	2543
Average				149.8		3165
Standard Deviation				8.6		1506

Table 2 Summary and Statistical Analysis of Dolomite Unconfined Compression Test Results

Boring No.	Sample No.	Depth (ft)	Feature in Sample	Unit Wt. (pcf)	Failure Mode	Strength (psi)
01-E	28	49.0	joint?	135.8	shear not on existing joint	2958
01-G	9	28.8	No apparent jointing	138.2	axial splitting along existing fractures	3702
01-H	11	11.0	No apparent fractures	138.9	shear	2434
01-I	38	159.5	2 healed joints 27 deg to axis	144.2	axial splitting	1834
01-I	40A	88.4	bedding at 69 deg to axis	142.0	axial splitting and bending	6373
01-I	42	44.0	-	141.5	axial splitting and shear	3504
OOBA-1	1-8B	146 ~ 147.2	joint	146.6	shear	5133
OOBA-1	1-9B	148.68 ~ 150	joint?	140.6	axial splitting	2625
OOBA-1	1-10	12.2 ~ 13.0	No apparent jointing	138.4	axial splitting	5284
OOBA-1	1-11	18.63 ~ 19.21	No apparent jointing	142.4	axial splitting	7190
OOBA-1	1-12	24.2 ~ 23.17	No apparent fractures	134.5	combined	4523
OOBA-1	1-14	45.8~49.63	no apparent fractures	143.1	axial splitting and bending	8649
Average				140.5		4517
Standard Deviation				3.5		2086

Table 3 Summary of Unconfined Compressive Strength of Intact Rocks

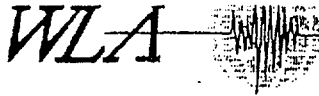
Boring No.	Sample No.	Depth (ft)	Unit Wt. (pcf)	Strength (psi)
01-A	1	19.5	161.4	2888
01-A	2	24.5	146.6	1113
01-B	18	26.5	147.3	4778
01-C	22	24.0	155.0	4504
01-E	28	49.0	135.8	2958
01-F	30	57.6	138.9	2543
01-G	9	28.8	138.2	3702
01-H	11	11.0	138.9	2434
01-I	38	159.5	144.2	1834
01-I	40A	88.4	142.0	6373
01-I	42	44.0	141.5	3504
OOBA-1	1-8B	146 ~ 147.2	146.6	5133
OOBA-1	1-9B	148.68 ~ 150	140.6	2625
OOBA-1	1-10	12.2 ~ 13.0	138.4	5284
OOBA-1	1-11	18.63 ~ 19.21	142.4	7190
OOBA-1	1-12	24.2 ~ 23.17	134.5	4523
OOBA-1	1-14	45.8~49.63	143.1	8649
Average			143.3	4120
Standard Deviation			6.8	1990

Table 4 Summary of Unconfined Compression Test Results Not Used in the Statistical Analysis

Boring No.	Sample No.	Depth (ft)	Feature in Sample	Unit Wt. (pcf)	Failure Mode	Strength (psi)
01-D	6	48.5	One joint about 32 deg from core axis and 1 axial fracture	147.1	shear on existing joint	959
01-E	26	22.0	Few healed shears	129.4	shear on healed shears	437
01-H	12	52.5	No visible fractures	155.1	multiple shears	10252
OOBA-2	2-E	50.9 ~ 51.4	Healed non-through going joints	160.9	axial splitting and shear on existing joints	10921
OOBA-1	1-13	40.88 ~ 41.37	Healed and partially healed joints	128.9	shear on existing joint	2079
01-B	19	38.0	joint at the end	132.4	shear not on existing joint	452
01-CTF-A	14	8.8	Partial plaster caps on both ends	128.8	shear	29
01-CTF-A	15	13.5	possible healed joints	138.3	shear	400
01-D	4	25.5	-	142.3	splitting/shear	207
01-G	10	69.0	-	130.7	shear and axial splitting	136
01-I	39A	130.4	open joint 12 deg to axis	140.3	shear not on existing joint	505

Table 5 Summary of Unconfined Compressive Strength of Intact Rocks Samples at ISFSI

	Unconfined Compressive Strength of Rock Samples	
	(psi)	(MPa)
Mean (Average) Strength	4120	28.4
Standard Deviation (SD)	1990	13.7
Mean + 1SD Strength	6110	42.1
Mean - 1SD Strength	2129	14.7



William Lettis & Associates, Inc.

1777 Botelho Drive, Suite 262, Walnut Creek, California 94596
Voice: (925) 256-6070 FAX: (925) 256-6076

Mr. Robert White
Geosciences Department
Pacific Gas & Electric Company
245 Market Street, Rm. 421-N4C
San Francisco, CA 94105

November 5, 2001

Re: Completion of Data Reports (formerly appendices)

Dear Rob:

This letter transmits to Geosciences the following Diablo Canyon ISFSI Data Reports (formerly called appendices) that were prepared under the WLA Work Plan, Additional Geologic Mapping, Exploratory Drilling, and Completion of Kinematic Analyses for the Diablo Canyon Power Plant Independent Spent Fuel Storage Installation Site, Rev. 2 (11/28/00) using data collected under that Work Plan and a second WLA Work Plan, Additional Exploratory Drilling and Geologic Mapping for the ISFSI Site, Rev. 1 (9/21/01).

Diablo Canyon ISFSI Data Report A - Geologic Mapping in the Plant Site and ISFSI Site Areas, Rev. 0, November 5, 2001, November 5, 2001, prepared by J. Bachhuber, 42 p.

Diablo Canyon ISFSI Data Report B - Borings in ISFSI Site Area, Rev. 0, November 5, 2001, prepared by J. Bachhuber, 244 p.

Diablo Canyon ISFSI Data Report C - 1998 Geophysical Investigations at the ISFSI Site Area, (Agabian Associates and GeoVision), Rev. 0, November 5, 2001, prepared by J. Bachhuber, 84 p.

Diablo Canyon ISFSI Data Report D - Trenches in the ISFSI Site Area, Rev. 0, November 5, 2001, prepared by J. Bachhuber, 66 p.

Diablo Canyon ISFSI Data Report E - Borehole Geophysical Data (NORCAL Geophysical Consultants, Inc.), Rev. 0, November 5, 2001, prepared by C. Brankman, 303 p.

Diablo Canyon ISFSI Data Report F - Field Discontinuity Measurements, Rev. 0, November 5, 2001, prepared by J. Bachhuber and C. Brankman, 85 p.

Diablo Canyon ISFSI Data Report G - Soil Laboratory Test Data (Cooper Testing Laboratory), Rev. 0, November 5, 2001, prepared by J. Sun, 63 p.

Diablo Canyon ISFSI Data Report H - Rock Strength Data and GSI Sheets, Rev. 0, November 5, 2001, prepared by J. Bachhuber, 37 p.

Diablo Canyon ISFSI Data Report I - Rock Laboratory Test Data (GeoTest Unlimited), Rev. 0, November 5, 2001, prepared by J. Sun, 203 p.

Diablo Canyon ISFSI Data Report J - Petrographic Analysis and X-Ray Diffraction of Rock Samples (Spectrum Petrographics, Inc.), Rev. 0, November 5, 2001, prepared by J. Bachhuber, 204 p.

Diablo Canyon ISFSI Data Report K - Petrographic and X-Ray Diffraction Analyses of Clay Beds (Schwein/Christensen Laboratories, Inc.), Rev. 0, November 5, 2001, prepared by J. Bachhuber, 36 p.

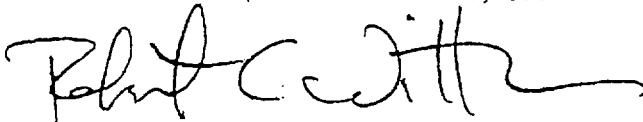
In addition to the revisions of those reports required under the various Work Plans, Mr. Scott Lindvall, the WLA ITR for the ISFSI project, has performed independent technical reviews of the Diablo Canyon ISFSI Data Reports as part of his review of Calculation Package GEO.DCPP.01.21, Analysis of Bedrock Stratigraphy and Geologic Structure at the DCPD ISFSI Site. He finds that the reports clearly and accurately compile and organize the data.

Mr. Albert Tafoya from the Diablo Canyon ISFSI Project Office in San Luis Obispo, Mr. Dale Marcum, NQS Technical Oversight for the project, and William Page of your office provided comments on the August versions of the Diablo Canyon ISFSI Data Reports (formerly called appendices) and their comments have been addressed.

These reports are submitted to you as per the PG&E Geosciences Department Calculation Procedure GEO.001, Rev. 04 (10/10/01).

We look forward to any comments you may have.

Sincerely,
WILLIAM LETTIS & ASSOCIATES, INC.



Robert C. Witter
Project Manager

CC: William Page

~~11 of 20~~
12 of 21



TRANSMITTAL

DATE: April 23, 2001 TIME: 9:08 AM
 TO: Chris Hartz PHONE: 8-691-4032
 DCPN NQS FAX: 8-691-4635
 FROM: Joseph Sun *J. Sun* PHONE: 415-973-2460
 Geolabs, Inc. FAX: 415-973-5778

RE: Independent Reviewer Documentation Report
 CC: Al Tafoya

Message

Dear Chris,

At the request of Bill Page of PG&E Geosciences Department, and in accordance with the Independent Verification By Peer Reviewer Plan entitled "Rock Sample Selection and Rock Testing for the Diablo Canyon Power Plant Independent Spent Fuel Storage Installation Site", I visited Diablo Canyon Power Plant (DCPP) Independent Spent Fuel Storage Installation Site (ISFSI) on April 19, 2000 where additional borings were being drilled to investigate the pad foundation and in the cut slope area behind the pad. The purpose of my visit was to observe and evaluate the basis of selecting appropriate rock samples for testing and the appropriateness of sample packaging for shipment as described in the GeoTest Unlimited Work Plan entitled, "Rock Sample Selection and Rock Testing for the Diablo Canyon Power Plant Independent Spent Fuel Storage Installation Site".

I arrived on site at 9:30 am on April 19, 2000 and departed at 8:00 pm the same day. During this period, I reviewed the available cores and discussed with Jeff Bachhuber, engineering geologist of William Lettis and Associates (WLA), regarding the basis of selecting rock samples for testing and reviewed his initial selection of the rock samples. Subsequently, I discussed with Anders Bro of GeoTest Unlimited (GTU) regarding the sample packaging approach he planned to use and observed him packaging all samples for shipment to his testing laboratory located near Nevada City.

Brief discussions were also made with Bill Page and Al Tafoya on site regarding my overall assessment, and I also witnessed signing of the Chain-of-Custody form for the 17 rock samples by Bill Page and Anders Bro. My observations and conclusions of the visit are summarized as follows:

Observations:

1. Rock cores from five borings were neatly laid out in the open area close to the proposed CTF site. These five borings were 01-A, 01-D, 01-G, 01-H, and CTF-A.
2. Geophysical investigation by Norcal was also underway in borings 01-A and CTF-A during the time of my visit.
3. The cores showed mostly massive dolomite or cemented sandstone. Occasional zone of altered sandstone were encountered, however, the amount of these weaker rock was limited compared to the massive dolomite and cemented sandstone in these five boreholes.
4. Cores from borehole 01-D appeared more broken up than others. I discussed this with Bill Page and he suspected that this may be due to the drilling process because the drillers were not that familiar with the site conditions and this was their first borehole on site. Subsequent cores retrieved showed improvement in quality.
5. Based on the approved work plan for WLA, the purpose for the current investigation (April, 2001) program is to investigate the ISFSI pad footprint and CTF footprint areas to characterize the foundation rock conditions and to assess the overall rock mass behavior in association with the discontinuity characteristics in the cut slope. On this basis, I concur with Jeff Bachhuber regarding the sample selection criteria which are: samples selected will be representative of the "average" foundation material as a whole, and consideration will be given and samples will be taken to address potential variations of the material, especially on the weaker side of the variation. Samples tested in the cut slope area will be focused more on the geological characterization.
6. I observed that in each of the five boreholes drilled, at least three samples were selected. Usually with one sample representing the typical rock mass, one sample representative of the weaker zone, and a third sample may be selected for a number of reasons including: testing of special features, testing for geological characterization purposes, or testing a second sample of the more representative material within the sample borehole. The selection criteria meet the requirements stated in the corresponding GTU work plan.
7. In sampling packaging, I observed Anders Bro carefully remove the selected samples from the core boxes, and wrap them with heat shrink plastic. The plastic wrap was then sealed and heated to shrink onto the sample to support the sample and to reduce sample desiccation. The samples were then labeled and placed in a plastic box, and packed with bubble wrap to prevent sample movement during transport. Anders used a sample holder to transport samples between the core boxes and his working area. In my opinion, samples thus prepared meet state-of-the-practice procedure and samples should experience minimum disturbance during transport. The procedures used meet the requirements stated in the GTU work plan.
8. Both Jeff Bachhuber, responsible for selection of testing samples, and Anders Bro, responsible for packaging samples for laboratory testing, are experienced professionals with over 10 years of experience in their respective fields. In my

opinion, both of them exceed the minimum experience stated in the personnel qualification section of the GTU work plan.

9. I have witnessed the signing of Chain-of-Custody form by representatives from PG&E and the rock testing facility. I have also cross checked the samples taken from the site against those listed on the Chain-of-Custody form and am satisfied with the documentation accuracy.

Conclusions:

1. I have witnessed a sufficient portion of the sample selection and packaging and verify that sample collection, identification, and handling and packaging were performed according to accepted standards and the established work plan.
2. I have review 17 rock samples from five boreholes and verify that the shrink-wrapped samples have been legibly and accurately marked with job name, borehole number, sample depth intervals, and intended tests.
3. I have reviewed the quality of the 17 samples and verify that samples have been properly packaged and secured for transport.
4. I have discussed my findings and my acceptance of the procedures implemented for sample selection and sample packaging with Bill Page and Al Tafoya on site prior to leaving the DCP.
5. I have concluded that the work described above meets the requirements stated in the GTU work plan entitled "Rock Sample Selection and Rock Testing for the Diablo Canyon Power Plant Independent Spent Fuel Storage Installation Site".



TRANSMITTAL

DATE: May 12, 2001 TIME: 11:18 AM
 TO: Chris Hartz PHONE: 8-691-4032
 DCPD NQS FAX: 8-691-4635
 FROM: Joseph Sun *J. A.* PHONE: 415-973-2460
 Geolabs, Inc. FAX: 415-973-5778

RE: Independent Reviewer Documentation Report of GeoTest Unlimited Rock Testing Facility located in Nevada City, CA.

CC: Al Tafoya

Message

Dear Chris,

In accordance with Revision 0 of the Verification Plan entitled "Independent Verification by Peer Reviewer, Rock Sample Selection and Rock Testing for the Diablo Canyon Power Plant Independent Spent Fuel Storage Installation Site," I conducted an independent review of the GeoTest Unlimited (GTU) testing facility in Nevada City on May 7, 2001 for work performed under revision 0 of the GTU Work Plan entitled "Laboratory Testing of Rock Samples for the Diablo Canyon Power Plant, Independent Spent Fuel Storage Installation Site". This was the second review of GTU facilities, the first being documented in a Geosciences report by Mr. Robert White dated 1/22/01. The objectives of my visit are summarized as follows:

1. Transport a third group of rock samples obtained at the DCPD ISFSI site from William Lettis and Associates' office in Walnut Creek to GTU's testing facility.
2. Review chain-of-custody forms for the three groups of rock samples transported from Diablo Canyon Power Plant (DCPD) to GTU testing facility.
3. Review with Dr. Anders Bro, who is responsible for testing and interpretation of test results at GTU, the scope and objectives of the GTU work plan.
4. Review accuracy of statements made in the GTU Statement of Qualification submitted to PG&E at the beginning of the previous phase of investigation in December of 2000.
5. Review qualifications of the personnel responsible for conducting the tests.
6. Witness a direct shear test from sample preparation to completion of test.

Activities and Observations:**1. Sample Delivery**

I arrived at William Lettis & Associates' office in Walnut Creek at 8:00 am on, May 7, 2000 to meet with Jeff Bachhuber and arrange for samples pick-up. Jeff had just returned from the DCCP ISFSI site over the weekend and brought back samples from Boring 01-I. The samples were tightly wrapped with thick plastic sheets and electrical tapes. Cushion material was used to separate the samples that were securely packed in a cardboard storage box. The sample container was stored inside WLA's office over the weekend. I laid out the 9 samples and checked them against the listing on the chain-of-custody form. I signed the form after confirming that all samples were correctly accounted for. I arrived at GTU testing facility in Nevada City about 11:30 am and delivered the samples to Anders Bro. Anders signed the chain-of-custody form after confirming all samples on the list were delivered (Attachment A). The previous two sets of samples had been transported to the lab separately under Dr. Bro' instructions. I had previously witnessed samples packed at DCCP (see my transmittal to you dated 23 April 2001).

2. Review of Chain-of-Custody Form

I also reviewed the previous chain-of-custody forms signed on April 20 and 23, 2001, by Bill Page, Al Tafoya, and Anders Bro (Attachments B and C). My review concluded that all three chain-of-custody forms, dated 4/20/01, 4/23/01, and 5/7/01, were in order.

In the first two chain-of-custody forms, samples were numbered sequentially (e.g., on the first form, samples were numbered from 1 through 17; and on the second form, samples were numbered from 18 through 35). The sample numbers identified on these forms, along with their borehole numbers and sample depths, were used in the reporting of the test results. On the third chain-of-custody form, the sample numbers were re-started again from 1. Although test results still could be tracked through borehole numbers and sample depths, having duplicate sample numbers could be confusing. Accordingly, sample numbers on the third chain-of-custody form (signed on May 7, 2001) were renumbered as shown below, and Anders confirmed the renumbering via his fax to PG&E on May 8, 2001 (Attachment D).

Sample Number on Chain-of-Custody form signed on May 7, 2001	Boring No.	Sample Depth (ft)	Revised Sample Number Shown on Rock Test Data Sheets
1	01-I	174.0	36
2	01-I	168.0 - 169.0	37
3	01-I	159.5	38
4	01-I	130.4	39
5a	01-I	88.4	40a
5b	01-I	88.8	40b
6a	01-I	45.6	41a
6b	01-I	46.1	41b
7	01-I	44.0	42

3. Work Plan Scope and Objectives:

- Work Plan Objectives

I discussed with Anders the objectives of this phase of the investigation, which has a significant amount of borings, made within the ISFSI pad footprint area. He was informed that the stiffness (expressed in terms of spring constants) of the foundation material is needed for the design analysis of the concrete pad. Prior to the current phase of the investigation, Young's moduli were estimated based on in-situ wave velocities and we would like to confirm the Young moduli with laboratory tests. In addition to the stiffness properties, we are also interested in the strength of the foundation material, both in the stronger dolomitic sandstone, and in the weaker altered sandstone. I concluded that Anders has a reasonably good understanding of the Work Plan objectives.

- Elastic Property Measurements

Anders discussed how he would measure the properties we need. For the stronger dolomitic sandstone samples, he can measure the Young's modulus and Poisson's ratio during the unconfined compression tests. Since the elastic properties of this well cemented material would be relatively insensitive to the confining pressure range of interest to this project, the values measured from unconfined strength tests would be appropriate to compare with results from in-situ wave velocity measurement.

However, for the weaker altered friable sandstone samples, their stiffness will be sensitive to the confining pressures applied, just like typical sands are. Anders can only measure Young's modulus in his unconfined compression testing apparatus and not in his triaxial chamber where confining pressure would be applied. As a result, the Young's moduli reported for the altered sandstone samples were measured outside the triaxial cell,

in a way similar to an unconfined compression test. Moduli thus measured without confining pressures for the altered sandstone samples were typically very low and do not represent their in-situ conditions. To resolve this issue, an approach described in the following paragraph will be used.

Young's moduli measured in the laboratory for the dolomitic sandstone samples will be checked against the values derived from in-situ wave velocity measurements. If the comparison is reasonable, then it would imply that using in-situ wave velocity measurements to estimate Young's modulus is appropriate, and Young's modulus and Poisson ratio for the altered sandstone material could be estimated using velocity measurements as well.

Based on my review of the two types of samples and the limitation of the testing apparatus, I understand the difficulties regarding testing of these weak rocks and conclude that the approach described above to resolve the difficulty is appropriate.

- Strength Property Measurements

Because Anders had begun tests on samples obtained prior to my visit, he provided me test results for review while on site. Preliminary results of unconfined compression tests on dolomitic sandstone show reasonable values comparable to those measured in December 2000. Preliminary results of triaxial tests on the friable altered sandstone indicate that the material appeared clayey, exhibiting ductile (plastic) stress-strain behaviors. In addition, the samples were suspected to have generated excess pore pressures upon shearing and did not have sufficient time to drain (water was observed oozing out of several of the samples during testing). This typically would result in low friction angles and high cohesion intercepts. In addition, since no specific consolidation time was specified for consolidation of rock samples required by ASTM D-2664¹, and these multi-stage triaxial tests that followed ASTM do not have pore pressure measurements, the results of the first five tests (on samples no. 3, 5, 13, 17, and 32) should be viewed (and used) as unsaturated, unconsolidated, undrained triaxial tests.

After reviewing these results, I have recommended a soil triaxial testing procedure with pore pressure measurements (ASTM D-4767²) in order to obtain the effective and total friction angle of this friable altered sandstone material. Although this procedure is not listed in the current revision of the GTU Work Plan, based on the material behaviors in these tests and the preliminary test results, it is my opinion that changing the test procedure from rock triaxial (without pore pressure measurements) to soil triaxial (with pore pressure measurements) is important and appropriate. The above findings were discussed with Robert White of PG&E Geosciences Department, who concurred with the recommendation.

4. Verification of Laboratory Statement of Qualifications (SOQ) for GTU

¹ ASTM D-2664, Test Method for Triaxial Compression Strength of Undrained Rock Core Specimens without Pore Pressure Measurements.

² ASTM D-4767, Consolidated-Isotropically Drained Triaxial Test with Back Pressure Measurements (CIU)

The required documentation of laboratory qualifications was found to be adequately represented in the GTU's company brochure (copy previously attached to the 1/22/01 report). I inspected the direct shear testing apparatus, the triaxial loading frame with its cells and membrane, the closed circuit data acquisition system, and the Morehouse proving ring used for calibrating pressure transducers and load cells during my visit. In my opinion, the GTU capabilities stated in its company brochure are well -represented in the testing facility, and the equipment used for this project meets the standard of state-of-practice.

The same testing facility was used by PG&E for the testing of Scott Dam foundation materials. Anders Bro and the laboratory testing services by GTU were recommended by Prof. Richard Goodman of U.C. Berkeley for Scott Dam.

5. Verification of Personnel Qualifications for GTU

Qualifications of Anders Bro, who is responsible for conducting the rock tests and interpreting the test results, are presented in his resume sent to PG&E dated December 13, 2000 (copy previously attached to the 1/22/01 report) for the DCP. ISFSI project. His experience was found to exceed the 10-year minimum work experience requirement stated in the GTU Work Plan. On this basis, and based on my discussion with him, and observation of him performing a direct shear test, it is my opinion that Anders Bro is qualified to perform and interpret the tests required by this project.

6. Witness Direct Shear Test

During the time I was at the GTU testing facility, I witnessed Anders prepare and test a direct shear sample (Boring 01-B at depth of 48.8 ft). This sample had a joint inclined at about 60 degrees from the axis of the core. The joint was held together with cloth strings to prevent it from breaking apart during the sampling preparation process. The sample was placed in the shear box at an inclined angle of 30 degrees such that the joint face was aligned with the shear direction and located roughly at the middle of the opening between the upper and lower shear boxes. The core sample was securely fixed in the shear boxes with high strength plaster. The plastered upper and lower shear boxes were then moved to the testing apparatus to be sheared.

Both the normal load and shear force were applied hydraulically. The applied loads were constantly monitored by load cells. Six LVDT's were used to monitor the displacements of the upper shear box in the direction of the applied shear load and along the side and top of the upper shear box.

In order to perform multi-stage tests without excessive shearing, subsequent stages of normal loads were applied to the sample immediately upon the samples showing leveling off of shear resistance from the applied normal load. Since the tests followed ASTM standards for rock testing, no time was allowed for the sample to consolidate between stages. Corrections to shear areas to account for the reducing contact area with increasing shear displacements were applied. In my opinion, the test was performed consistent with ASTM standards and the GTU Work Plan.

7. Equipment Calibration

Calibration data for load cells, pressure transducers and LVDT's used in the unconfined, triaxial, and direct shear tests were collected in December 2000 and reviewed in the 1/22/01 report. Within the past 4 months since the calibrations were made, none of the devices malfunctioned. In my opinion, and in accordance with the Work Plan that required equipment must be calibrated within 12 months, I conclude that the measuring devices used in this project are reasonably accurate and reliable for the duration of this project.

8. Other Observations

During this and my past visit to GTU, I noticed that the lab does not have a moist room for storing samples. However, considering the fact that samples tested were rock and sealed in shrink wrapped plastic, and duration of storage at GTU was relatively short (typically less than 1 week before testing), and also by examining the condition of the stored samples, it is my opinion that not storing samples in a moist room has no measurable affect on the test results.

Conclusions:

1. I have reviewed the chain-of-custody forms dated 4/20/01, 4/23/01, and 5/7/01 and am satisfied with their accuracy and the manner in which the samples were transported from the DCPD ISFSI site to GTU facility.
2. I have reviewed the GTU Statement of Qualification in the form of a company brochure, and verified the statement's accuracy based on a site visit. In my opinion, the qualifications of GTU are accurate and GTU is qualified to perform the tests required for this investigation.
3. I have reviewed Anders Bro's qualifications to perform the tests and met with him regarding the objectives of the Work Plan. In my opinion, Dr. Bro is qualified to perform these tests and he has the qualifications to interpret the test results.
4. Based on my review of the preliminary test results for the friable altered sandstone, it appeared that testing this type of clayey material, which tends to generate excess pore pressure during shearing, using triaxial testing procedures for rocks without pore pressure measurements may not be appropriate for the objective of measuring the material's strength properties. In my opinion, a modified triaxial test procedure obtaining pore pressure measurements during sample shearing would be more appropriate. This was discussed with Mr. Robert White of PG&E Geosciences Department, and the recommended procedure has been implemented at GTU for the remaining triaxial tests of the same material.
5. In my opinion, GTU has performed activities in general accordance with the GTU work plan entitled "Laboratory Testing of Rock Samples for the Diablo Canyon Power Plant Independent Spent Fuel Storage Installation Site".

PACIFIC GAS AND ELECTRIC COMPANY
GEOSCIENCES DEPARTMENT
CALCULATION DOCUMENT

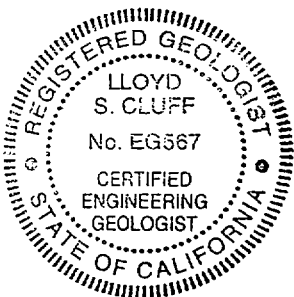
Calc Number GEO.DCPP.01.18
Revision 2
Date 11/19/01
Calc Pages: 30
Verification Method: A
Verification Pages: 1

TITLE: Determination of basic friction angle along rock discontinuities at DCPD
ISFSI based on laboratory tests.

PREPARED BY: Robert K White DATE 11/19/01
Robert K White Geosciences
Printed Name Organization

VERIFIED BY: Joseph Sun DATE 11/19/01
Joseph Sun Geosciences
Printed Name Organization

APPROVED BY: Lloyd Cluff DATE 11/19/01
Lloyd Cluff Geosciences
Printed Name Organization



Expires 12/31/02

**Determination of basic friction angle along rock discontinuities at DCPD ISFSI
based on laboratory tests.
Calc. Number GEO.DCPD.01.18**

Record of Revisions

Rev. No.	Reason for Revision	Revision Date
1	Separated dolomite and sandstone clean rock to rock joint data previously lumped together. Clarified assumptions. Minor changes to Table 1. Replotted and added additional figures:	7/23/01
2	Added references to relevant calculations. Revised References section, added Attachments section. Revised assumptions based on approved calculation 21. Revised order of methodology to more closely match Analysis. Removed separate analyses for dolomite and sandstone based on revised classifications in Bachhuber, 11/19/01.	11/19/01

DCPP ISFSI GEOTECHNICAL CALCULATION PACKAGE

Title: Determination of basic friction angle along rock discontinuities at DCP
ISFSI based on laboratory tests

Calc Number: GEO.DCPP.01.18

Revision: 2

Author: Robert K. White

Date: 11/19/01

Verifier: Joseph I. Sun

PURPOSE

As required by Geosciences Work Plan GEO 2001-03, Appendix N, this calculation package documents the evaluation and statistical analysis of the laboratory direct shear test results on rock discontinuities and develops the basic friction angle along the discontinuities. The basic friction angle determined from direct shear tests will be used in a separate calculation (GEO.DCPP.01.20), in conjunction with other geological indices describing discontinuity properties, to develop the overall discontinuity strength. The discontinuity strengths will then be applied to wedge-type slope stability analyses (GEO.DCPP.01.23).

ASSUMPTIONS

1. Basic frictional strengths of rock discontinuities have no adhesion (or cohesion) component. Thus, failure envelopes of the rock discontinuities all go through the origin and a similar restriction will be applied to the statistical analysis when developing the envelopes. This is a reasonable assumption, based on the definition of the basic friction angle in chapter 4, page 61, of Hoek (2000), attached..
2. The post-peak friction angle determined as a result of laboratory tests on discontinuities is approximately equivalent to the basic friction angle, as described in chapter 4, page 61, Hoek (2000), attached.
3. The friction angle derived from multi-stage direct shear tests on discontinuities is not significantly different from the friction angle developed from single stage tests. This is a conservative assumption, as the multistage test generally underestimates peak

strength, because each stage of the test is ended at or before the peak strength is reached.

4. Partially clay-coated discontinuities occur randomly throughout both sandstone and dolomite at the site. That is, they are not restricted to a certain rock type or zone, nor are they completely clay-filled. This is a reasonable assumption, as documented in GEO.DCPP.01.21, pages 50 and 51.

DESIGN INPUTS

1. Laboratory test results from Witter, 11/5/01, Data Report I.
2. Direct shear sample classification table, as provided in Bachhuber, 11/19/01.

METHODOLOGY

1. Obtain laboratory test results for all December 2000 and May 2001 direct shear tests from Witter (11/5/01), Data Report I. A total of 21 multi-stage direct shear tests were performed. Review direct shear laboratory test sheets, transfer strength test data to Table 1, and identify unreliable tests in accordance with Bachhuber, 11/19/01.
2. Classify discontinuity of samples as sandstone or dolomite rock-rock contact, clay-rock or clay coating, and clay bed/seam ($> \frac{1}{4}$ inch thick) in accordance with Bachhuber, 11/19/01.
3. Aggregate rock-rock contact and clay-rock contact test results.
4. Perform statistical analysis based on aggregated samples and test results.

SOFTWARE

Statistical analysis used to determine the least squares best fit strength envelopes presented on the attached Figures was based on built-in statistical functions in Microsoft Excel 2000.

ANALYSIS

Out of the 21 direct shear tests listed in Bachhuber (11/19/01) and transferred to Table 1, ten were classified as clean rock-rock contacts, seven were clay-rock contacts or joints with clay coating, and four were clay seams or clay beds. Of the ten clean rock samples, all were dolomite (Tofb-1). Clay beds and clay seams typically are thicker than $\frac{1}{4}$ inch. The results are discussed below.

Rock-Rock Contact

For the ten rock-rock contact samples (30 data points), the variation of data points for both their peak strengths and post peak strengths are developed in Figures 1 through 4 and summarized in Table 2. A normal stress of 70 psi is chosen as a cutoff in some of the plots because 0 to 70 psi is anticipated to be the most representative stress range for joints in the cutslope analyses (GEO.DCPP.01.23), and this range removes the influence of six values at much higher normal stresses not duplicated in clay film sample tests. Based on the best-fit strength envelope in Figure 4, the post-peak friction angle for rock-rock contact is 35 degrees.

Clay-Rock Contact or Clay Coated Joints

The thickness of the clay coatings or clay films is usually less than ¼ inch for seven rock-clay or clay coated samples. Many of the clay coatings were not clearly visible during the sample selection process in the field. Some of them were only visible after the tests when samples were taken apart to expose the joints.

Of the seven samples tested, three tests were discarded. Sample No. 33 from boring 01-F was discarded because the clay seam in the sample may have experienced plastic deformation under high normal loads, and the asperities may have extruded through the clay seams and interfered with the test results. Sample No. 34 from Boring 01-CTF-A was discarded because the shear box rotated significantly during the test. This resulted in unreliable shear displacement and shear stress plots, thus creating difficulties in selecting the peak shear stress under each normal load. Sample 35 from Boring 01-H was discarded because the 0.1 to 0.4 inch thick clay seam compressed under the normal load and caused steel-to-steel contact between the shear boxes. Constant peak shear stresses for the first two normal loads also suggests that contact between the upper and lower shear boxes may have occurred earlier than the application of the 3rd normal stress.

The peak and post-peak shear strengths for the remaining 4 samples (accounting for 14 data points for peak strength measurements and 12 for post-peak strength measurements) are developed in Figure 5 and summarized in Table 3, with corresponding friction angles of 18° and 14°, respectively.

Clay beds

Four clay bed samples, typically with clay thickness over ¼ inch thick were tested. None of the test results were included in the analysis. The reason for discarding these tests is because of the rock direct shear test set up. Unlike soil direct shear apparatus, which have minimum gap between the upper and lower shear boxes, the rock direct shear boxes have a wide gap between the shear boxes. In addition, the clay bed material was not set in the plaster and thus does not receive any lateral support (confinement) during the application of normal loads. Often, the thick clay beds failed in compression and were squeezed out of the shear box when the normal loads were applied, producing inconsistent or contradictory results. Sample 31 from Boring 01-F, for example, exhibited lower shear resistance under higher normal loads. On the above basis, it was judged that the rock direct shear device is not appropriate to test and characterize the clay bed strength.

RESULTS

Joint Characteristics Evaluation

Based on the random occurrence of clay-coated discontinuities as described in the Assumptions section, above, the strength test results for the rock-rock contact and the clay-rock contact are aggregated in performing the statistical analyses, below.

Statistical Analysis

For the fourteen rock-rock and clay film samples, the variation of data points for both their peak strengths and post peak strengths are developed in Figures 6 through 9, and resulting best-fit strength envelopes shown on the Figures are summarized in Table 4. Based on the best-fit strength envelope in Figure 9, the post peak friction angle for the aggregated rock-rock and clay film samples is 28 degrees.

CONCLUSIONS

1. Based on classification of discontinuity types in Bachhuber (11/19/01), there appears to be a relatively equal chance that any given point along a discontinuity may be either clean (rock-rock) or clay-coated (in this case, ten samples were clean and seven coated).

2. On the above basis, aggregating the direct shear strength data from clean and clay coated joints and developing a best-fit envelope through all data appears to represent a reasonable average of the discontinuity strength.
3. A conservative approach was taken to discard higher strength test results that were tested with normal stress above 70 psi. The best-fit post-peak friction angle for clean samples is about 35 degrees. The best-fit post-peak friction angle for clay-coated samples is about 14 degrees. The best-fit post-peak friction angle for the aggregated samples is about 28 degrees.
4. These post-peak friction angles should be used as the basic friction angles to characterize the discontinuity strength in further wedge-type slope stability analyses (GEO.DCPP.01.23).

REFERENCES

1. Geosciences Work Plan GEO 2001-03, Development of Engineering Properties for ISFSI and CTF Foundation Design, ISFSI Slope Analyses, and ISFSI Cut and Fill Slope Reinforcement Design for The DCPD ISFSI Site, rev. 1.
2. Witter (11/5/01): letter from Rob Witter to Rob White, entitled "Completion of Data Reports," dated 11/5/01, and accompanying:
Data Report B, Borings in ISFSI Site Area, rev. 0, and
Data Report I, Rock Laboratory Test Data, rev. 0.
3. Hoek, E., 2000, Rock engineering course notes: chapter 4 of on-line webpage document at www.rocscience.com, latest revision date 11/27/00.
4. Geosciences Calculation GEO.DCPP.01.20, Development of Strength Envelopes for Shallow Discontinuities at DCPD ISFSI using Barton Equations, rev. 1.
5. Geosciences Calculation GEO.DCPP.01.21, Analysis of Bedrock Stratigraphy and Geologic Structure at the DCPD ISFSI Site, rev. 1.
6. Geosciences Calculation GEO.DCPP.01.23, Pseudostatic wedge analysis of DCPD ISFSI Cutslope (SWEDGE Analysis), rev. 0.
7. Bachhuber (11/19/01): letter from Jeff Bachhuber to Rob White, dated 11/19/01, and referenced attachment Direct Shear Test Sample Classification Table.

ATTACHMENTS

1. Table 1, Direct Shear Test Summary, pages 7 through 9.
2. Tables 2, 3, and 4, page 10.
3. Figures 1 through 9, pages 11 through 19.
4. Witter (11/5/01): letter from Rob Witter to Rob White, entitled "Completion of Data Reports," dated 11/5/01 (without attachments), pages 20 and 21.
5. Hoek, E., 2000, Rock engineering course notes: chapter 4 of on-line webpage document at www.rocsience.com, latest revision date 11/27/00, cover page and page 61, pages 22 and 23.
6. Bachhuber (11/19/01): letter from Jeff Bachhuber to Rob White, dated 11/19/01, and referenced attachment, Direct Shear Test Sample Classification Table, pages 24 through 30.

Table 1
Direct Shear test Results

DIRECT SHEAR TEST SUMMARY

Boring No.	Sample I.D.	Depth (ft)	Discontinuity Inclination (degrees)	Bedrock Description	Bedrock Unit	Discontinuity Description	Laboratory Sample Description	Normal Stress (psi)	Rock-rock surface		Clay-rock or clay		Clay Bed/Seam	
									Peak Shear Stress (psi)	Post peak Shear Stress (psi)	Peak Shear Stress (psi)	Post peak Shear Stress (psi)	Peak Shear Stress (psi)	Post peak Shear Stress (psi)
01-B	20	48.8	40 (WLA) 50 (Lab)	Altered clayey dolomitic sandstone in contact with sandstone fine to med grained.	Tofb-2	Bonded contact, irregular, between altered and non-altered rock. Irregular clay-coated shear surface on post-test sample, sheared partly through weak rock.	Slightly wavy contact between hard dolomite and soft clayey altered dolomite	13.0 18.0 25.0 40.0 55.0 15.0 20.0 28.0			11.8 14.0 17.0 25.0 30.5	12.0 14.0 17.0		
01-C	23	41.4	20 (WLA) 44 (Lab)	Dolomitic sandstone to semi-friable dolomitic sandstone, med. to coarse grained.	Tofb-2	De-bonded fault plane with clay-coated slickensides.	Very thin clay coated slickensided joint in gray medium grained sandstone. Joint slightly disturbed during preparation. Actual break deviated from intended joint plane.	20.2 40.0 62.3 21.4 41.3 66.2			4.5 7.8 11.7	6.0 9.0 11.8		
01-C	24	44.3	30 (WLA) 30 (Lab)	Cemented dolomitic sandstone, medium grained	Tofb-2	Partly bonded joint plane	Wavy lightly bonded joint with thin tan clay coating in tan medium grained sandstone	20.8 41.2 61.0 22.5 45.2 66.3			4.5 6.2 7.8	5.8 7.3 10.0		
01-E	29	51.8	0 to 5 (WLA) 6 (Lab) Bedding	Cemented dolomite, fine grained.	Tofb-1	Mechanical break 0 to 5 degrees along possible bedding lamination.	Planar well mated bedding joint in tan fine to medium grained sandstone	17.0 30.0 46.8 17.5 34.0 50.2	19.0 30.2 44.5					
01-F DISCARD	31	117	8 to 12 (WLA) 15 (Lab)	Cemented dolomite, medium grained - friable medium to coarse grained clayey sandstone	Tofb-1a / Tofb-2a	De-bonded joint interface 8 to 12 deg between harder and softer rock with 1cm thick clay seam. Irregular clayey seam with multiple clay shear surfaces.	Tan sandy soft clay seam (0.5 to 1 inch) in tan fine to medium grained clayey sandstone. Sample extruded sideways under load. Separation surface is not shear surface.	12.5 20.4 38.7 13.2 21.6 40.3					4.0 3.9 3.4	5.1 4.7 4.0
01-F DISCARD	33	118.3	65 to 70	Friable clayey medium and coarse grained sandstone in contact with cemented medium grained sandstone	Tofb-2a / Tofb-2	De-bonded joint interface 65 to 70 degrees between friable and hard rock. Irregular clay coated sheared surface in post-test sample, not a single planar joint.	Gray clay seam (0 to 0.05 inch thick) in gray medium grained clayey sandstone. Test may not have sheared through clay "seam", pulled apart through chewed up rock.	18.5 35.0 72.0 20.5 40.0 81.0 174.0			8.0 11.0 20.0	10.5 14.0 21.0 36.0		
01-CTF-A DISCARD	34	32.6	5 (WLA) 23 (Lab)	Medium grained sandstone in contact with silty clay.	Tofb-2	Partly De-bonded contact between cemented sandstone and silty clay bed/zone with polished clay surface. Very irregular shear surface not developed along a planar joint.	Contact between tan sandy clay and tan clayey fine to medium grained sandstone. Part of sample collapsed and sample underwent large rotation during testing. Lab recommended that the sample not be tested due to limited ability to clamp sample.	15.5 31.5 60.5			14.0 24.2 39.5			
01-H DISCARD	35	94.5	5 (WLA) 4 (Lab)		Tofb-2a	Partly de-bonded low angle clay filled joints possibly along bedding. Very irregular shear	Irregular dark gray clay filled joint (0.1 to 0.4 in. thick) in gray clayey medium grained	14.0 24.3 47.2			2.6 2.6 3.5			

page 7 of 30

Table 1
Direct Shear test Results

Boring No.	Sample I.D.	Depth (ft)	Discontinuity Inclination (degrees)	Bedrock Description	Bedrock Unit	Discontinuity Description	Laboratory Sample Description	Normal Stress (psi)	Peak Shear Stress (psi)	Post peak Shear Stress (psi)	Peak Shear Stress (psi)	Post peak Shear Stress (psi)	Peak Shear Stress (psi)	Post peak Shear Stress (psi)
				Frable medium grained sandstone		surface involving multiple irregular subparallel clayey surface, not developed along angle planar joint.	sandstone. Sample compressed during final testing stages causing steel-to-steel shear box contact.	16.0 29.0 53.2				6.5 6.5 8.8		
01-1	36	174	0 (WLA) 14 (Lab) Bedding	Cemented medium grained dolomite, laminated.	Tofb-1	De-bonded bedding plane joint/mechanical break.	Planar bedding joint in tan thinly bedded very fine grained dolomitic sandstone. Leaf fossil observed on joint surface.	86.0 175.0 352.0 93.0 190.0 384.0	76.0 144.0 264.0	61.0 121.0 237.0				
01-1	37	168.5	10 (WLA) 14 (Lab)	Cemented dolomite, medium grained, laminated in contact with stiff clay	Tofb-1	De-bonded joint/bedding partings along 10 degree clay seam 1/8" to 1/4" thick.	Bedding plane joint in tan fine grained dolomitic sandstone with a thin lamination and clay coating. Sample rotated and joint slides probably ground into contact through the clay.	16.2 27.5 52.3 16.5 28.1 54.5			6.8 9.6 18.5	7.9 11.1 20.0		
01-1 DISCARD	39B	130.4	10 (WLA) 8 (Lab)	Cemented fine to medium grained dolomite in contact with stiff clay	Tofb-1	Partly bonded low angle contact between hard dolomite and a 1/2 to 1 cm thick clay bed. Irregular failure surface partly in rock, partly along clayey discontinuous joint surface.	Tan clay seam (0.1 to 0.2 inch thick) in tan fine grained dolomitic sandstone. Sample slid on soft clay.	13.1 25.6 47.8 14.2 28.1 52.2					4.8 7.2 10.6	5.5 7.3 11.0
01-1	40B	88.8	20 (WLA) 16 (Lab) Bedding	Cemented fine grained dolomite, laminated.	Tofb-1	De-bonded bedding plane joint, subparallel to laminations.	Planar bedding joints in tan fine grained dolomitic sandstone.	47.0 90.0 178.0 49.0 96.0 194.0	42.0 73.0 133.0	32.0 59.0 113.0				
01-1 DISCARD	41A	45.6	10 to 15 (WLA) 17 (Lab)	Cemented fine grained dolomite, laminated.	Tofb-1	partly bonded low angle clay bed-rock contact, clay 2 cm thick, tight contact. Clay not observed in returned sample (removed?).	Tan clay seam about 3/4-inch thick in tan fine grained sandstone. Sample rocked and developed open fractures during shearing. Slickensides observed on sample surface.	9.5 13.5 26.5 10.5 16.5 28.5					8.0 9.0 14.0	7.0 9.0 12.0
01-1	41B	46.1	20 (WLA) 14 (Lab) Bedding	Cemented fine grained dolomite, laminated.	Tofb-1	De-bonded low angle bedding joint between rock surfaces.	Planar bedding joint in tan fine grained dolomitic sandstone.	23.5 48.0 93.0 25.5 51.5 100.0	28.5 54.5 96.0	20.0 40.0 75.0				
OOBA-1	1-1	18.2	30 to 40 (WLA) 30 (Lab)	Cemented fine to medium grained dolomite.	Tofb-1	De-bonded joint, rock to rock surface, oxidized.	Poorly mated rough joint in molted tan and brown dolomite with black oxide and light brown coating.	10.6 20.1 41.2 11.3 21.4 43.7	13.0 21.3 35.3	9.0 16.6 31.2				
OOBA-1	1-2	34.2	64 (WLA) 64 (Lab)	Cemented fine to medium grained dolomitic sandstone.	Tofb-1	De-bonded steep wavy joint, rock-rock contact.	Rough, well-mated joint in tan dolomite with black and brown oxidation staining.	10.3 20.1 41.0 10.0 21.6 44.1	16.1 25.6 43.8	9.0 18.3 33.0				
OOBA-1	1-3	37.3	12 (WLA) 12 (Lab) Bedding	Cemented fine to medium grained dolomitic sandstone.	Tofb-1	De-bonded joint, subparallel to bedding, laminations, rock-rock contact.	Bedding plane in brown dolomite	10.1 20.5 41.3 10.9 22.2 44.7	8.0 14.7 27.5	6.9 12.4 23.4				

09 to 8 sand

Table 1
Direct Shear test Results

Boring No.	Sample I.D.	Depth (ft)	Discontinuity Inclination (degrees)	Bedrock Description	Bedrock Unit	Discontinuity Description	Laboratory Sample Description	Normal Stress (psi)	Peak Shear Stress (psi)	Post peak Shear Stress (psi)	Peak Shear Stress (psi)	Post peak Shear Stress (psi)	Peak Shear Stress (psi)	Post peak Shear Stress (psi)	
OOBA-1	1-4	41.9	12 (WLA) 13 (Lab) Bedding	Cemented fine to medium grained dolomitic sandstone	Tofb-1	De-bonded mechanical break, subparallel to fault bedding, lamination, rock-rock contact.	Mechanical break possibly along bedding in fine grained tan dolomitic sandstone.	13.8 24.0 44.6 15.8 27.2 50.5	25.3 31.0 46.9	10.8 18.1 31.7					
OOBA-1	1-6	88.8	21 (WLA) 21 (Lab)	Cemented fine to medium grained dolomitic sandstone.	Tofb-1	De-bonded joint, rock-rock contact.	Moderately rough, well-mated joint with a thin flakey coating in the tan dolomitic sandstone	20.6 40.1 82.0 24.2 47.0 96.2	24.2 42.4 71.0	13.3 23.7 45.0					
OOBA-1	1-7	142	55 (WLA) 55 (Lab)	Cemented fine to medium grained dolomite.	Tofb-1	Steep wavy joint, rock-rock contact.	Wavy poorly mated joint with a black oxide coating and tan flakey coating (possibly clay) in tan dolomite sandstone	20.5 41.8 83.0 22.9 46.7 92.8	21.8 41.8 76.8	19.0 37.0 71.0					
OOBA-1 DISCARD	1-18	56.5	5 to 15 (WLA) 15 (Lab)	Cemented fine grained dolomite - claybed.	Tofb-1	Low angle contact between dolomite and 0.7 in thick stiff clay bed, tight and relatively planar clay rock contact.	Tan rock/clay seam interface with a dark brown staining in the vicinity of the interface.	5.8 10.0 20.2 37.2 6.5 10.7 21.9 40.3				7.8 10.7 15.2 19.1	4.9 6.3 9.4 12.0		

Page 9 of 30

Table 2 Clean rock joints

Figure	Joint set plotted	ϕ_{peak}	$\phi_{\text{post peak}}$
1	Peak all rock	39	
2	Peak all rock with sign < 70 psi	45	
3	Post peak all rock		32
4	Post peak all rock with sign < 70 psi		35

Table 3 Clay film joints

Figure	Joint set plotted	ϕ_{peak}	$\phi_{\text{post peak}}$
5	peak all rock	18	
5	post peak all rock		14

Table 4 Clean rock joints and clay film joints together

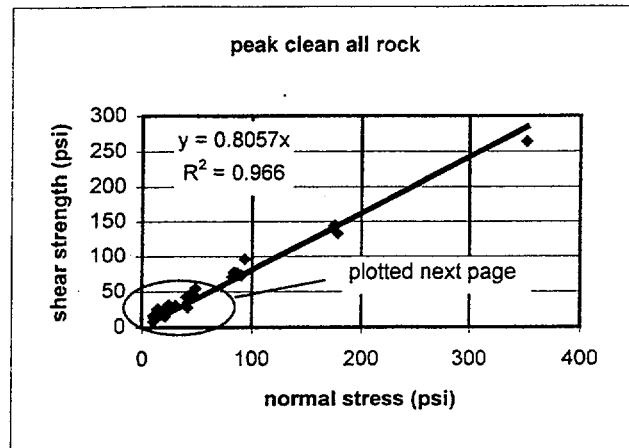
Figure	Joint set plotted	ϕ_{peak}	$\phi_{\text{post peak}}$
6	Peak all rock	38	
7	Peak all rock with sign < 70 psi	34	
8	Post peak all rock		31
9	Post peak all rock with sign < 70 psi		28

Notes:

1. The term "sign" in the tables is "sigma normal," or normal stress applied to sample.
2. All best fits to obtain ϕ angle in plots are straight lines through the origin.

Peak clean all rock data

Boring No.	Sample I.D.	Rock Type	normal stress	peak strength
01-E	29	Tofb-1	17.0	19.0
	29		30.0	30.2
	29		46.8	44.5
01-I	36	Tofb-1	86.0	76.0
	36		175.0	144.0
	36		352.0	264.0
01-I	40B	Tofb-1	47.0	42.0
	40B		90.0	73.0
	40B		178.0	133.0
01-I	41B	Tofb-1	23.5	28.5
	41B		48.0	54.5
	41B		93.0	96.0
OOBA-1	1-1	Tofb-1	10.6	13.0
	1-1		20.1	21.3
	1-1		41.2	35.3
OOBA-1	1-2	Tofb-1	10.3	16.1
	1-2		20.1	25.6
	1-2		41.0	43.8
OOBA-1	1-3	Tofb-1	10.1	8.0
	1-3		20.5	14.7
	1-3		41.3	27.5
OOBA-1	1-4	Tofb-1	13.8	25.3
	1-4		24.0	31.0
	1-4		44.6	46.9
OOBA-1	1-6	Tofb-1	20.6	24.2
	1-6		40.1	42.4
	1-6		82.0	71.0
OOBA-1	1-7	Tofb-1	20.5	21.8
	1-7		41.8	41.8
	1-7		83.0	76.8

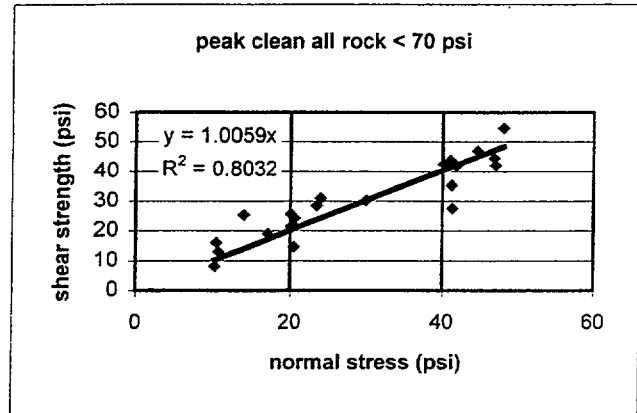


line slope = 0.8057
phi = 38.9 degrees

Figure 1

peak clean all rock with normal stress < 70 psi

Boring No.	Sample I.D.	Rock Type	normal stress	peak strength
01-E	29	Tofb-1	17.0	19.0
			30.0	30.2
			46.8	44.5
01-I	40B	Tofb-1	47.0	42.0
01-I	41B	Tofb-1	23.5	28.5
			48.0	54.5
OOBA-1	1-1	Tofb-1	10.6	13.0
			20.1	21.3
			41.2	35.3
OOBA-1	1-2	Tofb-1	10.3	16.1
			20.1	25.6
			41.0	43.8
OOBA-1	1-3	Tofb-1	10.1	8.0
			20.5	14.7
			41.3	27.5
OOBA-1	1-4	Tofb-1	13.8	25.3
			24.0	31.0
			44.6	46.9
OOBA-1	1-6	Tofb-1	20.6	24.2
			40.1	42.4
OOBA-1	1-7	Tofb-1	20.5	21.8
			41.8	41.8

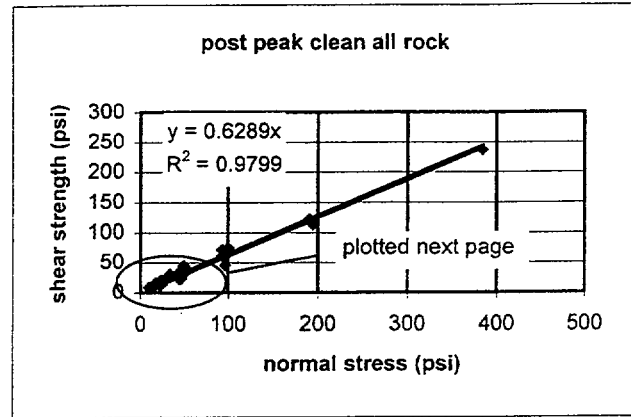


line slope = 1.0059
 phi = 45.2 degrees

Figure 2

post peak clean all rock data

Boring No.	Sample I.D.	Rock Type	normal stress	post peak strength
01-E	29	Tofb-1	17.5	16.0
	29		34.0	31.0
	29		50.2	45.0
01-I	36	Tofb-1	93.0	61.0
	36		190.0	121.0
	36		384.0	237.0
01-I	40B	Tofb-1	49.0	32.0
	40B		96.0	59.0
	40B		194.0	113.0
01-I	41B	Tofb-1	25.5	20.0
	41B		51.5	40.0
	41B		100.0	75.0
OOBA-1	1-1	Tofb-1	11.3	9.0
	1-1		21.4	16.6
	1-1		43.7	31.2
OOBA-1	1-2	Tofb-1	10.0	9.0
	1-2		21.6	18.3
	1-2		44.1	33.0
OOBA-1	1-3	Tofb-1	10.9	6.9
	1-3		22.2	12.4
	1-3		44.7	23.4
OOBA-1	1-4	Tofb-1	15.8	10.8
	1-4		27.2	18.1
	1-4		50.5	31.7
OOBA-1	1-6	Tofb-1	24.2	13.3
	1-6		47.0	23.7
	1-6		96.2	45.0
OOBA-1	1-7	Tofb-1	22.9	19.0
	1-7		46.7	37.0
	1-7		92.8	71.0



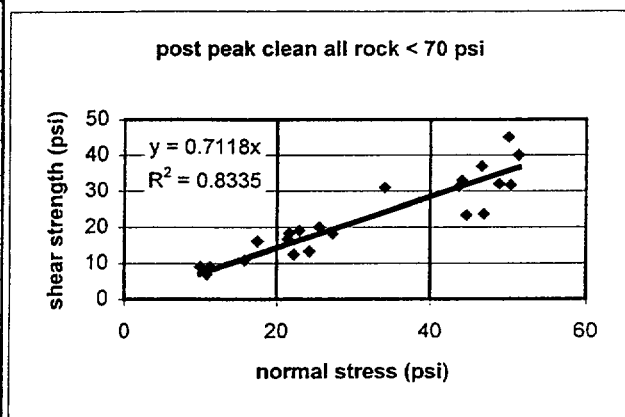
line slope = 0.6289
 phi = 32.2 degrees

✓

Figure 3

post peak clean all rock with normal stress < 70 psi

Boring No.	Sample I.D.	Rock Type	normal stres	post peak strength
01-E	29	Tofb-1	17.5	16.0
	29		34.0	31.0
	29		50.2	45.0
01-I	40B	Tofb-1	49.0	32.0
01-I	41B	Tofb-1	25.5	20.0
	41B		51.5	40.0
OOBA-1	1-1	Tofb-1	11.3	9.0
	1-1		21.4	16.6
	1-1		43.7	31.2
OOBA-1	1-2	Tofb-1	10.0	9.0
	1-2		21.6	18.3
	1-2		44.1	33.0
OOBA-1	1-3	Tofb-1	10.9	6.9
	1-3		22.2	12.4
	1-3		44.7	23.4
OOBA-1	1-4	Tofb-1	15.8	10.8
	1-4		27.2	18.1
	1-4		50.5	31.7
OOBA-1	1-6	Tofb-1	24.2	13.3
	1-6		47.0	23.7
OOBA-1	1-7	Tofb-1	22.9	19.0
	1-7		46.7	37.0

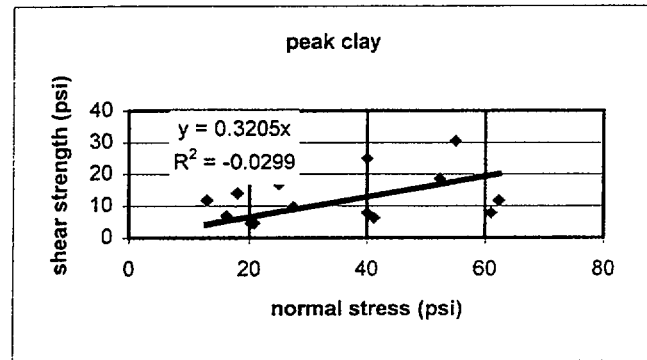


line slope = 0.7118
 phi = 35.4 degrees

Figure 4

Peak clay film

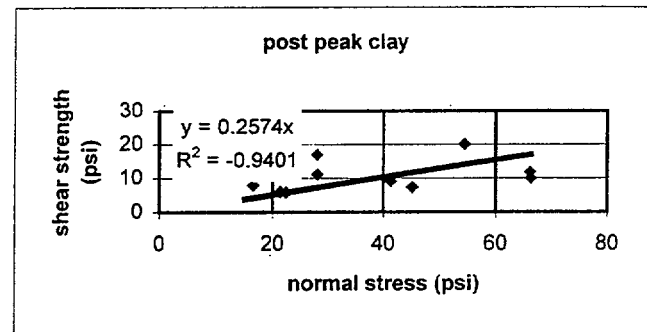
Boring No.	Sample I.D.	Rock Type	normal stress	peak strength**
01-B	20	Tofb-2	13.0	11.8
	20		18.0	14.0
	20		25.0	17.0
	20		40.0	25.0
	20		55.0	30.5
01-C	23	Tofb-2	20.2	4.5
	23		40.0	7.8
	23		62.3	11.7
01-C	24	Tofb-2	20.8	4.5
	24		41.2	6.2
	24		61.0	7.8
01-I	37	Tofb-1	16.2	6.8
	37		27.5	9.6
	37		52.3	18.5



line slope = 0.3205
phi = 17.8 degrees

Post peak clay film

Boring No.	Sample I.D.	Rock Type	normal stress	post peak strength**
01-B	20	Tofb-2	15.0	12.0
	20		20.0	14.0
	20		28.0	17.0
01-C	23	Tofb-2	21.4	6.0
	23		41.3	9.0
	23		66.2	11.8
01-C	24	Tofb-2	22.5	5.8
	24		45.2	7.3
	24		66.3	10.0
01-I	37	Tofb-1	16.5	7.9
	37		28.1	11.1
	37		54.5	20.0



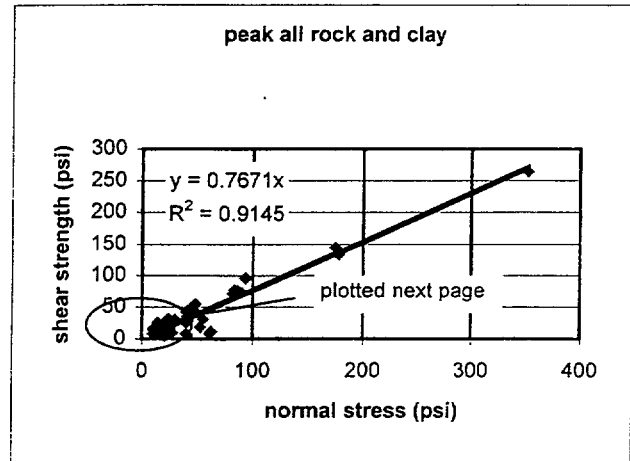
line slope = 0.2574
phi = 14.4 degrees

**clay film values in italics

Figure 5

Peak all clean rock and clay film

Boring	Sample	Rock	normal	peak
No.	I.D.	Type	stress	strength**
01-B	20	Tofb-2	13.0	11.8
	20		18.0	14.0
	20		25.0	17.0
	20		40.0	25.0
	20		55.0	30.5
01-C	23	Tofb-2	20.2	4.5
	23		40.0	7.8
	23		62.3	11.7
01-C	24	Tofb-2	20.8	4.5
	24		41.2	6.2
	24		61.0	7.8
01-E	29	Tofb-1	17.0	19.0
	29		30.0	30.2
	29		46.8	44.5
01-I	37	Tofb-1	16.2	6.8
	37		27.5	9.6
	37		52.3	18.5
01-I	36	Tofb-1	86.0	76.0
	36		175.0	144.0
	36		352.0	264.0
01-I	40B	Tofb-1	47.0	42.0
	40B		90.0	73.0
	40B		178.0	133.0
01-I	41B	Tofb-1	23.5	28.5
	41B		48.0	54.5
	41B		93.0	96.0
OOBA-1	1-1	Tofb-1	10.6	13.0
	1-1		20.1	21.3
	1-1		41.2	35.3
OOBA-1	1-2	Tofb-1	10.3	16.1
	1-2		20.1	25.6
	1-2		41.0	43.8
OOBA-1	1-3	Tofb-1	10.1	8.0
	1-3		20.5	14.7
	1-3		41.3	27.5
OOBA-1	1-4	Tofb-1	13.8	25.3
	1-4		24.0	31.0
	1-4		44.6	46.9
OOBA-1	1-6	Tofb-1	20.6	24.2
	1-6		40.1	42.4
	1-6		82.0	71.0
OOBA-1	1-7	Tofb-1	20.5	21.8
	1-7		41.8	41.8
	1-7		83.0	76.8



line slope = 0.7671
 phi = 37.5 degrees

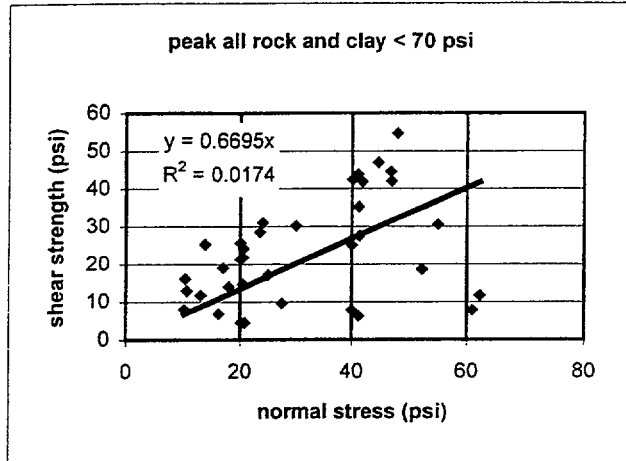
**clay film values in *italics*

Figure 6

Peak all clean rock and clay film with normal stress < 70 psi

Boring	Sample	Rock	normal	peak
No.	I.D.	Type	stress	strength**
01-B	20	Tofb-2	13.0	11.8
	20		18.0	14.0
	20		25.0	17.0
	20		40.0	25.0
	20		55.0	30.5
01-C	23	Tofb-2	20.2	4.5
	23		40.0	7.8
	23		62.3	11.7
01-C	24	Tofb-2	20.8	4.5
	24		41.2	6.2
	24		61.0	7.8
01-E	29	Tofb-1	17.0	19.0
	29		30.0	30.2
	29		46.8	44.5
01-I	37	Tofb-1	16.2	6.8
	37		27.5	9.6
	37		52.3	18.5
01-I	40B	Tofb-1	47.0	42.0
01-I	41B	Tofb-1	23.5	28.5
	41B		48.0	54.5
OOBA-1	1-1	Tofb-1	10.6	13.0
	1-1		20.1	21.3
	1-1		41.2	35.3
OOBA-1	1-2	Tofb-1	10.3	16.1
	1-2		20.1	25.6
	1-2		41.0	43.8
OOBA-1	1-3	Tofb-1	10.1	8.0
	1-3		20.5	14.7
	1-3		41.3	27.5
OOBA-1	1-4	Tofb-1	13.8	25.3
	1-4		24.0	31.0
	1-4		44.6	46.9
OOBA-1	1-6	Tofb-1	20.6	24.2
	1-6		40.1	42.4
OOBA-1	1-7	Tofb-1	20.5	21.8
	1-7		41.8	41.8

** clay film values in italics

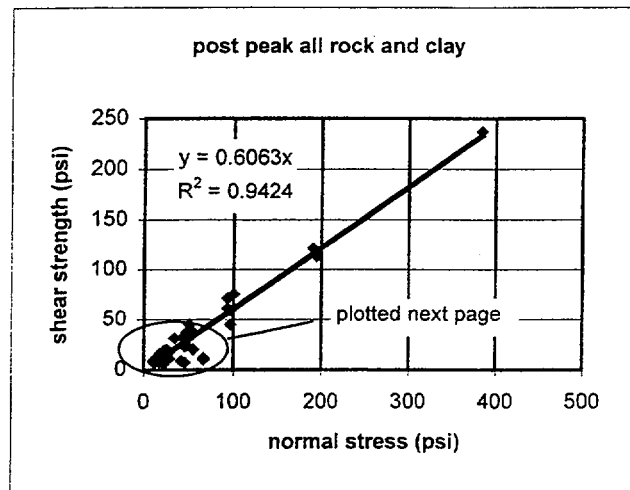


line slope = 0.6695
 phi = 33.8 degrees

Figure 7

Post Peak Clean Rock and Clay Film

Boring	Sample	Rock	normal	post peak
No.	I.D.	Type	stress	strength**
01-B	20	Tofb-2	15.0	12.0
	20		20.0	14.0
	20		28.0	17.0
01-C	23	Tofb-2	21.4	6.0
	23		41.3	9.0
	23		66.2	11.8
01-C	24	Tofb-2	22.5	5.8
	24		45.2	7.3
	24		66.3	10.0
01-I	37	Tofb-1	16.5	7.9
	37		28.1	11.1
	37		54.5	20.0
01-E	29	Tofb-1	17.5	16.0
	29		34.0	31.0
	29		50.2	45.0
01-I	36	Tofb-1	93.0	61.0
	36		190.0	121.0
	36		384.0	237.0
01-I	40B	Tofb-1	49.0	32.0
	40B		96.0	59.0
	40B		194.0	113.0
01-I	41B	Tofb-1	25.5	20.0
	41B		51.5	40.0
	41B		100.0	75.0
OOBA-1	1-1	Tofb-1	11.3	9.0
	1-1		21.4	16.6
	1-1		43.7	31.2
OOBA-1	1-2	Tofb-1	10.0	9.0
	1-2		21.6	18.3
	1-2		44.1	33.0
OOBA-1	1-3	Tofb-1	10.9	6.9
	1-3		22.2	12.4
	1-3		44.7	23.4
OOBA-1	1-4	Tofb-1	15.8	10.8
	1-4		27.2	18.1
	1-4		50.5	31.7
OOBA-1	1-6	Tofb-1	24.2	13.3
	1-6		47.0	23.7
	1-6		96.2	45.0
OOBA-1	1-7	Tofb-1	22.9	19.0
	1-7		46.7	37.0
	1-7		92.8	71.0



line slope = 0.6063
 phi = 31.2 degrees

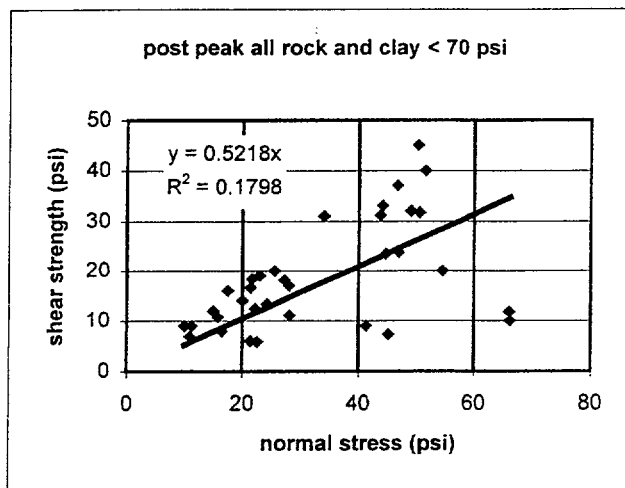
**clay film samples in italics

Figure 8

Post Peak Clean Rock and Clay Film with normal stress < 70 psi

Boring	Sample	Rock	normal	post peak
No.	I.D.	Type	stress	trength**E33
01-B	20	Tofb-2	15.0	12.0
	20		20.0	14.0
	20		28.0	17.0
01-C	23	Tofb-2	21.4	6.0
	23		41.3	9.0
	23		66.2	11.8
01-C	24	Tofb-2	22.5	5.8
	24		45.2	7.3
	24		66.3	10.0
01-E	29	Tofb-1	17.5	16.0
	29		34.0	31.0
	29		50.2	45.0
01-I	37	Tofb-1	16.5	7.9
	37		28.1	11.1
	37		54.5	20.0
01-I	40B	Tofb-1	49.0	32.0
01-I	41B	Tofb-1	25.5	20.0
	41B		51.5	40.0
OOBA-1	1-1	Tofb-1	11.3	9.0
	1-1		21.4	16.6
	1-1		43.7	31.2
OOBA-1	1-2	Tofb-1	10.0	9.0
	1-2		21.6	18.3
	1-2		44.1	33.0
OOBA-1	1-3	Tofb-1	10.9	6.9
	1-3		22.2	12.4
	1-3		44.7	23.4
OOBA-1	1-4	Tofb-1	15.8	10.8
	1-4		27.2	18.1
	1-4		50.5	31.7
OOBA-1	1-6	Tofb-1	24.2	13.3
	1-6		47.0	23.7
OOBA-1	1-7	Tofb-1	22.9	19.0
	1-7		46.7	37.0

** clay film values in italics



line slope = 0.5218
 phi = 27.6 degrees

Figure 9



Mr. Robert White
Geosciences Department
Pacific Gas & Electric Company
245 Market Street, Rm. 421-N4C
San Francisco, CA 94105

File - 24

November 5, 2001

Re: Completion of Data Reports (formerly appendices)

Dear Rob:

This letter transmits to Geosciences the following Diablo Canyon ISFSI Data Reports (formerly called appendices) that were prepared under the WLA Work Plan, Additional Geologic Mapping, Exploratory Drilling, and Completion of Kinematic Analyses for the Diablo Canyon Power Plant Independent Spent Fuel Storage Installation Site, Rev. 2 (11/28/00) using data collected under that Work Plan and a second WLA Work Plan, Additional Exploratory Drilling and Geologic Mapping for the ISFSI Site, Rev. 1 (9/21/01).

Diablo Canyon ISFSI Data Report A - Geologic Mapping in the Plant Site and ISFSI Site Areas, Rev. 0, November 5, 2001, November 5, 2001, prepared by J. Bachhuber, 42 p.

Diablo Canyon ISFSI Data Report B - Borings in ISFSI Site Area, Rev. 0, November 5, 2001, prepared by J. Bachhuber, 244 p.

Diablo Canyon ISFSI Data Report C - 1998 Geophysical Investigations at the ISFSI Site Area, (Agabian Associates and GeoVision), Rev. 0, November 5, 2001, prepared by J. Bachhuber, 84 p.

Diablo Canyon ISFSI Data Report D - Trenches in the ISFSI Site Area, Rev. 0, November 5, 2001, prepared by J. Bachhuber, 66 p.

Diablo Canyon ISFSI Data Report E - Borehole Geophysical Data (NORCAL Geophysical Consultants, Inc.), Rev. 0, November 5, 2001, prepared by C. Brankman, 303 p.

Diablo Canyon ISFSI Data Report F - Field Discontinuity Measurements, Rev. 0, November 5, 2001, prepared by J. Bachhuber and C. Brankman, 85 p.

Diablo Canyon ISFSI Data Report G - Soil Laboratory Test Data (Cooper Testing Laboratory), Rev. 0, November 5, 2001, prepared by J. Sun, 63 p.

Diablo Canyon ISFSI Data Report H - Rock Strength Data and GSI Sheets, Rev. 0, November 5, 2001, prepared by J. Bachhuber, 37 p.

Diablo Canyon ISFSI Data Report I - Rock Laboratory Test Data (GeoTest Unlimited), Rev. 0, November 5, 2001, prepared by J. Sun, 203 p.

Diablo Canyon ISFSI Data Report J - Petrographic Analysis and X-Ray Diffraction of Rock Samples (Spectrum Petrographics, Inc.), Rev. 0, November 5, 2001, prepared by J. Bachhuber, 204 p.

Diablo Canyon ISFSI Data Report K - Petrographic and X-Ray Diffraction Analyses of Clay Beds (Schwein/Christensen Laboratories, Inc.), Rev. 0, November 5, 2001, prepared by J. Bachhuber, 36 p.

In addition to the revisions of those reports required under the various Work Plans, Mr. Scott Lindvall, the WLA ITR for the ISFSI project, has performed independent technical reviews of the Diablo Canyon ISFSI Data Reports as part of his review of Calculation Package GEO.DCPP.01.21, Analysis of Bedrock Stratigraphy and Geologic Structure at the DCPD ISFSI Site. He finds that the reports clearly and accurately compile and organize the data.

Mr. Albert Tafoya from the Diablo Canyon ISFSI Project Office in San Luis Obispo, Mr. Dale Marcum, NQS Technical Oversight for the project, and William Page of your office provided comments on the August versions of the Diablo Canyon ISFSI Data Reports (formerly called appendices) and their comments have been addressed.

These reports are submitted to you as per the PG&E Geosciences Department Calculation Procedure GEO.001, Rev. 04 (10/10/01).

We look forward to any comments you may have.

Sincerely,
WILLIAM LETTIS & ASSOCIATES, INC.



Robert C. Witter
Project Manager

CC: William Page

ROCK ENGINEERING

Course notes by Evert Hoek



Shear strength of planar surfaces

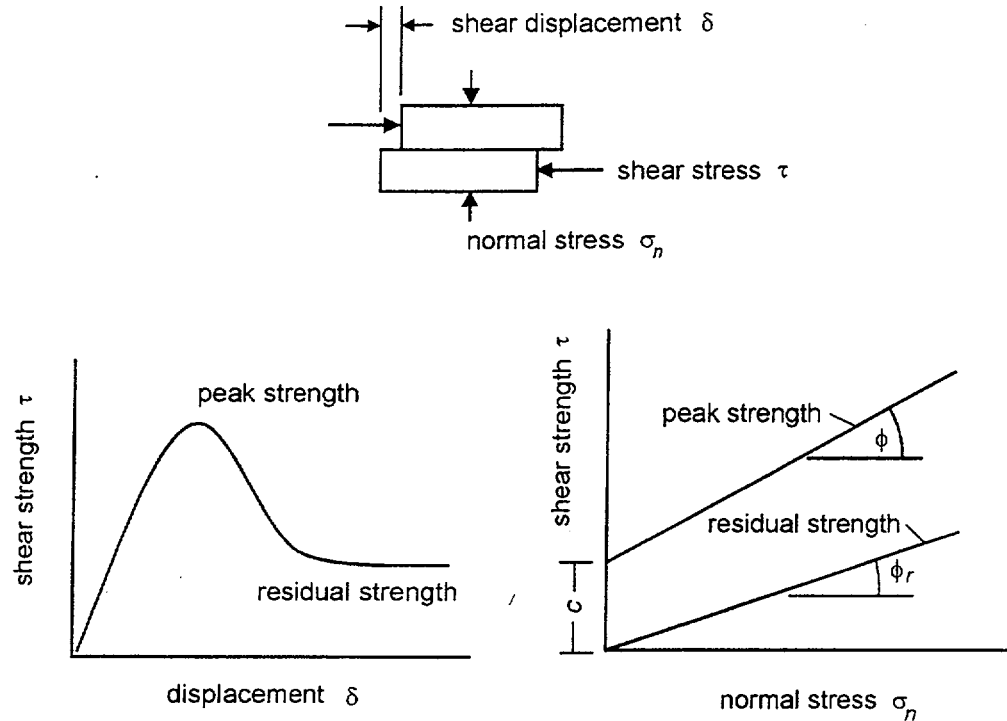


Figure 4.1: Shear testing of discontinuities

In the case of the residual strength, the cohesion c has dropped to zero and the relationship between ϕ_r and σ_n can be represented by:

$$\tau_r = \sigma_n \tan \phi_r \quad (4.2)$$

where ϕ_r is the residual angle of friction.

This example has been discussed in order to illustrate the physical meaning of the term cohesion, a soil mechanics term, which has been adopted by the rock mechanics community. In shear tests on soils, the stress levels are generally an order of magnitude lower than those involved in rock testing and the cohesive strength of a soil is a result of the adhesion of the soil particles. In rock mechanics, true cohesion occurs when cemented surfaces are sheared. However, in many practical applications, the term cohesion is used for convenience and it refers to a mathematical quantity related to surface roughness, as discussed in a later section. Cohesion is simply the intercept on the τ axis at zero normal stress.

The basic friction angle ϕ_b is a quantity that is fundamental to the understanding of the shear strength of discontinuity surfaces. This is approximately equal to the residual friction angle ϕ_r but it is generally measured by testing sawn or ground rock surfaces. These tests, which can be carried out on surfaces as small as 50 mm × 50 mm, will produce a straight line plot defined by the equation :

$$\tau_r = \sigma_n \tan \phi_b \quad (4.3)$$

WLA

William Lettis & Associates, Inc.

1777 Botelho Drive, Suite 262, Walnut Creek, California 94596
Voice: (925) 256-6070 FAX: (925) 256-6076

Robert K. White
PG&E Geosciences
P.O. Box 770000,
Mail Code N4C
San Francisco, CA 94177

November 19, 2001

RE: Re-confirmation of Direct Shear Test Classification Table

Rob:

Per your request, I have performed an additional review of direct shear sample rock classifications and the "Appendix I Direct Shear Test Sample Classification" table, dated June 12, 2001, that I prepared and sent to you via email on June 19, 2001. As you pointed out during our telephone discussion of November 16, 2001, four of the rock samples from boring 00BA-1 (samples 1-2, 1-3, 1-4, and 1-6) were incorrectly classified as sandstone, and instead should be classified as dolomite. The sandstone classification was in conflict with the detailed boring logs and summary logs in Data Report B. In addition to correction of rock classifications for these samples, we have also corrected classification for boring O1-G sample No. 23 that should be classified as "friable" rock. I have attached a four-page edited table including these revisions.

Please make the corrections in tables and references in Data Report I, and perform a re-evaluation of the rock test data for possible implications for the engineering analyses.

Please call me if you have any questions regarding this letter or need additional information.

Sincerely,

WILLIAM LETTIS & ASSOCIATES, INC.

Jeff Bachhuber, C.E.G.
Principal Geologist-ISFSI Project Geologist

Attachment: 4-page table, "Direct Shear Test Summary", revised 11/19/01

Attachment A

Appendix I Direct Shear Test Sample Classification

						Modeled Condition		
						Rock-Rock Surface	Clay-Rock or Clay Coating	Clay bed/seam (>1/4" thick)
Geo Test Lab	Sample No.	Boring	Depth	Bedrock Type and Unit	Geologic Description of Discontinuity	Laboratory Description		
	20	01-B	48.8'	Altered clayey dolomitic sandstone in contact with sandstone, fine-to medium-grained (Tofb-2)	Bonded 40° contact, irregular, between altered and non-altered rock *irregular clay-coated shear surface on post-test sample, shear partly through weak rock.	Slightly wavy intact contact between hard dolomite and soft clayey altered dolomite		X
	23	01-C	41.4'	Dolomitic sandstone to semi-friable dolomitic sandstone, medium-to coarse-grained (Tofb-2)	De-bonded 20° Fault plane with clay-coated slickensides.	Very thin clay coated, slickensided joint in gray, medium-grained sandstone. *Joint slightly disturbed during preparation. Actual break deviated from intended joint plane.		X
	24	01-C	44.3'	Cemented dolomitic sandstone, medium-grained (Tofb-2)	Partly bonded 30° joint plane	Wavy lightly bonded joint with thin, tan clay coating in tan medium-grained sandstone		X ?
	29	01-E	51.8'	Cemented dolomite fine-grained (Tofb-1)	Mechanical break 0-5° along possible bedding lamination	Planar, well-mated bedding joint in tan fine-to medium-grained sandstone.	X bddg.	

08 ft. SA Rod

GE O.D.M.P. 01.18 Rev. 2

Appendix I Direct Shear Test Sample Classification

						Modeled Condition		
						Rock-Rock Surface	Clay-Rock or Clay Coating	Clay bed/seam (>1/4" thick)
Geo Test Lab	Sample No.	Boring	Depth	Bedrock Type and Unit	Geologic Description of Discontinuity	Laboratory Description		
	31	01-F	117'	Cemented dolomite, med. grained in contact with friable, med.-to coarse-grained clayey sandstone (Tofb-1a/Tofb-2a)	De-bonded joint interface 8-12" between harder and softer rock with 1 cm thick clay seam *irregular clayey seam with multiple clay shear surfaces	Tan, sandy, soft clay seam (1/2-1 inch thick) in tan, fine-to medium-grained clayey sandstone. *Sample extruded sideways under load. Separation surface is not shear surface.		X
	33 (discard?)	01-F	118.3	Friable clayey medium-to coarse grained sandstone in contact with cemented medium-grained sandstone. (Tofb-2a/Tofb-2)	Debonded joint interface 65-70" between friable and hard rock *Irregular clay coated sheared surface on post-test sample, not a single planar joint	Gray clay seam (0 to 0.05-inch thick) in gray, med.-grained weak clayey sandstone *Test may not have sheared through clay "seam", pulled apart through chewed up rock	X	
	34 (discard?)	01-CTFA	32.6'	Medium-grained sandstone in contact with silty clay (Tofb-2)	Partly debonded contact, 5", between cemented sandstone and silty clay bed/zone with polished clay surface *Very irregular shear surface not developed along a planar joint	Contact between tan, sandy clay and tan, clayey fine-to medium-grained sandstone. *Part of sample collapsed and sample underwent large rotations during testing. Lab recommended that the sample not be tested due to limited ability to clamp sample.	X	

off to the road

GED.DCWP.01.18 Rev 2

Appendix I Direct Shear Test Sample Classification

						Modeled Condition		
						Rock-Rock Surface	Clay-Rock or Clay Coating	Clay bed/seam (>1/4" thick)
Sample No.	Boring	Depth	Bedrock Type and Unit	Geologic Description of Discontinuity	Laboratory Description			
35 (discard?)	01-H	94.5'	Friable, medium-grained sandstone (Tofb-2a)	Partly debonded low angle (5°±) clay-filled joints possibly along bedding. *Very irregular shear surface involving multiple irregular, subparallel clayey surfaces not developed along a single planar joint	Irregular dark gray clay-filled joint (0.1 to 0.4-inch thick) in gray clayey medium-grained sandstone. *Sample compressed during final testing stages causing steel-to-steel shear box contact		X	
36	01-I	174'	Cemented, medium-grained dolomite, laminated (Tofb-1)	Debonded bedding plane joint/mechanical break, flat (0°)	Planar bedding joint in tan, thinly bedded, very fine-grained dolomitic sandstone. *Leaf fossil observed on joint surface	X bddg.		
37	01-I	168.5'	Cemented dolomite, medium-grained, laminated-stiff clay (Tofb-1)	Debonded joints/bedding partings along 10° clay seams 1/8" to 1/4" thick.	Bedding plane joint in tan, fine-grained dolomitic sandstone with a thin lamination and clay coating *Sample rotated and joint sides probably ground into contact through the clay.		X	

page 17 of 30

GEO.DCPR.01.18 Rev 2

Appendix I Direct Shear Test Sample Classification

						Modeled Condition		
						Rock-Rock Surface	Clay-Rock or Clay Coating	Clay bed/seam (>1/4" thick)
Geo Test Lab	Sample No.	Boring	Depth	Bedrock Type and Unit	Geologic Description of Discontinuity	Laboratory Description		
	39B	01-I	130.4'	Cemented, fine-to medium grained dolomite in contact with stiff clay (Tofb-1)	Partly bonded, low angle contact, 10°, between hard dolomite and 1/2-1cm thick clay bed. *Irregular failure surface partly in rock, partly along clayey discontinuous joint surfaces.	Tan clay seam (0.1 to 0.2-inch thick) in tan fine-grained dolomitic sandstone. *Sample slid on soft clay		X
	40B	01-I	88.8'	Cemented, fine-grained dolomite, laminated (Tofb-1)	Debonded bedding plane joint, 20°, subparallel to laminations	Planar bedding joint in tan fine-grained dolomitic sandstone	X bddg.	
	41A	01-I	45.6'	Cemented fine grained dolomite, laminated (Tofb-1)	Partly bonded low angle clay/bed-rock contact, 10-15°, clay 2cm thick, tight contact. Clay not observed in returned sample (removed?)	Tan clay seam about 3/4-inch thick in tan, fine-grained sandstone *Sample rocked and developed open fissures during shearing, slickensides observed on sample surface		X

0.5 to 1.0 ft

GEO-DUPP.01.18 Rev 2

Appendix I Direct Shear Test Sample Classification

Geo Test Lab						Modeled Condition		
						Rock-Rock Surface	Clay-Rock or Clay Coating	Clay bed/seam (>1/4" thick)
Sample No.	Boring	Depth	Bedrock Type and Unit	Geologic Description of Discontinuity	Laboratory Description			
41B	01-I	46.1'	Cemented, fine-grained dolomite, laminated (Tofb-1)	Debonded, low angle bedding joint, 20°, between rock surfaces	Planar bedding joint in tan fine-grained dolomitic sandstone	X bddg.		
1-1	00BA-1	17.8-18.6'	Cemented, fine-to medium grained dolomite (Tofb-1)	Debonded joint, 30-40°, rock-rock surfaces, oxidized	poorly mated rough joint in mottled tan and brown dolomite (?) with black oxide and light brown coating	X		
1-2	00BA-1	34-34.4'	Cemented, fine-to medium grained dolomitic sandstone (Tofb-2)	Debonded, steep, wavy joint, 64° rock-rock contact	Rough, well-mated joint in tan dolomite (?) with black and brown oxide staining	X		
1-3	00BA-1	36.9-37.6'	Cemented, fine-to medium grained dolomitic sandstone (Tofb-2)	Debonded joint, 12°, subparallel to bedding (?) laminations, rock-rock contact	Bedding plane in dark brown dolomite (?)	X bddg.		

page 29 of 30

GE0.DUPP.01.18 Rev 2

Appendix I Direct Shear Test Sample Classification

						Modeled Condition		
						Rock-Rock Surface	Clay-Rock or Clay Coating	Clay bed/seam (>1/4" thick)
Sample No.	Boring	Depth	Bedrock Type and Unit	Geologic Description of Discontinuity	Laboratory Description			
1-4	00BA-1	41.7-42.2'	Cemented, fine-to medium grained dolomitic sandstone (Tofb-2)	Debonded, mechanical break subparallel to faint bedding (?) laminations, 12°, rock-rock contact	Mechanical break (possibly along bedding) in fine-grained tan dolomitic sandstone	X bddg.		
1-6	00BA-1	88.2-89.5'	Cemented, fine-to medium grained dolomitic sandstone (Tofb-2)	Debonded joint, 21°, rock-rock contact	Moderately rough well mated joint with a thin flakey coating in tan dolomitic sandstone	X		
1-7	00BA-1	141.4-142.5'	Cemented, fine-to medium grained dolomite (Tofb-1)	Steep wavy joint, 55°, rock-rock contact	Wavy poorly mated joint with a black oxide coating (probably clay) in tan dolomitic sandstone	X		
1-18	00BA-1	55.3-56.5'	Cemented, fine-grained dolomite-clay bed (Tofb-1)	Low angle contact between dolomite and 0.7-foot thick stiff clay bed. 5-15°, tight and relatively planar clay-rock contacts	Tan rock/clay seam interface with a dark brown staining in the vicinity of the interface			X

OK to OK sand

GEO-DUPP. 01.18 Rev 2

Title: Calculation Cover Sheet

PACIFIC GAS AND ELECTRIC COMPANY
GEOSCIENCES DEPARTMENT
CALCULATION DOCUMENT

Calc Number: DEO.DCPP. 01.19

Revision: 1

Date: November 6, 2001

No. of Calc Pages: 92

Verification Method: A

No. of Verification Pages: 1

TITLE Development of Strength Envelopes for Jointed Rock Mass at DCPD ISFSI using Hoek-Brown Equations

PREPARED BY

Jeffrey L. Bachhuber
Jeffrey L. Bachhuber
Printed Name

DATE November 6, 2001

William Lettis & Associates, Inc.
Organization

VERIFIED BY

Robert K. White
Robert K. White
Printed Name

DATE 11/12/01

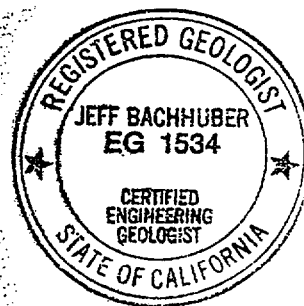
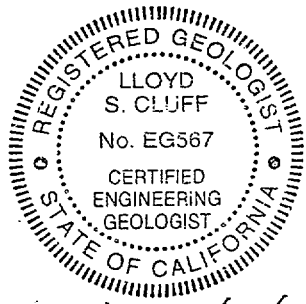
PG&E Geosciences Department
Organization

APPROVED BY

Lloyd S. Cluff
Lloyd S. Cluff
Printed Name

DATE 11/13/01

Geosciences
Organization



Title: Record of Revision

Calc Number: GEO DCPD 01.19

**Development of strength envelopes for jointed rock mass at DCPD ISFSI
Using Hoek-Brown equations**

Rev. No.	Reason for Revision	Revision Date
0	Original Report issued for signatures	8/8/01
1	Added text to Section 7.0, edited text, added 50° line to strength envelopes	11/6/01

DCPP ISFSI

CALCULATION PACKAGE GEO.DCPP.01.19

Development of Strength Envelopes for Jointed Rock Mass

At DCPD ISFSI Using Hoek-Brown Equations

DCPP ISFSI
CALCULATION PACKAGE GEO.DCPP.01.19
Development of Strength Envelopes for Jointed Rock Mass
At DCPD ISFSI Using Hoek-Brown Equations

Table of Contents

	<u>Page</u>
1.0 PURPOSE	6
2.0 INPUTS	8
3.0 ASSUMPTIONS	9
4.0 METHOD	9
5.0 SOFTWARE	12
6.0 ANALYSIS	13
7.0 RESULTS	13
8.0 CONCLUSIONS	14
9.0 REFERENCES	14

List of Tables

Table 19-1. GSI and m_i Values for Dolomite (Tof_{b-1})	17
Table 19-2. GSI and m_i Values for Sandstone (Tof_{b-2})	20
Table 19-3. Unconfined Compressive Strength of Dolomite and Sandstone, ISFSI Site Area	21

List of Figures

Figure 19-1. Material index (m_i) value for rocks in ISFSI site area using the Hoek field classification chart.....	22
Figure 19-2. Field estimates of Hoek-Brown geologic strength index for rocks in ISFSI site area.	23
Figure 19-3. Curve D-1	24
Figure 19-4. Curve D-2	25
Figure 19-5. Curve D-3	26
Figure 19-6. Curve D-4	27
Figure 19-7. Curve SS-1	28
Figure 19-8. Curve SS-2	29
Figure 19-9. Curve SS-3	30
Figure 19-10. Curve SS-4	31

Table of Contents (continued)

Page

List of Attachments

Attachment 1	Rock engineering course notes, chapter 11 (version dated Nov. 27, 2000) E. Hoek, 2000.	32
Attachment 2	Hoek-Brown criterion spreadsheet verification runs.	58
Attachment 3	ISFSI site Hoek-Brown criterion shear strength calculation runs.	66

DCPP ISFSI GEOTECHNICAL CALCULATION PACKAGE

Title: Development of strength envelopes for jointed rock mass at DCPD ISFSI using Hoek-Brown equations

Calc Number: GEO.DCPP.01.19

Revision: Rev. 1

Author: Jeff L. Bachhuber

Date: November 7, 2001

Verifier: Robert K. White

1.0 PURPOSE

This Calculation Package documents the development of in situ rock mass shear strength estimates using the Hoek-Brown criterion (Hoek, 2000) for in situ dolomite (geologic map unit Tof_{b-1}) and sandstone (unit Tof_{b-2}) bedrock at the ISFSI and CTF Sites, and within the slope above the ISFSI pads as part of the assessment of subsurface conditions required under William Lettis & Associates, Inc. (WLA) Work Plan "Additional Geologic Mapping, Exploratory Drilling, and Completion of Kinematic Analyses for the Diablo Canyon Power Plant, Independent Spent Fuel Storage Installation Site", Rev. 2, November 28, 2000.. The Hoek-Brown criterion is described in an online document entitled "Rock Engineering Course Notes" by Evert Hoek, with a latest revision date of December 2000. Excerpts from Chapter 11, "Rock Mass Properties" of the course notes that describe the Hoek-Brown criterion for development of rock strength envelopes are included in Attachment 1 of this Calculation Package. The referenced chapter also contains the equations used for derivation of the Hoek-Brown shear strength envelopes.

The Hoek-Brown criterion is an empirically-based approach that develops non-linear shear strength envelopes for a rock mass, and accounts for the strength influence of discontinuities (joints, bedding planes, faults), mineralogy and cementation, rock origin (e.g., sedimentary or igneous), and weathering. The resulting rock mass shear strength envelopes are used for evaluation of the ISFSI pads and CTF facility foundation properties, and for stability analyses of potential bedrock failures within jointed, confined rock at the ISFSI site. The Hoek-Brown methodology is intended to be used for rock masses in which there is a sufficient density of intersecting discontinuities, with similar

surface characteristics, such that isotropic behavior involving failure along multiple discontinuities can be assumed. The method is not intended for use when failure is anticipated to occur largely through intact rock blocks, or along discrete, weak, continuous failure planes (such as weak bedding interfaces). The structure (or failure) geometry must be relatively large with respect to individual block size. The rock mass conditions and relative size differences between rock blocks, potential deep-seated rock slide masses, and ISFSI/CTF foundations for which the Hoek-Brown criterion is being applied are appropriate, and meet these rock mass requirements.

Block sizes in the rock mass exhibit a significant range, but typically are on the order of 2 to 3 feet and locally up to about 14 feet in maximum dimension, and exhibit irregular intersections and low persistence (refer to William Lettis & Associates, Inc., 2001, Diablo Canyon ISFSI Data Report F). Potential deep-seated rock slide failures are on the order of hundreds of feet in dimension.

The Hoek-Brown criterion is appropriate at the ISFSI site for the fractured, confined rock mass below surficial zones of weathering and stress relief. A zone of surficial dilated and weathered rock was observed in exploratory trenches and borings extending about 4 feet deep (refer to boring logs, trench logs, and Optical Televiewer logs in William Lettis & Associates, Inc., 2001, Diablo Canyon ISFSI Data Reports B, D, and E, respectively), and conservatively estimated to extend to a maximum depth of about 20 feet below the ground surface or behind planned excavation slopes. Unconfined, stress-relieved rock in the near surface and in future excavation cuts, is free to dilate along pre-existing discontinuities. The shear strength of shallow rock within the dilated surficial zone is estimated using the method of Barton and Choubey (1977) in Calculation Package GEO.DCPP.01.20 for modeling potential shallow wedge and topple sliding that could occur along discrete discontinuity surfaces in cut slopes.

The Hoek-Brown criterion is not appropriate for estimating the shear strength of localized zones of very weak to weak, friable dolomite (geologic map unit Tof_{b-1a}) and friable sandstone (map unit Tof_{b-2a}) that were observed in some test pits, exploratory borings, and road cuts. Typically, the friable rocks are relatively massive with poorly-developed discontinuities and weak cementation, and shear strength appears to be largely controlled by cementation strength of rock blocks, rather than the strength along discontinuities. Therefore, the use of the Hoek-Brown criterion is restricted to the relatively harder, stronger, dolomite and sandstone. Laboratory multi-stage triaxial testing was used to

develop shear strength envelopes for the friable rock zones, as described in Calculation Package GEO.DCPP.01.16. Furthermore, the Hoek-Brown criterion is not applicable for determination of shear strength along distributed clay beds and seams in the rock mass that may be laterally persistent. The shear strength of discrete clay beds in the rock mass was evaluated by laboratory testing of clay samples as described in Calculation Package GEO.DCPP.01.31.

2.0 INPUTS

The Hoek-Brown method uses three input parameters to estimate rock mass strength: (1) uniaxial compressive strength (U_c) of intact rock blocks; (2) material index (m_i) related to rock mineralogy, cementation, and origin (Figure 19-1); and, (3) Geological Strength Index (GSI) that factors the intensity and surface characteristics of rock mass discontinuities (Figure 19-2).

Rock mass field and laboratory data are the basis for the Hoek-Brown spreadsheet parameters. These data were obtained by field examination and classification of in situ rock mass exposures, mostly from exploratory trenches (William Lettis & Associates, Inc., 2001, Diablo Canyon ISFSI Data Report H) and laboratory testing of diamond core boring samples (William Lettis & Associates, Inc., 2001, Diablo Canyon ISFSI Data Report I). These data were compiled and evaluated using Microsoft Excel spreadsheet functions. Data tables for GSI and m_i are presented in Tables 19-1 and 19-2. Table 19-3 summarizes U_c data used for the spreadsheet input as documented in Calculation Package GEO.DCPP.01.17. The following input values were used.

Dolomite: U_c range 13 to 60 Megapascals (MPa), mean 32.1 MPa, standard deviation 14.7 MPa;
GSI range 35 to 72, average 55.7, standard deviation 9.3;
 m_i range 12 to 20, average 15.4, standard deviation 2.0.

Sandstone: U_c range 8 to 33 MPa, mean 21.6 MPa, standard deviation 9.3 MPa;
GSI range 60 to 69, average 64.8, standard deviation 3.1;
 m_i range 16 to 19, average 17.8, standard deviation 1.0.

3.0 ASSUMPTIONS

1. Rock mass shear strength is dependant on confining pressure, and the non-linear failure envelope predicted by the Hoek-Brown failure criterion closely approximates the rock mass strength at the DCPD ISFSI. This assumption is generally reasonable as described in Attachment 1.
2. In situ characterization of rock mass properties at the DCPD ISFSI site (e.g. lithology, GSI, m_i) represents the mean, minimum, and maximum range of properties in the in situ rock mass. This assumption is reasonable because of the large set of field observations as documented in William Lettis & Associates, Inc., 2001, Diablo Canyon ISFSI Data Report H.
3. Unconfined compression tests on rock core obtained from the ISFSI site area and CTF sites capture the range in strength for intact rock blocks at the site, and appropriately model in situ rock block strength. This assumption is reasonable as documented in GEO.DCPD.01.17.
4. Rock below the uppermost stress-relieved surface zone is sufficiently confined to force failure surfaces to propagate around rock blocks and not cause significant dilation of the rock mass and localization of failure along any single, persistent, continuous weak zone as described in Attachment 1.

4.0 METHOD

The three rock mass input parameters are processed either by a spreadsheet or by hand calculations, to develop non-linear stress-strain failure envelopes using empirically- and laboratory-based curve fitting equations developed by Hoek and Brown (Hoek, 2000). The stress-strain failure envelopes are established by fitting a linear regression curve to a series of synthetic triaxial shear test values generated, based on the input parameters and established stress range.

The step-by-step methodology used for generation of the Hoek-Brown failure envelopes is listed below:

- Step 1. Compilation and statistical evaluation of input U_c , m_i , and GSI data presented in William Lettis & Associates, Inc., 2001, Diablo Canyon ISFSI Data Reports H and I;
- Step 2. Verification of Hoek (2001) Excel spreadsheet;
- Step 3. Data entry into the Hoek (2001) Excel spreadsheet; and,
- Step 4. Preparation of summary failure envelope graphs.

Step 1

For the ISFSI project, uniaxial strength (U_c) is based on laboratory testing of intact rock core samples obtained from diamond core exploratory borings made in the ISFSI and CTF pads, and the slope above the ISFSI pad. The laboratory tests were performed by GeoTest Unlimited, Ltd. (Nevada City, California), and are presented in William Lettis & Associates, Inc., 2001, Diablo Canyon ISFSI Data Report I. Reported U_c strength values were segregated according to rock type (dolomite or sandstone), and compiled in Table 19-3 in this Calculation Package, and as documented in Calculation Package GEO.DCPP.01.17. The Excel spreadsheet functions were used to calculate the U_c mean and one-sigma standard deviation values separately for dolomite and sandstone. The mean and standard deviation range of values of U_c were used for input into the Hoek-Brown equations.

The material indices (m_i) for ISFSI site rocks were determined by comparing the rock mineralogical and sedimentological characteristics against values for similar rock types presented in a table by Hoek (1998), shown in Figure 19-1 of this Calculation Package. Values of m_i were estimated for rocks exposed in exploratory trenches at the ISFSI site, and recorded on field data sheets included in William Lettis & Associates, Inc., 2001, Diablo Canyon ISFSI Data Report H. Tables 19-1 and 19-2 of this Calculation Package summarize the m_i values, and present the mean and one-sigma standard deviations for the tabulated values. The mean and standard deviation range of m_i values were used for input in the Hoek-Brown analyses.

The Geological Strength Index (GSI) values were estimated for dolomite and sandstone bedrock exposures in exploratory trenches and road cuts, and recorded on field data sheets in William Lettis & Associates, Inc., 2001, Diablo Canyon ISFSI Data Report H. GSI values were estimated by visual and descriptive comparison of rock mass structure and discontinuity surface condition against a classification table developed by Hoek-

Brown (Hoek, 2000), and are presented in Figure 19-2, and tabulated in Tables 19-1 and 19-2.

Values of m_i and GSI were estimated by each member in a two- to three-person team of field geologists, and the average values were recorded on field sheets. This method served to reduce bias, and improve consistency in evaluating the rock mass.

Step 2

Examples of strength parameters derived using the Hoek-Brown criterion presented in Hoek (2000) were used to verify the Hoek (2001) Excel spreadsheet obtained from Dr. Hoek (Hoek, email transmittal June 6, 2001). Input parameters from the problems were entered into the spreadsheet, and the output was compared. The spreadsheet successfully produced correct solutions. Copies of the problem pages and spreadsheet verification output files are included in Attachment 2.

Step 3

Data were entered into the verified Hoek (2001) Excel spreadsheet by Jeff Bachhuber of WLA. Individual workbook files were established for dolomite and sandstone analyses, and separate spreadsheets were prepared within each workbook to evaluate the sensitivity of shear strength to variations in the input parameters. The mean and standard deviation spread of values were entered for each of the three input parameters (U_c , GSI, m_i).

Step 4

The Hoek spreadsheet output files were used to develop a series of stress-strain failure envelopes for the rock. Each failure envelope was first plotted in Microsoft Excel, and then re-plotted in the program SPSS DeltaGraph to obtain exact 1:1 vertical and horizontal scales for accurate plotting of the failure envelopes and evaluation of angle of internal friction (ϕ angle) and cohesion intercept (c). Failure envelopes were grouped into sets of graphs as follows:

- Comparison of strength ranges; upper bound, mean, and lower bound
- Comparison of GSI ranges; upper bound, mean, and lower bound
- Comparison of m_i ranges; upper bound, mean, and lower bound
- Comparison of U_c ranges; upper bound, mean, and lower bound

5.0 SOFTWARE

Statistical analyses and derivation of the Hoek-Brown shear strength failure envelopes were performed using Microsoft Excel and plotted using SPSS DeltaGraph software on a DELL Inspiron model 8000 laptop computer. The software specifications are as follows:

Microsoft Windows ME - Version 4.90.3000, 2000

Microsoft Excel - Version 9.03821 SR-1, 2000

SPSS DeltaGraph - Version 4.0.5C, 1997

The Hoek-Brown calculations were performed using the most current version of a spreadsheet developed by E. Hoek, which was transmitted electronically to Jeff Bachhuber by Dr. Hoek (Hoek, electronic transmittal, June 6, 2001). The spreadsheet was verified as described in Step 2 above, using method 1 of GEO.001 Section 4.2.2, identical copies were made for use in the analyses, and the following were identified:

- a) Spreadsheet name: hoek0.19rmstrrev1-dol.xls (for dolomite rock parameters), and hoek0.19rmstrrev1-ss.xls (identical version for sandstone rock parameters)
- b) Spreadsheet version: (not applicable)
- c) Spreadsheet revision: 7/11/01 (both spreadsheets)
- d) Computer platform compatibility: Windows ME
- e) Spreadsheet capabilities and limitations: The spreadsheet generates shear strength failure envelopes using the Hoek-Brown criteria. The spreadsheet is a modified version of the spreadsheet described in Attachment 1. The modified spreadsheet contains a revised curve fitting equation for low stress conditions commonly encountered for analyses of slope stability and shallow foundations. Strength envelopes are valid when ranges of input variables are within those described in Attachment 1.
- f) Spreadsheet test cases: described in Attachment 2.
- g) Instructions for use: input values for variables U_c (σ_{ci}), m_i , GSI, depth of failure surface, and unit weight as described in Attachment 1.
- h) Spreadsheet author: Jeff Bachhuber
- i) Identification of individual responsible for controlling the software or executables: see Geosciences QA procedure CF2.GEI.
- j) Change control: see Geosciences QA procedure CF2.GEI.
- k) Verification methods used: method 1 as shown in Attachment 2

6.0 ANALYSIS

Multiple iterations of the Hoek spreadsheet were performed to evaluate the differences in shear strength between dolomite and sandstone, and to assess the sensitivity of shear strength to variations in the three input parameters (U_c , GSI, m_i). Spreadsheet output files are included in Attachment 3, as well as calculated shear strength failure envelopes. The output files and failure envelopes were visually compared against each other, to ascertain the influence of rock lithology and variation in input parameters to rock mass shear strength, and results of this comparison follow.

7.0 RESULTS

The calculated shear strength envelopes developed by the Hoek-Brown Excel spreadsheet were plotted in the DeltaGraph program for presentation of results. The final failure envelope plots are presented in Figures 19-3 to 19-10. These shear strength envelopes show the range in strength related to the mean and one sigma variations for the three input parameters (U_c , GSI, m_i), and the differences in strength between dolomite and sandstone.

All failure envelopes exhibit typical non-linear shapes that are characteristic of jointed, relatively sound rock. The estimated rock mass shear and compressive strengths are considerably lower than the laboratory test uniaxial compressive strengths for intact rock blocks. Derived rock mass strength properties are similar to those reported in case studies by Hoek (2000) for "very poor" to "average" rock mass conditions.

Comparison of the shear strength envelopes shows that the dolomite is somewhat stronger than the sandstone, and that the sandstone shear strength envelope flattens more rapidly with increasing confining stress (more-rapid reduction in strength rate), compared to the dolomite. The in situ modulus predicted by the Hoek-Brown spreadsheet is considerably lower for the sandstone than for the dolomite, suggesting that the sandstone is more deformable. This corresponds to the observed field characteristics of the rock: dolomite generally appears to be significantly harder and more brittle than the sandstone, and commonly is stronger in hand sample. The shear strength of both the dolomite and the sandstone appears to be more sensitive to changes in U_c strength of the rock blocks, and GSI, than m_i , although the results are influenced by the statistical variation in the input parameters. It is observed that the mean Hoek-Brown strength envelopes for

dolomite (Figure 19-3) and sandstone (Figure 19-7) plot higher than a line inclined at 50 degrees from horizontal and passing through the origin at all calculated normal stresses. The lower-bound (low probability) Hoek-Brown envelopes cross below this line in some cases, thus making the line unconservative as a strength envelope, but only at normal stresses equivalent to nearly 250 feet of overburden in the dolomite and over 350 feet of overburden in the sandstone. Because depths of identified and analyzed potential rock slides along clay beds daylighting at or above the ISFSI site are not likely to exceed these values (GEO.DCPP.01.21, Fig. 21-22), the 50-degree line is shown as the lower-bound strength envelope for all portions of failure planes in dolomite and sandstone rock for large-scale rock slides along clay beds.

8.0 CONCLUSIONS

The final shear strength failure envelopes for ISFSI site dolomite and sandstone calculated using the Hoek-Brown criterion are suitable for representation of the in situ rock mass strength and deformation properties for the following uses: (1) slope stability analyses of deep rock slide failures extending through the confined, jointed rock mass below the surficial stress relieved surface zone; and, (2) foundation evaluation and design for foundation elements that extend into undisturbed, confined, jointed rock below the ISFSI pads and CTF subgrade. Analyses should consider the entire range in strength (mean, upper and lower bound) shown by the failure envelope curves (Figures 19-3 to 19-10). The mean strength curves for the dolomite and the sandstone bedrock are believed to be appropriate for analyses of ISFSI pads foundation stability and deep-seated rock slope stability of the hillside above the pads.

A line inclined at 50 degrees and passing through the origin is observed to pass well below the mean strength curves for both rock types and is shown as the lower-bound strength envelope for purposes of slope stability analyses of deep rock slide failures along clay beds.

9.0 REFERENCES

Barton, N.R. and Choubey, V., 1977, The shear strength of rock joints in theory and practise: Rock Mechanics, Vol. 10 (1-2), pp. 1-54.

Hoek, E., 2001, electronic transmittal June 6, Excel spreadsheet for calculation of rock mass shear strength, in files.

Hoek, E., June 6, 2001, personal communication in files.

Hoek, E., 2000, Rock engineering course notes: on-line webpage document at www.rocscience.com, latest revision date December 2000.

Hoek, E., and Brown, E.T., 1988, The Hoek-Brown failure criterion - a 1988 update: Proceedings 15th Canadian Rock Mechanics Symposium, in, ed. Curran, J.H., Civil Engineering Department University of Toronto, pp. 31-38.

Microsoft Excel '98, Microsoft Corporation, Redmond, WA.

SPSS Delta Graph, 1997.

William Lettis & Associates, Inc., 2001, Letter to Robert White, PG&E Geosciences from Robert C. Witter, November 5, 2001, Completion of Data Reports transmitting Data Reports A through K to PG&E Geosciences Department;

Diablo Canyon ISFSI Data Report B - Borings in ISFSI Site Area, Rev. 0,
November 5, 2001, prepared by J. Bachhuber, 244 p.

Diablo Canyon ISFSI Data Report D - Trenches in the ISFSI Site Area, Rev. 0,
November 5, 2001, prepared by J. Bachhuber, 66 p.

Diablo Canyon ISFSI Data Report E, - Borehole Geophysical Data (NORCAL Geophysical Consultants, Inc.), Rev. 0, November 5, 2001, prepared by C. Brankman and J. Bachhuber, 350 p.

Diablo Canyon ISFSI Data Report F - Field Discontinuity Measurements, Rev. 0,
November 5, 2001, prepared by C. Brankman and J. Bachhuber, 85 p.

Diablo Canyon ISFSI Data Report H - Rock Strength Data and GSI Sheets, Rev. 0,
November 5, 2001, prepared by J. Bachhuber, 37 p.

Diablo Canyon ISFSI Data Report I - Rock Laboratory Test Data (GeoTest Unlimited), Rev. 0, November 5, 2001, prepared by J. Sun, 203 p.

Geosciences Calculation packages

- GEO.DCPP.01.16 Development of strength envelopes for non-jointed rock at DCPD ISFSI based on laboratory data, Rev. 1
- GEO.DCPP.01.17 Determination of mean and standard deviation unconfined compression strengths for hard rock at DCPD ISFSI based on laboratory tests, Rev. 1
- GEO.DCPP.01.20 Development of strength envelopes for shallow discontinuities at DCPD ISFSI using Barton equations, Rev. 0

- GEO.DCPP.01.21 Analysis of bedrock stratigraphy and geologic structure at the DCP
ISFSI, Rev. 0
- GEO.DCPP.01.31 Development of strength envelopes for clay beds at DCP ISFSI based
on field and laboratory data, Rev. 0

QA Documents

PG&E Quality Assurance Procedure GEO.001, Development and Independent
Verification of Calculations for Nuclear Facilities, Rev. 4

William Lettis & Associates Work Plan, Additional Geologic Mapping, Exploratory
Drilling, and Completion of Kinematic Analyses for the Diablo Canyon
Power Plant, Independent Spent Fuel Storage Installation Site, Rev. 2,
November 28, 2000.

Table 19-1. GSI and m_i Values for Dolomite (Tof_{b-1})

Trench	GSI Values ⁽¹⁾	m_i Constant Range ⁽²⁾
T-1	60 58 55 55 52.5	15-18
T-2A	69 68 68 66 66 65.5 64.5 64	14-15
T-3	65 65 55.5 47	14-16 15-17
T-4	66 62 60 56	14-15
T-5	69.5 66 65.5 64 52 44	15-18 14-16 15-18
T-6	70 66	14 -16
T-11A	60.5 45 42	nr
T-11B	45 45 40	14-15

Table 19-1. GSI and m_i Values for Dolomite (Tof_{b-1}) (Cont'd)

Trench	GSI Values (1)	m_i Constant Range (2)
T-12	55	14
	60	
	60	
	37	12
	40	
	42.5	
	42.5	
	45	
T-13	66	13-14
	65	
	61	
	57	
	55	
	54	
	53	
	52	
	52	
	51	
	50	
T-14A	60	14-15
	60	
	55	
	55	
	35	12
	37	
	37.5	
T-15	68	14-15
	66	
	61	
	45	
	47	
	48	
	48	
	50	
	50	
	52	
T-17A	50	18-20
	46	18
	45	

Table 19-1. GSI and m_i Values for Dolomite (Tofb-1) (Cont'd)

Trench	GSI Values (1)	m_i Constant Range (2)
T-19	58	nr
T-20A	55.5	15
T-20B	52.5 52.5 69 72	12-20
T-21	56	nr
Road Cut	60.5 61 66	nr
GSI Average = 55.7		m_i constant Average = 15.43⁽³⁾
GSI standard deviation = 9.3		m_i constant standard deviation = 2.0⁽³⁾

Data for GSI and m_i obtained from DCPD ISFSI Section 2.6 Topical Report Appendix H.

Notes:

- (1) GSI = Geologic Strength Index (Hoek, 2000); GSI values typically estimated at multiple localities within each trench for a given rock type.
- (2) m_i = Material Index Constant (Hoek, 2000); a single value or range of m_i values was typically assigned for the rock type exposed in each trench; nr = not recorded.
- (3) The average and standard deviation of the m_i constant were simply derived from the minimum and maximum values of each estimate. These statistics do not represent a rigorous attempt to weight the m_i values based on lineal feet of exposure for each range of m_i assigned in the field.

Table 19-2. GSI and m_i Values for Sandstone (Tof_{b-2})

Trench	GSI Values (1)	m_i Constant Range(2)
T-1	65	18-19
T-1	63	
T-1	62	
T-1	60	
T-17A	67	16-18
	68	
T-17B	61	18
	66	
	67	
	69	
GSI Average =	64.8	m_i constant Average = 17.8 ⁽³⁾
GSI Standard Deviation =	3.1	m_i constant standard deviation = 1.0 ⁽³⁾

Data for GSI and m_i obtained from DCPD ISFSI SAR Section 2.6 Topical Report, Appendix H.

Notes:

- (1) GSI = Geologic Strength Index (Hoek, 2000); GSI values typically estimated at multiple localities within each trench for a given rock type.
- (2) m_i = Material Index Constant (Hoek, 2000); a single value or range of m_i values was typically assigned for the rock type exposed in each trench; nr = not recorded.
- (3) The average and standard deviation of the m_i constant were simply derived from the minimum and maximum values of each estimate. These statistics do not represent a rigorous attempt to weight the m_i values based on lineal feet of exposure for each range of m_i assigned in the field.

Values obtained from ISFSI SAR Section 2.6 Topical Report Appendix H.

Table 19-3. Unconfined Compressive Strength of Dolomite and Sandstone, ISFSI Site Area

ISFSI Unconfined Compressive Strength				
Dolomite (psi)	(Mpa)	Sandstone (psi)	Sandstone (MPa)	
3702	26	2888	20	
2434	17	1113	8	
1834	13	4778	33	
6373	44	4504	31	
3504	24	2958	20	
5133	35	2543	18	
2625	18	3131	21.6	mean
5284	36	1349	9.3	Std. Dev.
7190	50			
4523	31			
8649	60			
mean	4659	32.1		
Std. Dev.	2126	14.7		

Notes: Laboratory test samples were obtained from diamond core borings at, and above, the ISFSI pads and at the CTF site.

Laboratory testing was performed by GeoTest Unlimited, Ltd. (Nevada City, CA); ISFSI Section 2.6 and at the CTF site.

psi - pounds per square inch; MPa - Megapascals

Data compiled from DCPD ISFSI SAR Section 2.6 Calculation Package 01.17.

Rock type	Class	Group	Texture			
			Coarse	Medium	Fine	Very fine
SEDIMENTARY	Clastic		Conglomerate (22)	Sandstone 19 Sandstone (18) (18)	Siltstone 9 Greywacke	Claystone 4
	Non-Clastic	Organic	Chalk 7 Coal (8-21)			
		Carbonate	Breccia (20)	Sparitic Limestone (10)	Micritic Limestone 8	
		Chemical	Gypstone 16 Anhydrite 13			
	METAMORPHIC	Non Foliated		Marble 9	Hornfels (19)	Quartzite 24
Slightly foliated		Migmatite (30)	Amphibolite 25 - 31	Mylonite (6)		
Foliated*		Gneiss 33	Schist 4 - 8	Phyllite (10)	Slate 9	
IGNEOUS	Light	Granite 33		Rhyolite (16)	Obsidian (19)	
		Granodiorite (30)		Dacite (17)		
	Dark	Diorite (28)		Andesite 19		
		Gabbro 27 Norite 22	Dolerite (19)	Basalt (17)		
	Extrusive pyroclastic type		Agglomerate (20)	Breccia (18)	Tuff (15)	

Material index (m_i) values for intact rock, classified by rock group.

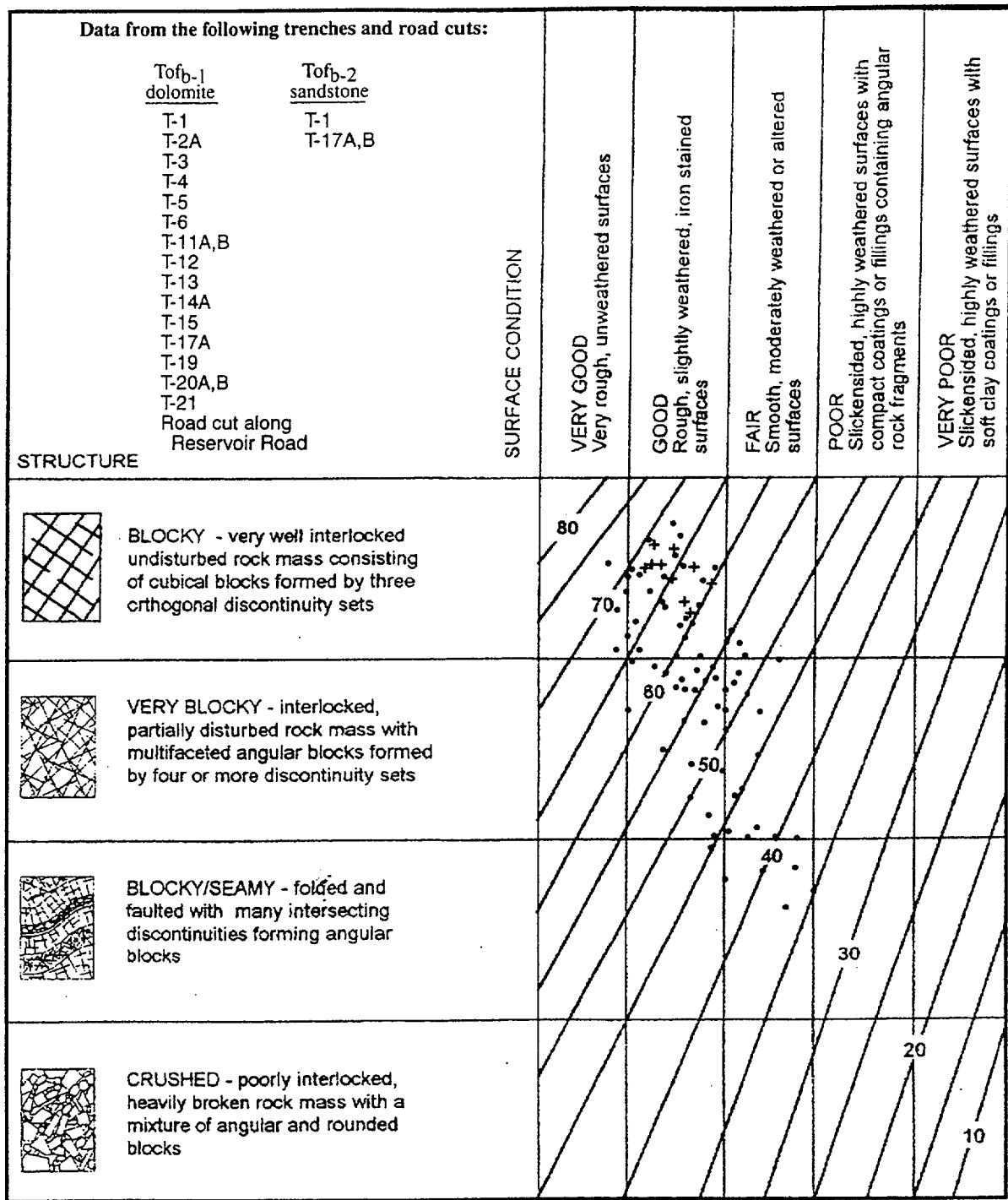
After Hoek, 1998

Refer to ISFSI SAR Section 2.6 Appendix H for description of site m_i values.

Explanation

- m_i values for dolomite and sandstone in the ISFSI site area, average m_i number indicated in parentheses.

Figure 19-1. Material index (m_i) value for rocks in ISFSI site area using the Hoek field classification chart.



07/23/01

Dolomite (Tof_{b-1}): average GSI = 55.7 (84 measurements[7 duplicate points]).

Sandstone (Tof_{b-2}): average GSI = 65 (10 measurements).

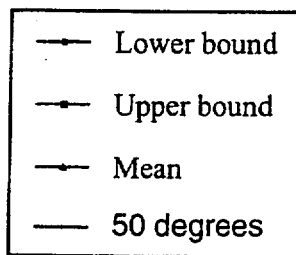
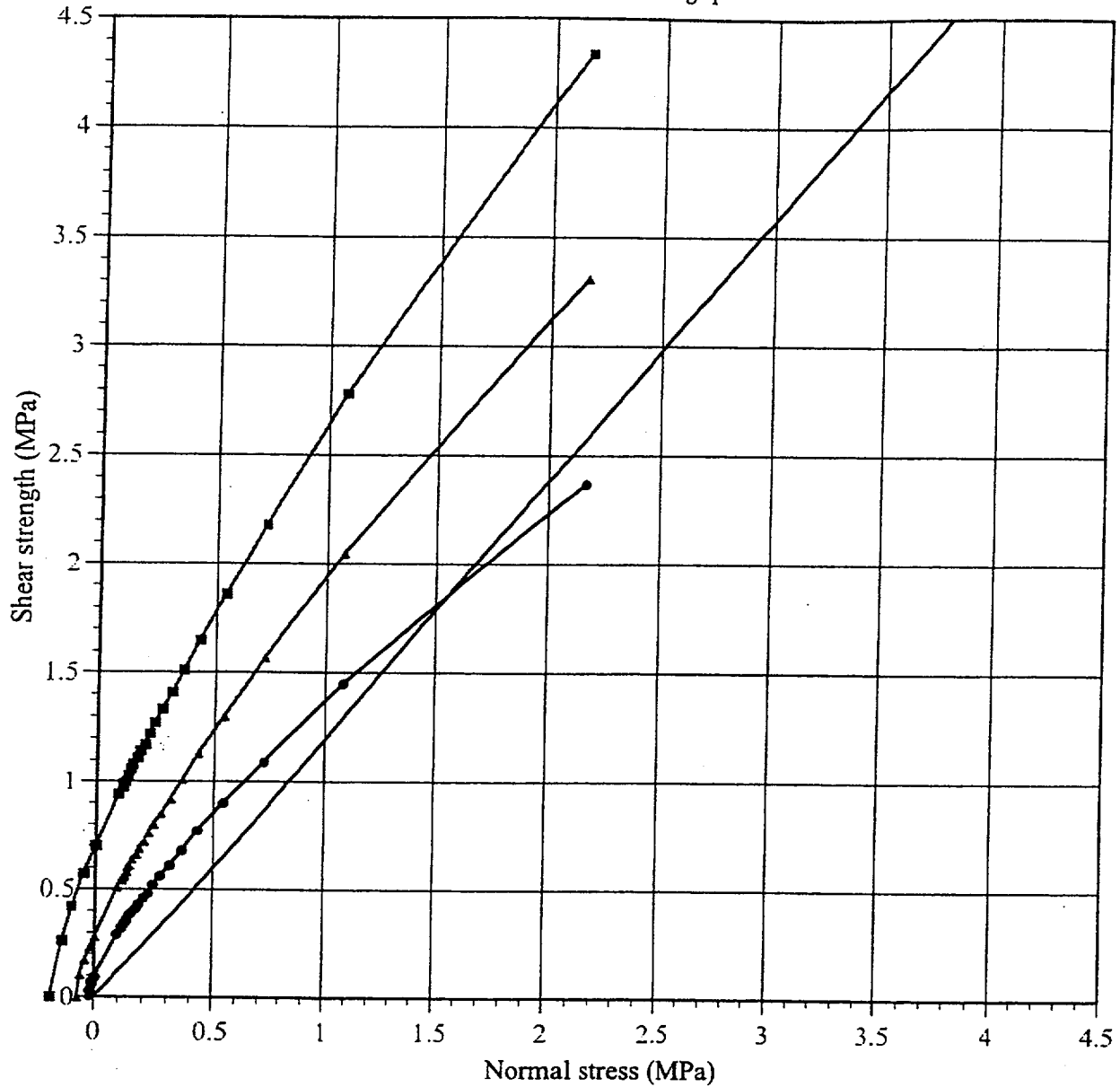
Explanation

- Dolomite (Tof_{b-1})
- + Sandstone (Tof_{b-2})

Refer to DCPD ISFSI SAR Section 2.6 Topical Report Appendix H for original GSI data sheets.

Figure 19-2. Field estimates of Hoek-Brown geologic strength index for rocks in ISFSI site area.

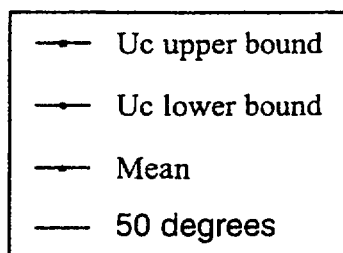
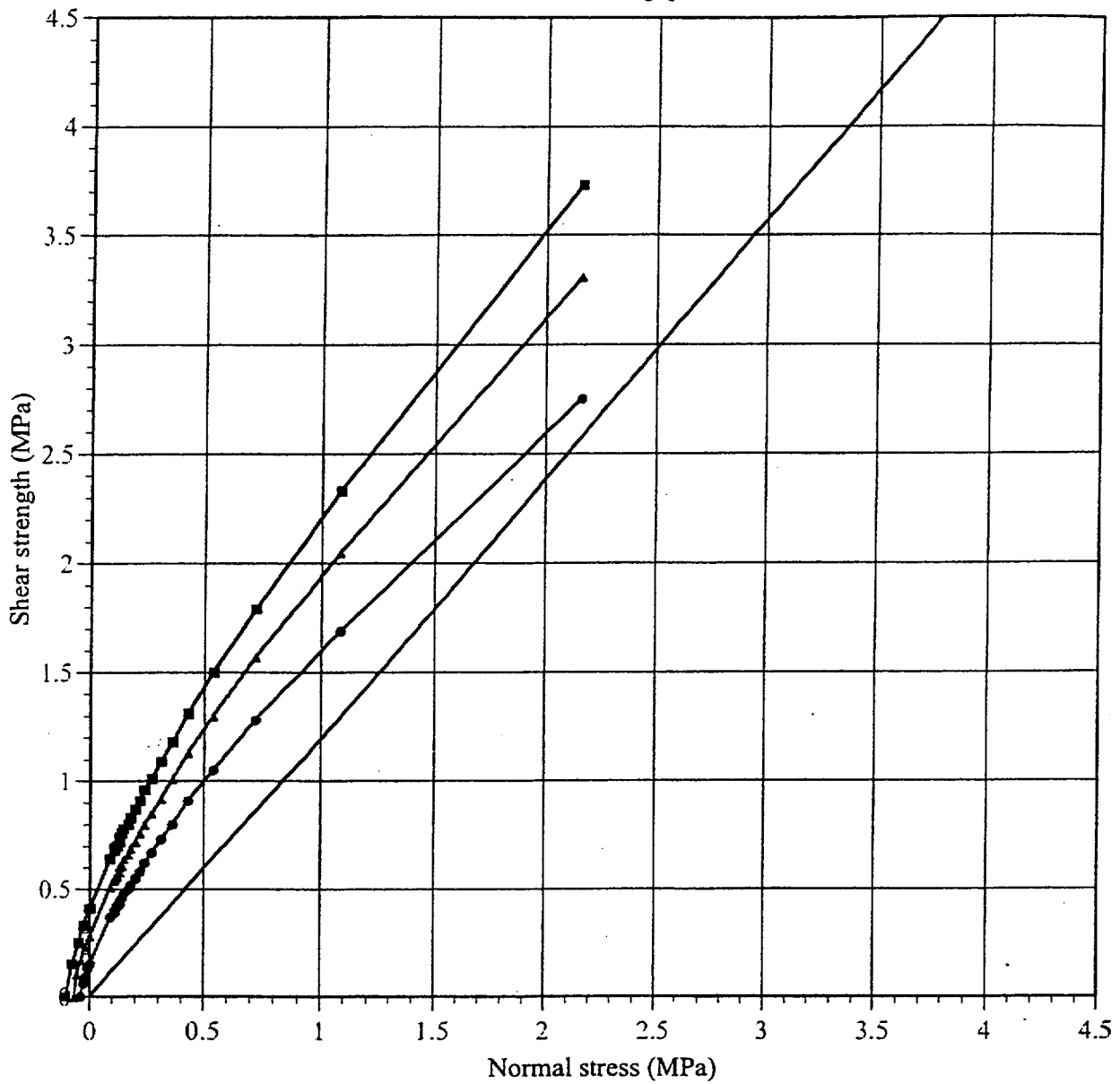
Comparison of strength ranges - Dolomite (Tof_{b-1}) - Hoek Brown Criterion



Note: Upper and lower bounds represent one standard deviation above and below the mean, respectively.

Figure 19-3. Curve D-1

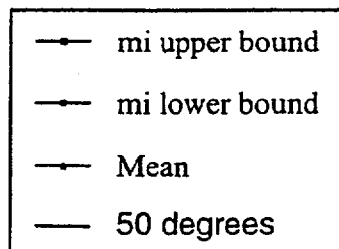
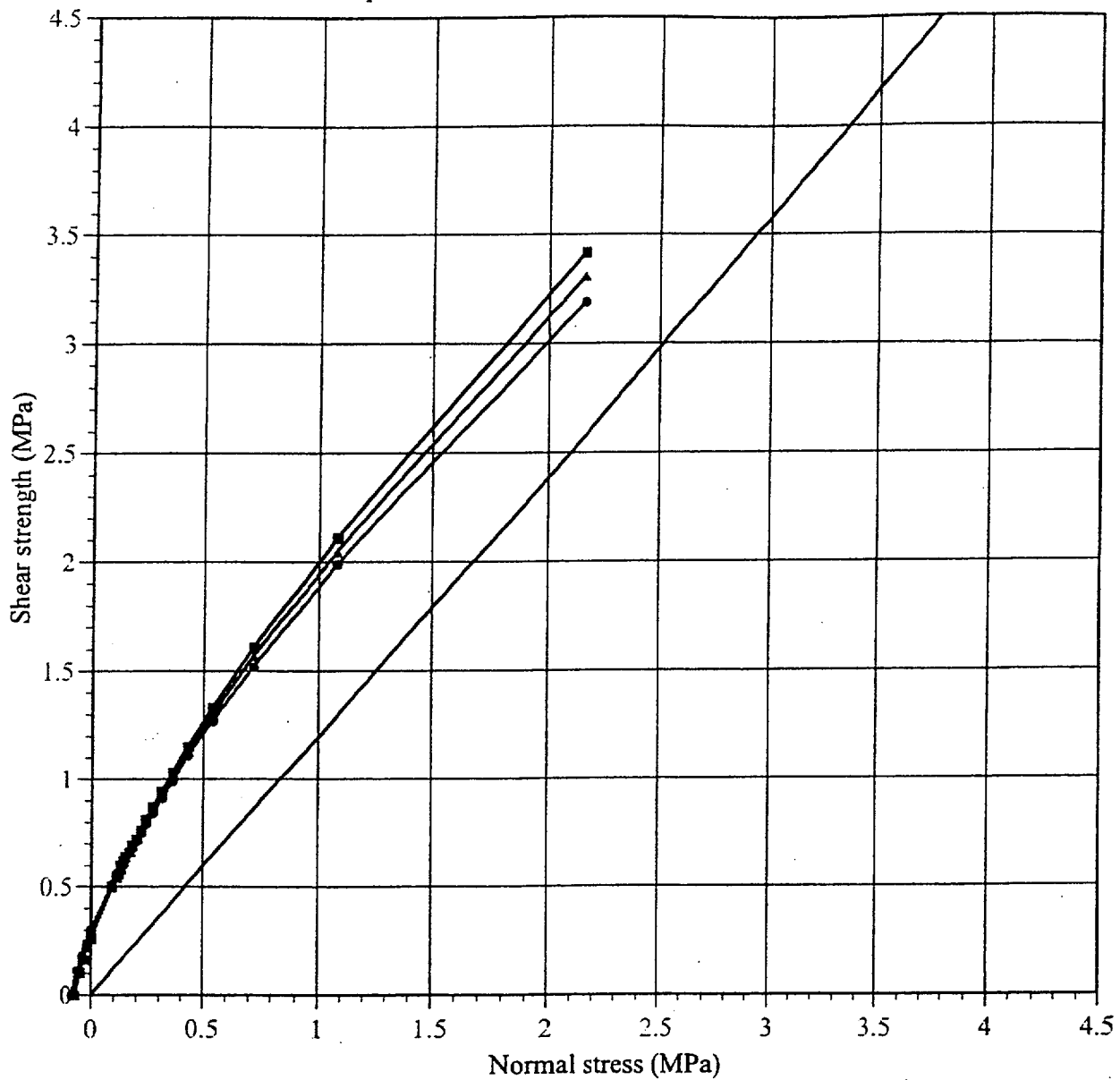
Sensitivity to U_c ranges - Dolomite ($T_{of_{b-1}}$) - Hoek Brown Criterion



Note: Upper and lower bounds represent one standard deviation above and below the mean, respectively.

Figure 19-4. Curve D-2

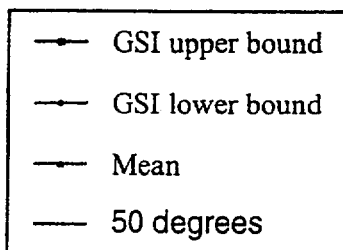
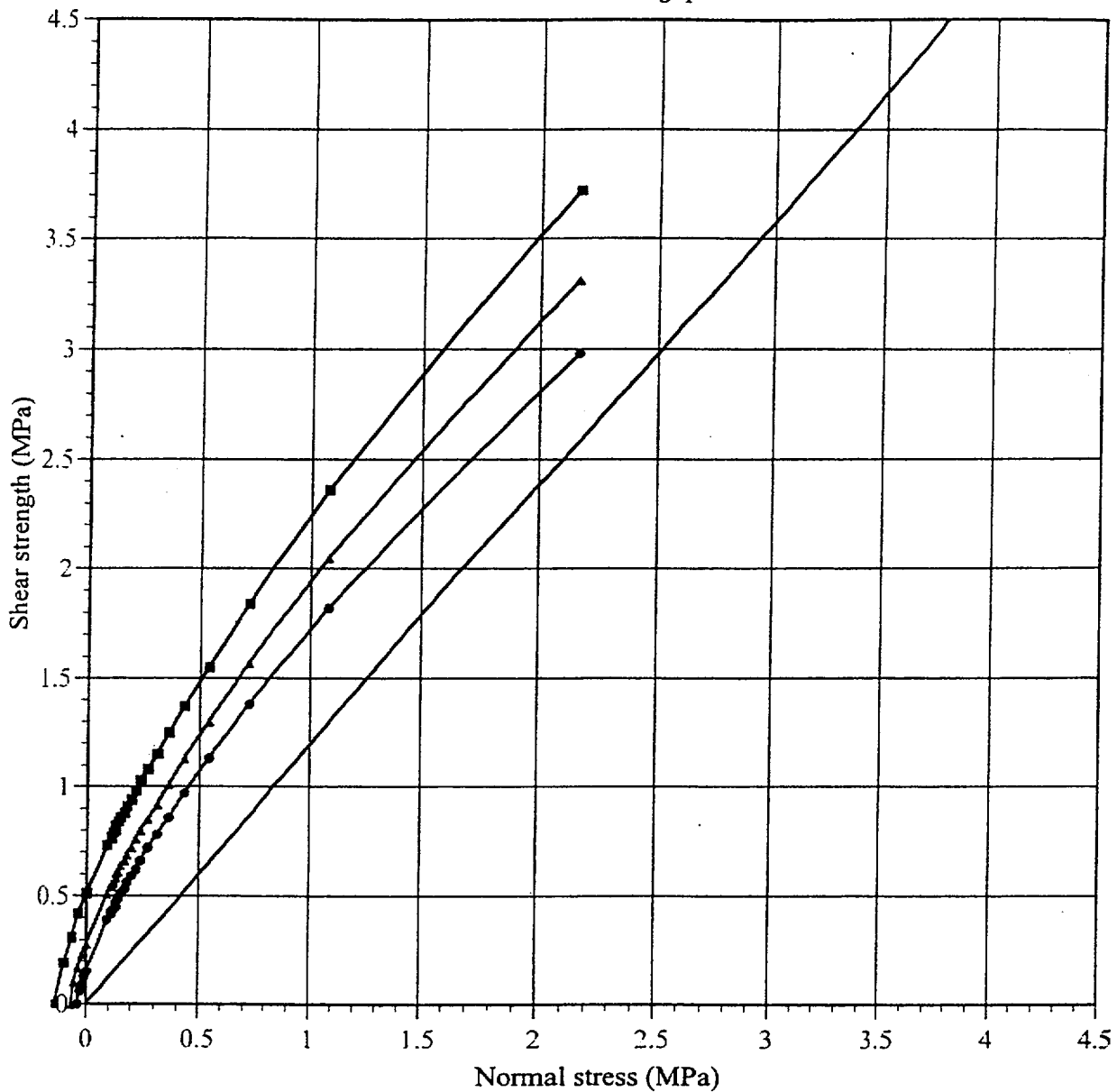
Sensitivity to m_i ranges - Dolomite (Tof_{b-1}) - Hoek Brown Criterion



Note: Upper and lower bounds represent one standard deviation above and below the mean, respectively.

Figure 19-5. Curve D-3

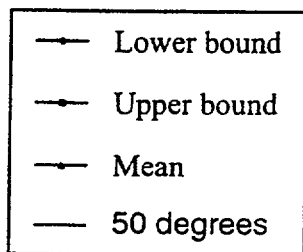
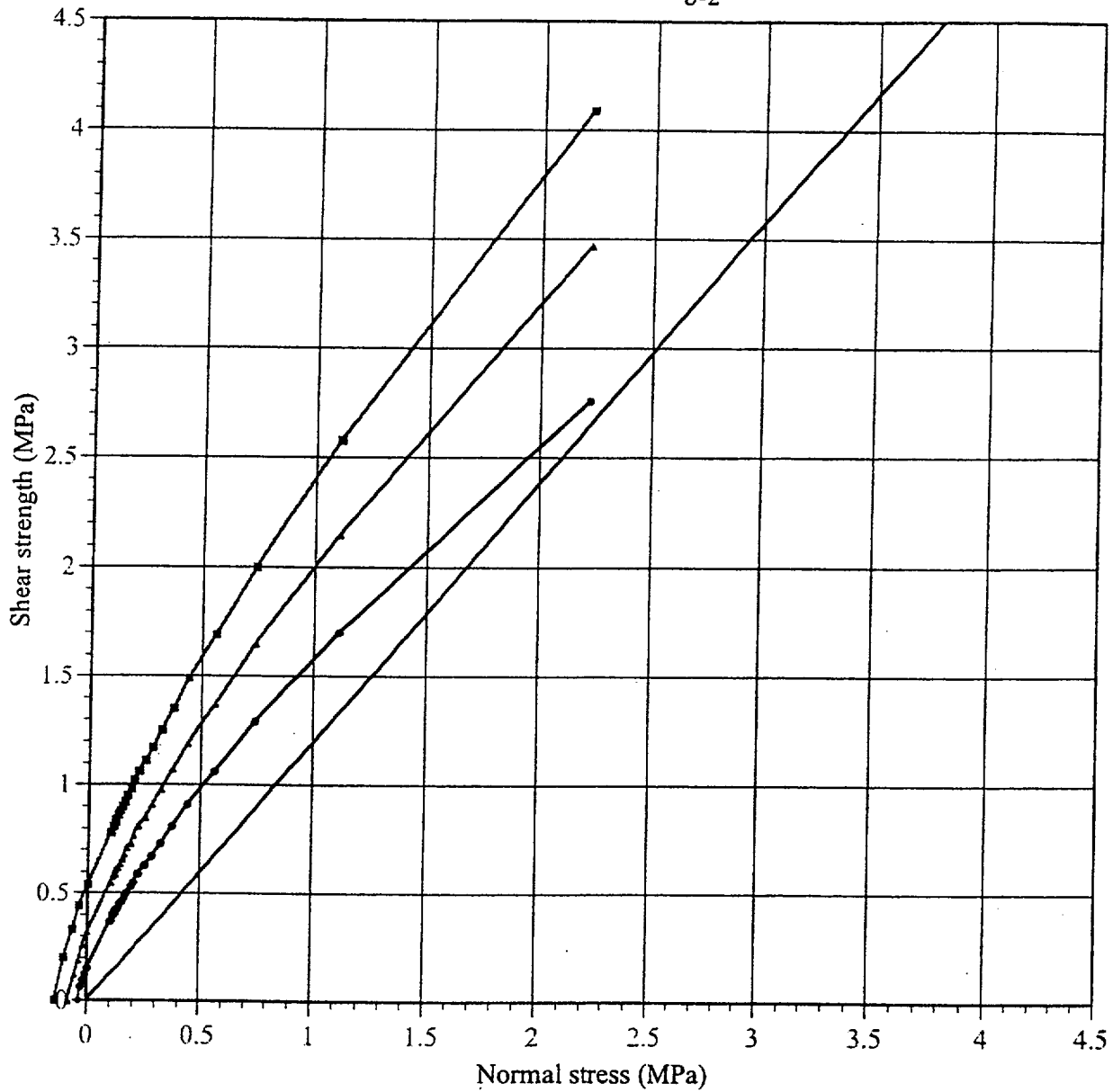
Sensitivity to GSI ranges - Dolomite ($T_{of_{b-1}}$) - Hoek Brown Criterion



Note: Upper and lower bounds represent one standard deviation above and below the mean, respectively.

Figure 19-6. Curve D-4
Page 27 of 92

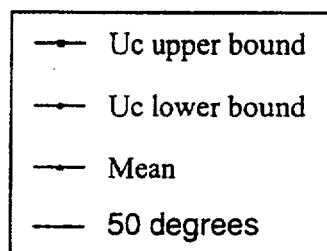
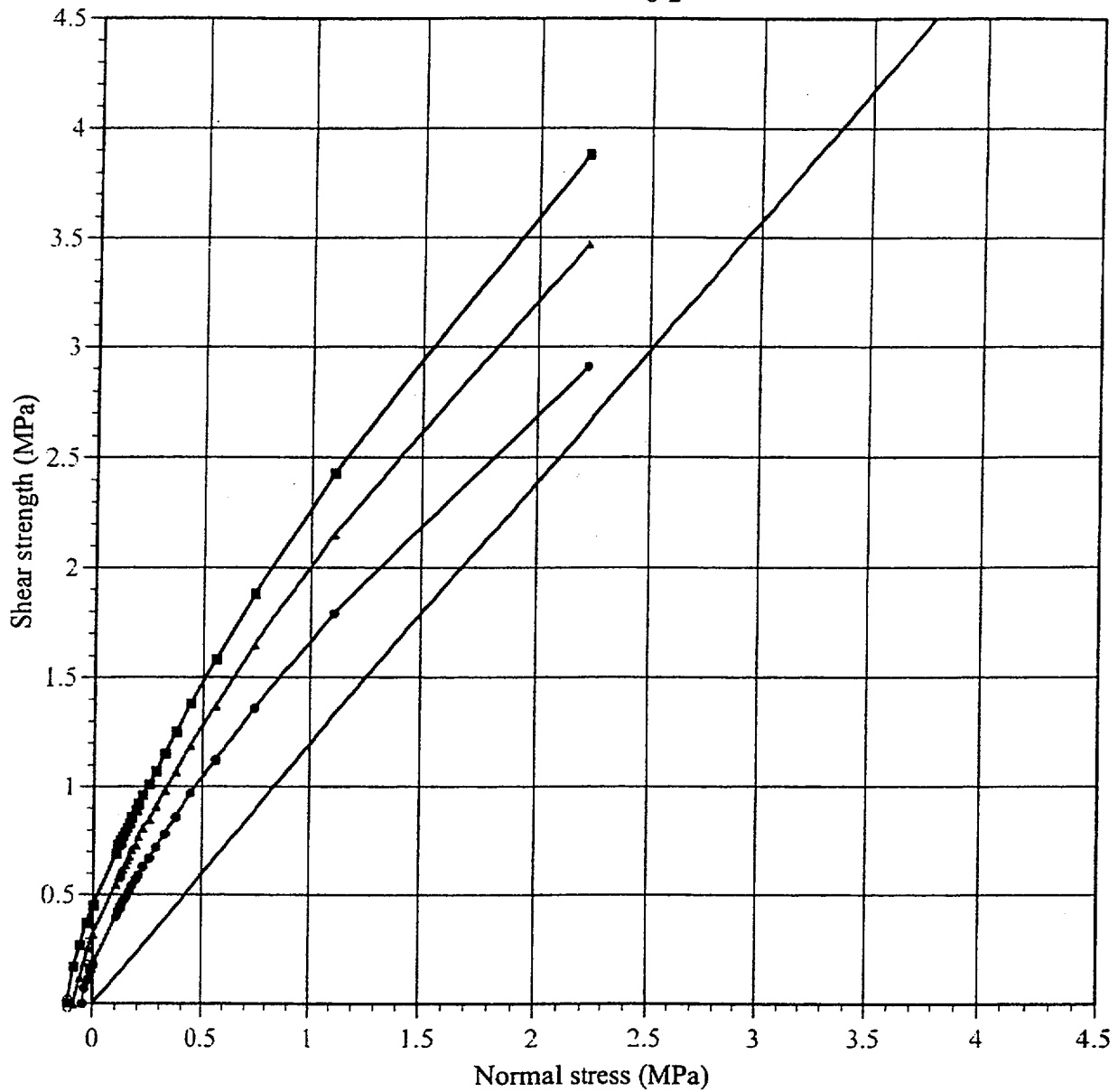
Comparison of strength ranges - Sandstone (σ_{b-2}) - Hoek Brown Criterion



Note: Upper and lower bounds represent one standard deviation above and below the mean, respectively.

Figure 19-7. Curve SS-1

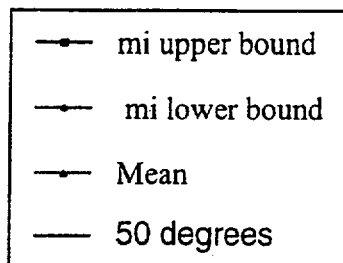
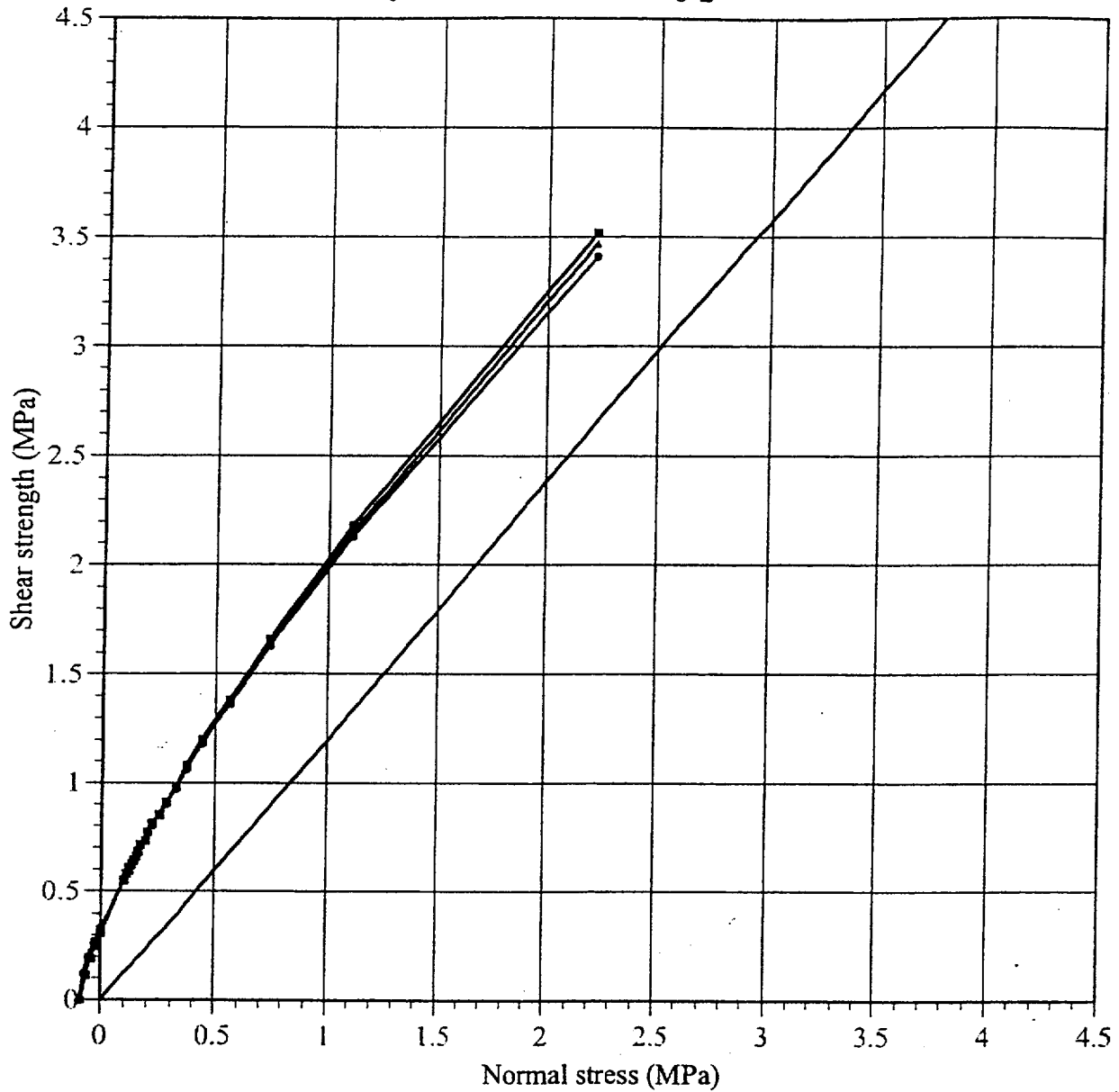
Sensitivity to U_c ranges - Sandstone (Tof_{b-2}) - Hoek Brown Criterion



Note: Upper and lower bounds represent one standard deviation above and below the mean, respectively.

Figure 19-8. Curve SS-2
Page 29 of 92

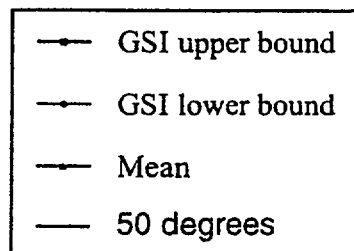
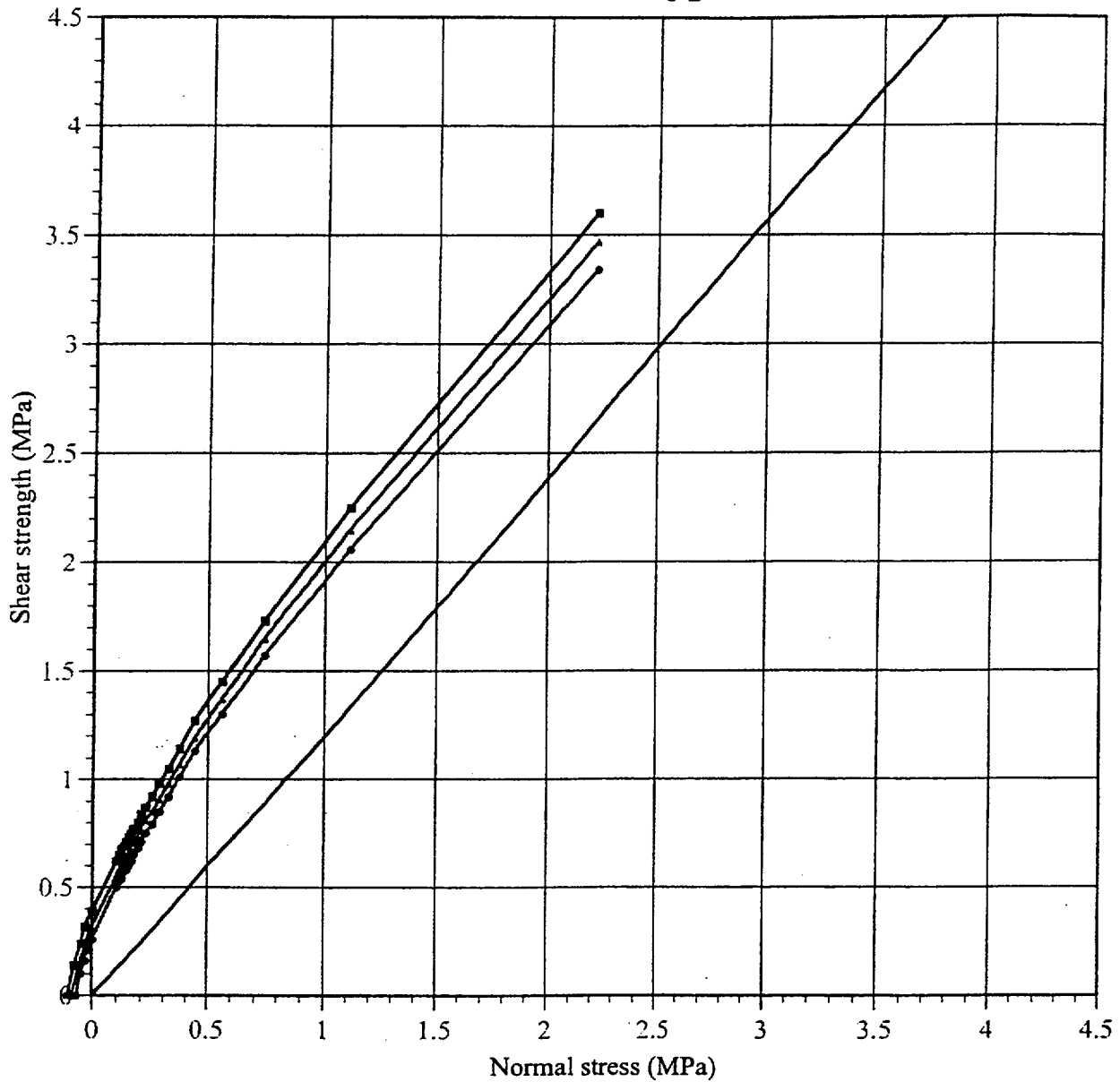
Sensitivity to m_i ranges - Sandstone (T_{b-2}) - Hoek Brown Criterion



Note: Upper and lower bounds represent one standard deviation above and below the mean, respectively.

Figure 19-9. Curve SS-3

Sensitivity to GSI ranges - Sandstone ($T_{of_{b-2}}$) - Hoek Brown Criterion



Note: Upper and lower bounds represent one standard deviation above and below the mean, respectively.

Figure 19-10. Curve SS-4

ATTACHMENT 1
Rock Engineering Course Notes, Chapter 11 (version dated Nov. 27, 2000)
E. Hoek, 2000

Downloaded from Rocscience website (www.rocscience.com) June 28, 2001

11

Rock mass properties

11.1 Introduction

Reliable estimates of the strength and deformation characteristics of rock masses are required for almost any form of analysis used for the design of slopes, foundations and underground excavations. Hoek and Brown (1980a, 1980b) proposed a method for obtaining estimates of the strength of jointed rock masses, based upon an assessment of the interlocking of rock blocks and the condition of the surfaces between these blocks. This method was modified over the years in order to meet the needs of users who were applying it to problems that were not considered when the original criterion was developed (Hoek 1983, Hoek and Brown 1988). The application of the method to very poor quality rock masses required further changes (Hoek, Wood and Shah 1992) and, eventually, the development of a new classification called the Geological Strength Index (Hoek, Kaiser and Bawden 1995, Hoek 1995, Hoek and Brown 1997). A review of the development of the criterion and of the equations proposed at various stages in this development is given in Hoek and Brown (1997).

This chapter presents the Hoek-Brown criterion in a form that has been found practical in the field and that appears to provide the most reliable set of results for use as input for methods of analysis in current use in rock engineering.

11.2 Generalised Hoek-Brown criterion

The Generalised Hoek-Brown failure criterion for jointed rock masses is defined by:

$$\sigma_1' = \sigma_3' + \sigma_{ci} \left(m_b \frac{\sigma_3'}{\sigma_{ci}} + s \right)^a \quad (11.1)$$

where σ_1' and σ_3' are the maximum and minimum effective stresses at failure,

m_b is the value of the Hoek-Brown constant m for the rock mass,

s and a are constants which depend upon the rock mass characteristics, and

σ_{ci} is the uniaxial compressive strength of the intact rock pieces.

The Mohr envelope, relating normal and shear stresses, can be determined by the method proposed by Hoek and Brown (1980a). In this approach, equation 11.1 is used to generate a series of triaxial test values, simulating full scale field tests, and a

statistical curve fitting process is used to derive an equivalent Mohr envelope defined by the equation:

$$\tau = A\sigma_{ci} \left(\frac{\sigma'_n - \sigma_{tm}}{\sigma_{ci}} \right)^B \quad (11.2)$$

where A and B are material constants

σ'_n is the normal effective stress, and

σ_{tm} is the 'tensile' strength of the rock mass.

This 'tensile' strength, which reflects the interlocking of the rock particles when they are not free to dilate, is given by:

$$\sigma_{tm} = \frac{\sigma_{ci}}{2} \left(m_b - \sqrt{m_b^2 + 4s} \right) \quad (11.3)$$

In order to use the Hoek-Brown criterion for estimating the strength and deformability of jointed rock masses, three 'properties' of the rock mass have to be estimated. These are

1. the uniaxial compressive strength σ_{ci} of the intact rock pieces,
2. the value of the Hoek-Brown constant m_i for these intact rock pieces, and
3. the value of the Geological Strength Index GSI for the rock mass.

11.3 Intact rock properties

For the intact rock pieces that make up the rock mass equation 11.1 simplifies to:

$$\sigma'_1 = \sigma'_3 + \sigma_{ci} \left(m_i \frac{\sigma'_3}{\sigma_{ci}} + 1 \right)^{0.5} \quad (11.4)$$

The relationship between the principal stresses at failure for a given rock is defined by two constants, the uniaxial compressive strength σ_{ci} and a constant m_i . Wherever possible the values of these constants should be determined by statistical analysis of the results of a set of triaxial tests on carefully prepared core samples.

Note that the range of minor principal stress (σ'_3) values over which these tests are carried out is critical in determining reliable values for the two constants. In deriving the original values of σ_{ci} and m_i , Hoek and Brown (1980a) used a range of $0 < \sigma'_3 < 0.5\sigma_{ci}$ and, in order to be consistent, it is essential that the same range be used in any laboratory triaxial tests on intact rock specimens. At least five data points should be included in the analysis.

One type of triaxial cell that can be used for these tests is illustrated in Figure 11.1. This cell, described by Hoek and Franklin (1968), does not require draining between tests and is convenient for the rapid testing of a large number of specimens. More sophisticated cells are available for research purposes but the results obtained from

the cell illustrated in Figure 11.1 are adequate for the rock strength estimates required for estimating σ_{ci} and m_i . This cell has the additional advantage that it can be used in the field when testing materials such as coals, shales and phyllites that are extremely difficult to preserve during transportation and normal specimen preparation for laboratory testing.

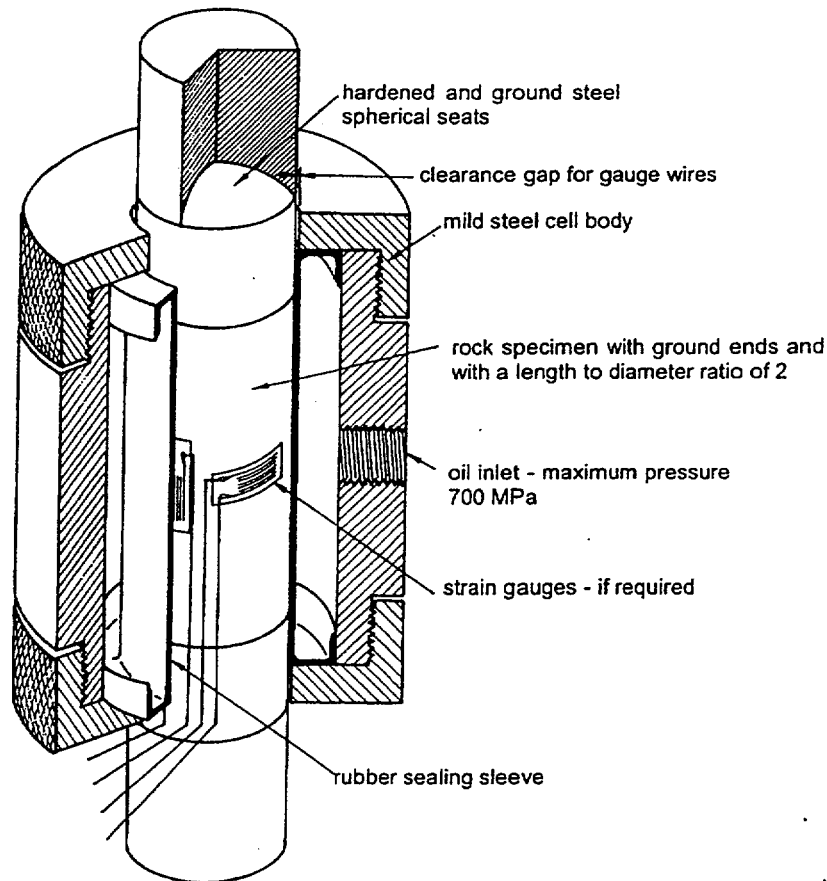


Figure 11.1: Cut-away view of a triaxial cell for testing rock specimens.

Laboratory tests should be carried out at moisture contents as close as possible to those which occur in the field. Many rocks show a significant strength decrease with increasing moisture content and tests on samples, which have been left to dry in a core shed for several months, can give a misleading impression of the intact rock strength.

Once the five or more triaxial test results have been obtained, they can be analysed to determine the uniaxial compressive strength σ_{ci} and the Hoek-Brown constant m_i as described by Hoek and Brown (1980a). In this analysis, equation 11.1 is re-written in the form:

$$y = m\sigma_{ci}x + s\sigma_{ci} \quad (11.5)$$

where $x = \sigma_3'$ and $y = (\sigma_1' - \sigma_3')^2$

For n specimens the uniaxial compressive strength σ_{ci} , the constant m_i and the coefficient of determination r^2 are calculated from:

$$\sigma_{ci}^2 = \frac{\sum y}{n} - \left[\frac{\sum xy - (\sum x \sum y/n)}{\sum x^2 - ((\sum x)^2/n)} \right] \frac{\sum x}{n} \quad (11.6)$$

$$m_i = \frac{1}{\sigma_{ci}} \left[\frac{\sum xy - (\sum x \sum y/n)}{\sum x^2 - ((\sum x)^2/n)} \right] \quad (11.7)$$

$$r^2 = \frac{[\sum xy - (\sum x \sum y/n)]^2}{[\sum x^2 - ((\sum x)^2/n)][\sum y^2 - ((\sum y)^2/n)]} \quad (11.8)$$

A spreadsheet for the analysis of triaxial test data is given in Table 11.1. Note that high quality triaxial test data will usually give a coefficient of determination r^2 of greater than 0.9.

When laboratory tests are not possible, Table 11.2 and Table 11.3 can be used to obtain estimates of σ_{ci} and m_i .

Short-term laboratory tests on very hard brittle rocks tend to overestimate the in situ rock mass strength. Laboratory tests and field studies on excellent quality Lac du Bonnet granite, reported by Martin and Chandler (1994), show that the in situ strength of this rock is only about 70% of that measured in the laboratory. This appears to be due to damage resulting from micro-cracking of the rock which initiates and develops critical intensities at lower stress levels in the field than in laboratory tests carried out at higher loading rates on smaller specimens. Hence, when analysing the results of laboratory tests on these types of rocks to estimate the values of σ_{ci} and m_i , it is prudent to reduce the values of the major effective principal stress at failure to 70% of the measured values.

Anisotropic and foliated rocks such as slates, schists and phyllites, the behaviour of which is dominated by closely spaced planes of weakness, cleavage or schistosity, present particular difficulties in the determination of the uniaxial compressive strengths.

Salcedo (1983) has reported the results of a set of directional uniaxial compressive tests on a graphitic phyllite from Venezuela. These results are summarised in Figure 11.2. It will be noted that the uniaxial compressive strength of this material varies by a factor of about 5, depending upon the direction of loading. Evidence of the behaviour of this graphitic phyllite in the field suggests that the rock mass properties are dependent upon the strength parallel to schistosity rather than that normal to it.

Table 11.1: Spreadsheet for the calculation of σ_{ci} and m_i from triaxial test data

Triaxial test data					
x		y	xy	xsq	ysq
sig3	sig1				
0	38.3	1466.89	0.0	0.0	2151766
5	72.4	4542.76	22713.8	25.0	20636668
7.5	80.5	5329.00	39967.5	56.3	28398241
15	115.6	10120.36	151805.4	225.0	102421687
20	134.3	13064.49	261289.8	400.0	170680899
47.5	441.1	34523.50	475776.5	706.3	324289261
sumx		sumy	sumxy	sumxsq	sumysq
Calculation results					
Number of tests	n =	5			
Uniaxial strength	sigci =	37.4			
Hoek-Brown constant	mi =	15.50			
Hoek-Brown constant	s =	1.00			
Coefficient of determination	r2 =	0.997			
Cell formulae					
$y = (\text{sig1} - \text{sig3})^2$					
$\text{sigci} = \text{SQRT}(\text{sumy}/n - (\text{sumxy} - \text{sumx} * \text{sumy}/n) / (\text{sumxsq} - (\text{sumx}^2)/n) * \text{sumx}/n)$					
$mi = (1/\text{sigci}) * ((\text{sumxy} - \text{sumx} * \text{sumy}/n) / (\text{sumxsq} - (\text{sumx}^2)/n))$					
$r2 = ((\text{sumxy} - (\text{sumx} * \text{sumy}/n))^2) / ((\text{sumxsq} - (\text{sumx}^2)/n) * (\text{sumysq} - (\text{sumy}^2)/n))$					

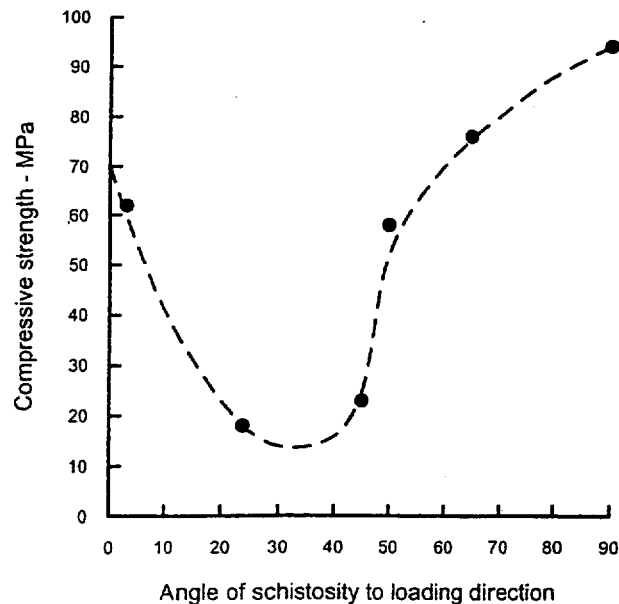


Figure 11.2: Influence of loading direction on the strength of graphitic phyllite tested by Salcedo (1983).

Table 11.2: Field estimates of uniaxial compressive strength.

Grade*	Term	Uniaxial Comp. Strength (MPa)	Point Load Index (MPa)	Field estimate of strength	Examples
R6	Extremely Strong	> 250	>10	Specimen can only be chipped with a geological hammer	Fresh basalt, chert, diabase, gneiss, granite, quartzite
R5	Very strong	100 - 250	4 - 10	Specimen requires many blows of a geological hammer to fracture it	Amphibolite, sandstone, basalt, gabbro, gneiss, granodiorite, limestone, marble, rhyolite, tuff
R4	Strong	50 - 100	2 - 4	Specimen requires more than one blow of a geological hammer to fracture it	Limestone, marble, phyllite, sandstone, schist, shale
R3	Medium strong	25 - 50	1 - 2	Cannot be scraped or peeled with a pocket knife, specimen can be fractured with a single blow from a geological hammer	Claystone, coal, concrete, schist, shale, siltstone
R2	Weak	5 - 25	**	Can be peeled with a pocket knife with difficulty, shallow indentation made by firm blow with point of a geological hammer	Chalk, rocksalt, potash
R1	Very weak	1 - 5	**	Crumbles under firm blows with point of a geological hammer, can be peeled by a pocket knife	Highly weathered or altered rock
R0	Extremely weak	0.25 - 1	**	Indented by thumbnail	Stiff fault gouge

* Grade according to Brown (1981).

** Point load tests on rocks with a uniaxial compressive strength below 25 MPa are likely to yield highly ambiguous results.

Table 11.3: Values of the constant m_i for intact rock, by rock group. Note that values in parenthesis are estimates.

Rock type	Class	Group	Texture			
			Coarse	Medium	Fine	Very fine
SEDIMENTARY	Clastic		Conglomerate (22)	Sandstone 19 —— Greywacke —— (18)	Siltstone 9	Claystone 4
	Non- Clastic	Organic	—— Chalk —— 7 —— Coal —— (8-21)			
		Carbonate	Breccia (20)	Sparitic Limestone (10)	Micritic Limestone 8	
		Chemical		Gypstone 16	Anhydrite 13	
	METAMORPHIC	Non Foliated		Marble 9	Hornfels (19)	Quartzite 24
Slightly foliated		Migmatite (30)	Amphibolite 25 - 31	Mylonites (6)		
Foliated*		Gneiss 33	Schists 4 - 8	Phyllites (10)	Slate 9	
IGNEOUS	Light	Dark	Granite 33		Rhyolite (16)	Obsidian (19)
			Granodiorite (30)		Dacite (17)	
			Diorite (28)		Andesite 19	
			Gabbro 27	Dolerite (19)	Basalt (17)	
			Norite 22			
	Extrusive pyroclastic type		Agglomerate (20)	Breccia (18)	Tuff (15)	

* These values are for intact rock specimens tested normal to bedding or foliation. The value of m_i will be significantly different if failure occurs along a weakness plane.

In deciding upon the value of σ_{ci} for foliated rocks, a decision has to be made on whether to use the highest or the lowest uniaxial compressive strength obtained from

results such as those given in Figure 11.1. Mineral composition, grain size, grade of metamorphism and tectonic history all play a role in determining the characteristics of the rock mass. The author cannot offer any precise guidance on the choice of σ_{ci} but suggest that the maximum value should be used for hard, well interlocked rock masses such as good quality slates. The lowest uniaxial compressive strength should be used for tectonically disturbed, poor quality rock masses such as the graphitic phyllite tested by Salcedo (1983).

Unlike other rocks, coal is organic in origin and therefore has unique constituents and properties. Unless these properties are recognised and allowed for in characterising the coal, the results of any tests will exhibit a large amount of scatter. Medhurst, Brown and Trueman (1995) have shown that, by taking into account the 'brightness' which reflects the composition and the cleating of the coal, it is possible to differentiate between the mechanical characteristics of different coals.

11.4 Influence of sample size

The influence of sample size upon rock strength has been widely discussed in geotechnical literature and it is generally assumed that there is a significant reduction in strength with increasing sample size. Based upon an analysis of published data, Hoek and Brown (1980a) have suggested that the uniaxial compressive strength σ_{cd} of a rock specimen with a diameter of d mm is related to the uniaxial compressive strength σ_{c50} of a 50 mm diameter sample by the following relationship:

$$\sigma_{cd} = \sigma_{c50} \left(\frac{50}{d} \right)^{0.18} \quad (11.9)$$

This relationship, together with the data upon which it was based, is illustrated in Figure 11.3.

The author suggests that the reduction in strength is due to the greater opportunity for failure through and around grains, the 'building blocks' of the intact rock, as more and more of these grains are included in the test sample. Eventually, when a sufficiently large number of grains are included in the sample, the strength reaches a constant value.

Medhurst and Brown (1996) have reported the results of laboratory triaxial tests on samples of 61, 101, 146 and 300 mm diameter samples of a highly cleated mid-brightness coal from the Moura mine in Australia. The results of these tests are summarised in Table 11.4 and Figure 11.4.

The results obtained by Medhurst and Brown show a significant decrease in strength with increasing sample size. This is attributed to the effects of cleat spacing. For this coal, the persistent cleats are spaced at 0.3 to 1.0 m while non-persistent cleats within vitrain bands and individual lithotypes define blocks of 1 cm or less. This cleating results in a 'critical' sample size of about 1 m above which the strength remains constant.

It is reasonable to extend this argument further and to suggest that, when dealing with large scale rock masses, the strength will reach a constant value when the size of individual rock pieces is sufficiently small in relation to the overall size of the

structure being considered. This suggestion is embodied in Figure 11.5 which shows the transition from an isotropic intact rock specimen, through a highly anisotropic rock mass in which failure is controlled by one or two discontinuities, to an isotropic heavily jointed rock mass.

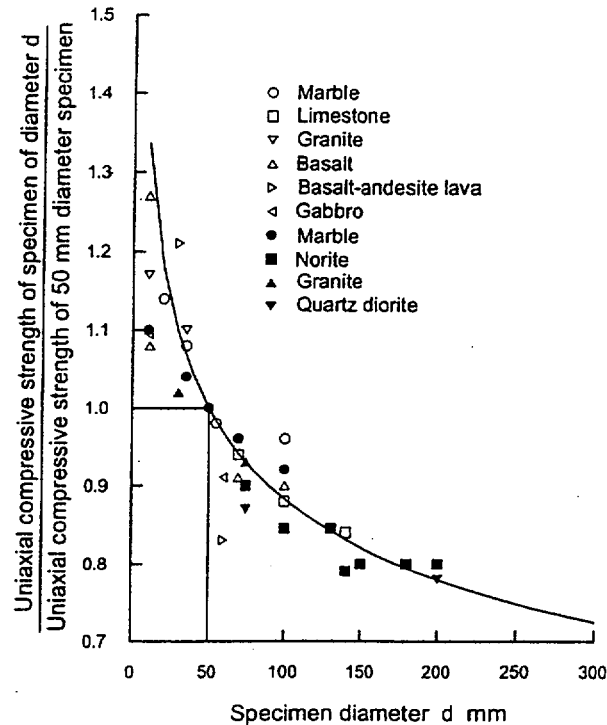


Figure 11.3 Influence of specimen size on the strength of intact rock. After Hoek and Brown (1980a).

Table 11.4 Peak strength of Moura DU coal in terms of the parameters contained in equation (11.1) based upon a value of $\sigma_{ci} = 32.7$ MPa.

Dia.(mm)	m_b	s	a
61	19.4	1.0	0.5
101	13.3	0.555	0.5
146	10.0	0.236	0.5
300	5.7	0.184	0.6
mass	2.6	0.052	0.65

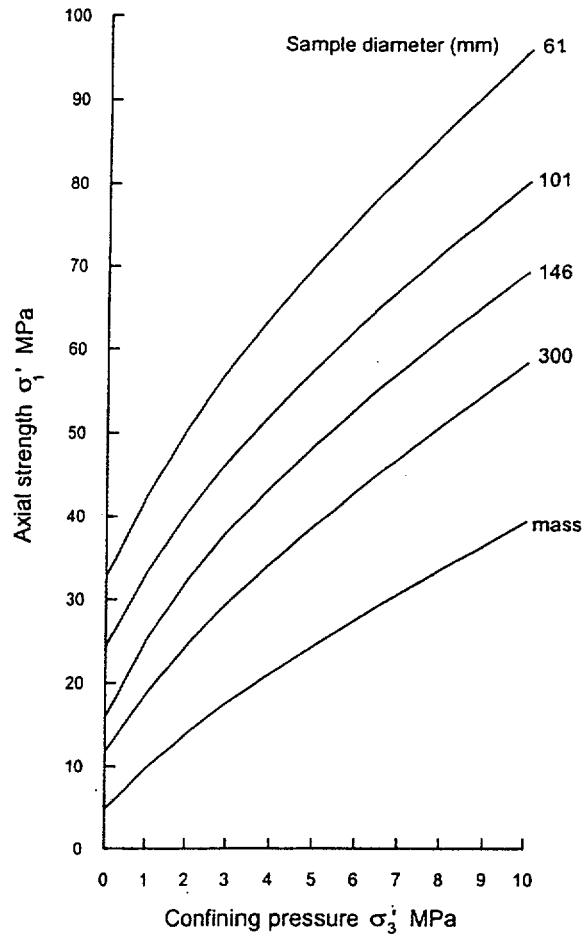


Figure 11.4 Peak strength for Australian Moura coal.
After Medhurst and Brown (1996).

The Hoek-Brown failure criterion, which assumes isotropic rock and rock mass behaviour, should only be applied to those rock masses in which there are a sufficient number of closely spaced discontinuities, with similar surface characteristics, that isotropic behaviour involving failure on discontinuities can be assumed. When the structure being analysed is large and the block size small in comparison, the rock mass can be treated as a Hoek-Brown material.

Where the block size is of the same order as that of the structure being analysed or when one of the discontinuity sets is significantly weaker than the others, the Hoek-Brown criterion should not be used. In these cases, the stability of the structure should be analysed by considering failure mechanisms involving the sliding or rotation of blocks and wedges defined by intersecting structural features.

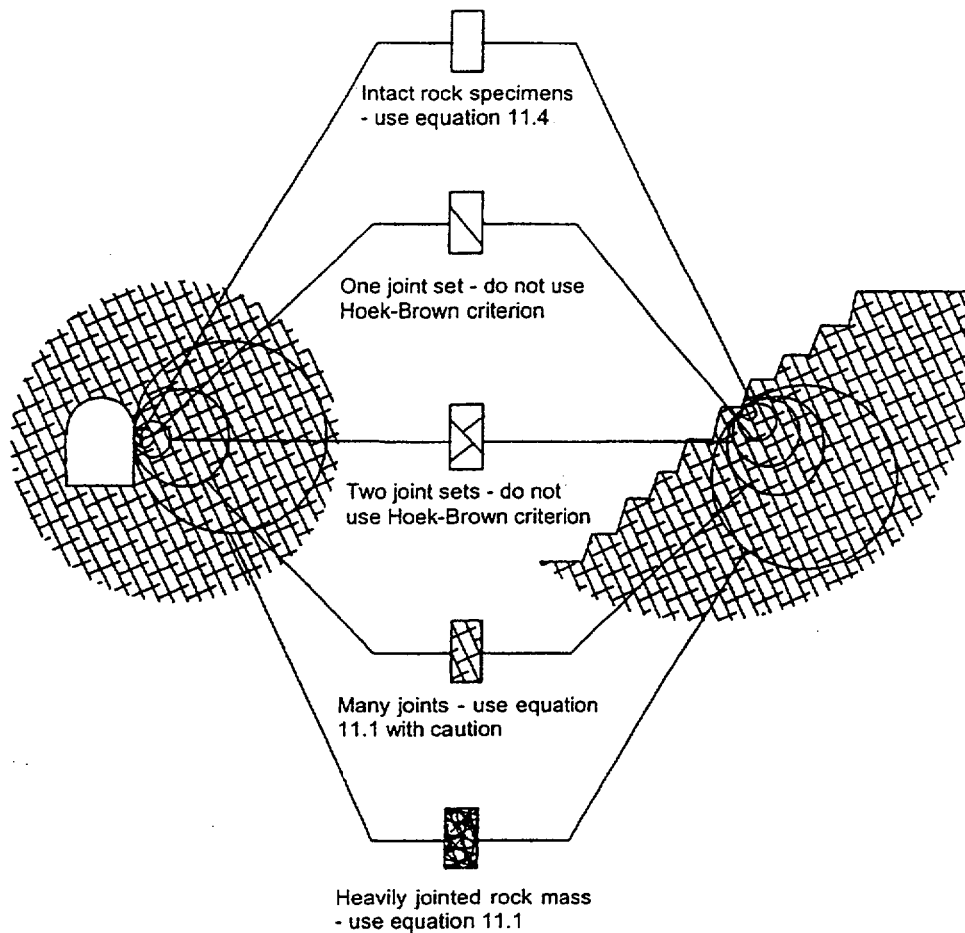


Figure 11.5: Idealised diagram showing the transition from intact to a heavily jointed rock mass with increasing sample size.

11.5 Geological strength Index

The strength of a jointed rock mass depends on the properties of the intact rock pieces and also upon the freedom of these pieces to slide and rotate under different stress conditions. This freedom is controlled by the geometrical shape of the intact rock pieces as well as the condition of the surfaces separating the pieces. Angular rock pieces with clean, rough discontinuity surfaces will result in a much stronger rock mass than one which contains rounded particles surrounded by weathered and altered material.

The Geological Strength Index (GSI), introduced by Hoek (1995) and Hoek, Kaiser and Bawden (1995) provides a system for estimating the reduction in rock mass strength for different geological conditions. This system is presented in Table 11.5 and Table 11.6. Experience has shown that Table 11.5 is sufficient for field

observations since the letter code that identifies each rock mass category can be entered into a field log. Later, these codes can be used to estimate the GSI value from Table 11.6.

Once the Geological Strength Index has been estimated, the parameters that describe the rock mass strength characteristics, are calculated as follows:

$$m_b = m_i \exp\left(\frac{GSI - 100}{28}\right) \quad (11.10)$$

For $GSI > 25$, i.e. rock masses of good to reasonable quality, the original Hoek-Brown criterion is applicable with

$$s = \exp\left(\frac{GSI - 100}{9}\right) \quad (11.11)$$

and

$$a = 0.5 \quad (11.12)$$

For $GSI < 25$, i.e. rock masses of very poor quality, the modified Hoek-Brown criterion applies with

$$s = 0 \quad (11.13)$$

and

$$a = 0.65 - \frac{GSI}{200} \quad (11.14)$$





The choice of $GSI = 25$ for the switch between the original and modified criteria is purely arbitrary. It could be argued that a switch at $GSI = 30$ would not introduce a discontinuity in the value of a , but extensive trials have shown that the exact location of this switch has negligible practical significance.

For better quality rock masses ($GSI > 25$), the value of GSI can be estimated directly from the 1976 version of Bieniawski's Rock Mass Rating, with the Groundwater rating set to 10 (dry) and the Adjustment for Joint Orientation set to 0 (very favourable) (Bieniawski 1976). For very poor quality rock masses the value of RMR is very difficult to estimate and the balance between the ratings no longer gives a reliable basis for estimating rock mass strength. Consequently, Bieniawski's RMR classification should not be used for estimating the GSI values for poor quality rock masses.

If the 1989 version of Bieniawski's RMR classification (Bieniawski 1989) is used, then $GSI = RMR_{89}' - 5$ where RMR_{89}' has the Groundwater rating set to 15 and the Adjustment for Joint Orientation set to zero.





One of the practical problems which arises when assessing the value of GSI in the field is related to blast damage. As illustrated in Figure 11.6, there is a considerable difference in the appearance of a rock face which has been excavated by controlled blasting and a face which has been damaged by bulk blasting. Wherever possible, the undamaged face should be used to estimate the value of GSI since the overall aim is to determine the properties of the undisturbed rock mass.

Table 11.5: Characterisation of rock masses on the basis of interlocking and joint alteration¹

ROCK MASS CHARACTERISTICS FOR STRENGTH ESTIMATES		SURFACE CONDITIONS				
Based upon the appearance of the rock, choose the category that you think gives the best description of the 'average' undisturbed in situ conditions. Note that exposed rock faces that have been created by blasting may give a misleading impression of the quality of the underlying rock. Some adjustment for blast damage may be necessary and examination of diamond drill core or of faces created by pre-split or smooth blasting may be helpful in making these adjustments. It is also important to recognize that the Hoek-Brown criterion should only be applied to rock masses where the size of individual blocks is small compared with the size of the excavation under consideration.		VERY GOOD Very rough, fresh unweathered surfaces	GOOD Rough, slightly weathered, iron stained surfaces	FAIR Smooth, moderately weathered or altered surfaces	POOR Slackensided, highly weathered surfaces with compact coatings or fillings of angular fragments	VERY POOR Slackensided, highly weathered surfaces with soft clay coatings or fillings
STRUCTURE		DECREASING SURFACE QUALITY ▼				
	BLOCKY - very well interlocked undisturbed rock mass consisting of cubical blocks formed by three orthogonal discontinuity sets	B/VG	B/G	B/F	B/P	B/VP
	VERY BLOCKY - interlocked, partially disturbed rock mass with multifaceted angular blocks formed by four or more discontinuity sets	VB/VG	VB/G	VB/F	VB/P	VB/VP
	BLOCKY/DISTURBED- folded and/or faulted with angular blocks formed by many intersecting discontinuity sets	BD/VG	BD/G	BD/F	BD/P	BD/VP
	DISINTEGRATED - poorly interlocked, heavily broken rock mass with a mixture of angular and rounded rock pieces	D/VG	D/G	D/F	D/P	D/VP

¹ In earlier versions of this table the terms **BLOCKY/SEAMY** and **CRUSHED** were used, following the terminology used by Terzaghi (1946). However, these terms proved to be misleading and they have been replaced, in this table by **BLOCKY/DISTURBED**, which more accurately reflects the increased mobility of a rock mass which has undergone some folding and/or faulting, and **DISINTEGRATED** which encompasses a wider range of particle shapes.

Table 11.6: Estimate of Geological Strength Index GSI based on geological descriptions.

GEOLOGICAL STRENGTH INDEX		SURFACE CONDITIONS					
From the letter codes describing the structure and surface conditions of the rock mass (from Table 4), pick the appropriate box in this chart. Estimate the average value of the Geological Strength Index (GSI) from the contours. Do not attempt to be too precise. Quoting a range of GSI from 36 to 42 is more realistic than stating that GSI = 38.		VERY GOOD Very rough, fresh unweathered surfaces					
		GOOD Rough, slightly weathered, iron stained surfaces					
		FAIR Smooth, moderately weathered or altered surfaces					
		POOR Slackensided, highly weathered surfaces with compact coatings or fillings of angular fragments					
		VERY POOR Slackensided, highly weathered surfaces with soft clay coatings or fillings					
STRUCTURE	DECREASING SURFACE QUALITY ▾						
	BLOCKY - very well interlocked undisturbed rock mass consisting of cubical blocks formed by three orthogonal discontinuity sets	80					
	VERY BLOCKY - interlocked, partially disturbed rock mass with multifaceted angular blocks formed by four or more discontinuity sets	70					
	BLOCKY/DISTURBED - folded and/or faulted with angular blocks formed by many intersecting discontinuity sets	60					
	DISINTEGRATED - poorly interlocked, heavily broken rock mass with a mixture of angular and rounded rock pieces	50					
		40					
			30				
				20			
					10		

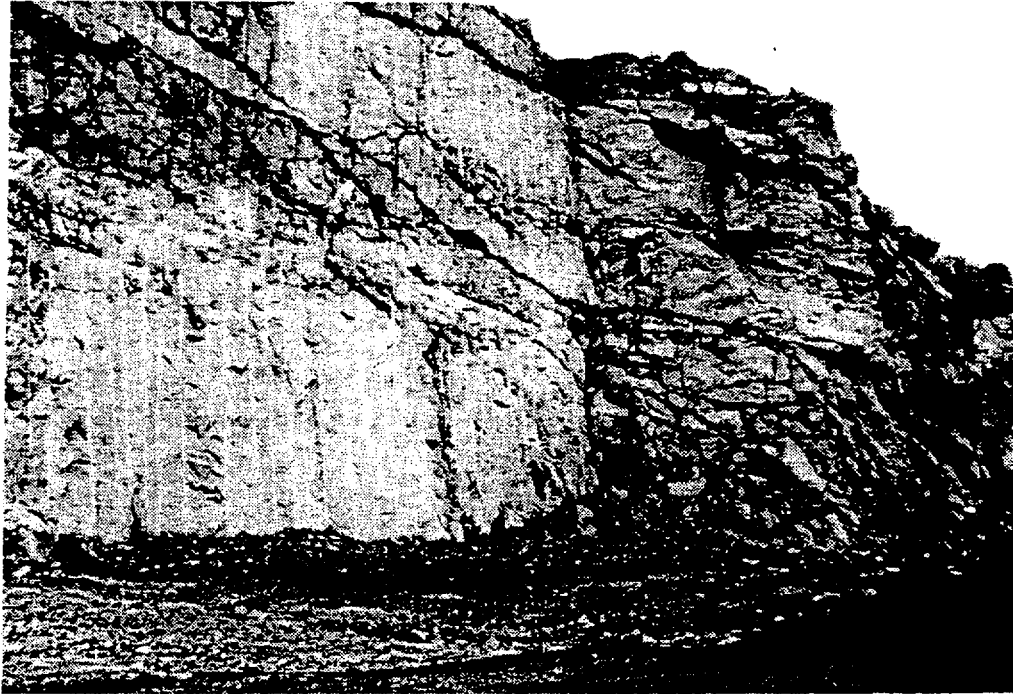


Figure 11.6: Comparison between the results achieved using controlled blasting (on the left) and normal bulk blasting for a surface excavation in gneiss.

Where all the visible faces have been damaged by blasting, some attempt should be made to compensate for the lower values of GSI obtained from such faces. In recently blasted faces, new discontinuity surfaces will have been created by the blast and these will give a GSI value that may be as much as 10 points lower than that for the undisturbed rock mass. In other words, severe blast damage can be allowed for by moving up one row in Table 11.5 and Table 11.6.

Where blast damaged faces have been exposed for a number of years, it may also be necessary to step as much as one column to the left in order to allow for surface weathering which will have occurred during this exposure. Hence, for example, a badly blast damaged weathered rock surface which has the appearance of a BLOCKY/DISTURBED and FAIR (BD/F in Table 11.5) rock mass may actually be VERY BLOCKY and GOOD (VB/G) in its unweathered and undisturbed in situ state.

An additional practical question is whether borehole cores can be used to estimate the GSI value behind the visible faces? For reasonable quality rock masses ($GSI > 25$) the best approach is to evaluate the core in terms of Bieniawski's RMR classification and then, as described above, to estimate the GSI value from RMR. For poor quality rock masses ($GSI < 25$), relatively few intact core pieces longer than 100 mm are recovered and it becomes difficult to determine a reliable value for RMR. In these circumstances, the physical appearance of the material recovered in the core should be used as a basis for estimating GSI.

11.6 Mohr-Coulomb parameters

Most geotechnical software is written in terms of the Mohr-Coulomb failure criterion in which the rock mass strength is defined by the cohesive strength c' and the angle of friction ϕ' . The linear relationship between the major and minor principal stresses, σ_1' and σ_3' , for the Mohr-Coulomb criterion is

$$\sigma_1' = \sigma_{cm} + k\sigma_3' \quad (11.15)$$

where σ_{cm} is the uniaxial compressive strength of the rock mass and k is the slope of the line relating σ_1' and σ_3' . The values of ϕ' and c' can be calculated from

$$\sin \phi' = \frac{k-1}{k+1} \quad (11.16)$$

$$c' = \frac{\sigma_{cm}(1 - \sin \phi')}{2 \cos \phi'} \quad (11.17)$$

There is no direct correlation between equation 11.15 and the non-linear Hoek-Brown criterion defined by equation 11.1. Consequently, determination of the values of c' and ϕ' for a rock mass that has been evaluated as a Hoek-Brown material is a difficult problem.

The author believes that the most rigorous approach available, for the original Hoek-Brown criterion, is that developed by Dr J.W. Bray and reported by Hoek (1983). For any point on a surface of concern in an analysis such as a slope stability calculation, the effective normal stress is calculated using an appropriate stress analysis technique. The shear strength developed at that value of effective normal stress is then calculated from the equations given in Hoek and Brown (1997). The difficulty in applying this approach in practice is that most of the geotechnical software currently available provides for constant rather than effective normal stress dependent values of c' and ϕ' .

Having evaluated a large number of possible approaches to this problem, it has been concluded that the most practical solution is to treat the problem as an analysis of a set of full-scale triaxial strength tests. The results of such tests are simulated by using the Hoek-Brown equation 11.1 to generate a series of triaxial test values. Equation 11.15 is then fitted to these test results by linear regression analysis and the values of c' and ϕ' are determined from equations 11.17 and 11.16. The steps required to determine the parameters A, B, c' and ϕ' are given below. A spreadsheet for carrying out this analysis, with a listing of all the cell formulae, is given in Figure 11.7.

The relationship between the normal and shear stresses can be expressed in terms of the corresponding principal effective stresses as suggested by Balmer (1952):

$$\sigma_n' = \sigma_3' + \frac{\sigma_1' - \sigma_3'}{\partial \sigma_1' / \partial \sigma_3' + 1} \quad (11.18)$$

$$\tau = (\sigma'_1 - \sigma'_3) \sqrt{\partial \sigma'_1 / \partial \sigma'_3} \quad (11.19)$$

For the $GSI > 25$, when $a = 0.5$:

$$\frac{\partial \sigma'_1}{\partial \sigma'_3} = 1 + \frac{m_b \sigma_{ci}}{2(\sigma'_1 - \sigma'_3)} \quad (11.20)$$

For $GSI < 25$, when $s = 0$:

$$\frac{\partial \sigma'_1}{\partial \sigma'_3} = 1 + am_b^a \left(\frac{\sigma'_3}{\sigma_{ci}} \right)^{a-1} \quad (11.21)$$

The tensile strength of the rock mass is calculated from:

$$\sigma_{tm} = \frac{\sigma_{ci}}{2} \left(m_b - \sqrt{m_b^2 + 4s} \right) \quad (11.22)$$

The equivalent Mohr envelope, defined by equation 11.2, may be written in the form:

$$Y = \log A + BX \quad (11.23)$$

where

$$Y = \log \left(\frac{\tau}{\sigma_{ci}} \right), \quad X = \log \left(\frac{\sigma'_n - \sigma_{tm}}{\sigma_{ci}} \right) \quad (11.24)$$

Using the value of σ_{tm} calculated from equation 11.22 and a range of values of τ and σ'_n calculated from equations 11.19 and 11.18 the values of A and B are determined by linear regression where :

$$B = \frac{\sum XY - (\sum X \sum Y)/T}{\sum X^2 - (\sum X)^2/T} \quad (11.25)$$

$$A = 10^{(\sum Y/T - B(\sum X/T))} \quad (11.26)$$

and T is the total number of data pairs included in the regression analysis.

The most critical step in this process is the selection of the range of σ'_3 values. As far as the author is aware, there are no theoretically correct methods for choosing this range and a trial and error method, based upon practical compromise, has been used for selecting the range included in the spreadsheet presented in Figure 11.7.

For a Mohr envelope defined by equation 11.2, the friction angle ϕ'_i for a specified normal stress σ'_{ni} is given by:

$$\phi'_i = \arctan \left(AB \left(\frac{\sigma'_{ni} - \sigma'_{tm}}{\sigma_{ci}} \right)^{B-1} \right) \quad (11.27)$$

The corresponding cohesive strength c'_i is given by:

$$c'_i = \tau - \sigma'_{ni} \tan \phi'_i \quad (11.28)$$

and the corresponding uniaxial compressive strength of the rock mass is :

$$\sigma_{cmi} = \frac{2c'_i \cos \phi'_i}{1 - \sin \phi'_i} \quad (11.29)$$

Note that the cohesive strength c'_i given by equation 11.29 is an upper bound value and that it is prudent to reduce this to about 75% of the calculated value for practical applications.

The values of c' and ϕ' obtained from this analysis are very sensitive to the range of values of the minor principal stress σ'_3 used to generate the simulated full-scale triaxial test results. On the basis of trial and error, it has been found that the most consistent results are obtained when 8 equally spaced values of σ'_3 are used in the range $0 < \sigma'_3 < 0.25\sigma_{ci}$.

An example of the results, which are obtained from this analysis, is given in Figure 11.8. Plots of the values of the ratio c'/σ_{ci} and the friction angle ϕ' , for different combinations of GSI and m_i are given in Figure 11.9.

The spreadsheet includes a calculation for a tangent to the Mohr envelope defined by equation 11.2. A normal stress has to be specified in order to calculate this tangent and, in Figure 11.8, this stress has been chosen so that the friction angle ϕ' is the same for both the tangent and the line defined by $c' = 3.3$ MPa and $\phi' = 30.1^\circ$, determined by the linear regression analysis described earlier. The cohesion intercept for the tangent is $c' = 4.1$ MPa which is approximately 25% higher than that obtained by linear regression analysis of the simulated triaxial test data.

Fitting a tangent to the curved Mohr envelope gives an upper bound value for the cohesive intercept c' . It is recommended that this value be reduced by about 25% in order to avoid over-estimation of the rock mass strength.

There is a particular class of problem for which extreme caution should be exercised when applying the approach outlined above. In some rock slope stability problems, the effective normal stress on some parts of the failure surface can be quite low, certainly less than 1 MPa. It will be noted that in the example given in Figure 11.8, for values of σ'_n of less than about 5 MPa, the straight line, constant c' and ϕ' method overestimates the available shear strength of the rock mass by increasingly significant amounts as σ'_n approaches zero. Under such circumstances, it would be prudent to use values of c' and ϕ' based on a tangent to the shear strength curve in the range of σ'_n values applying in practice.

Figure 11.7 Spreadsheet for calculation of Hoek-Brown and equivalent Mohr-Coulomb parameters

Hoek-Brown and equivalent Mohr Coulomb failure criteria

Input:	sigci = 85 MPa	mi = 10	GSI = 45
Output:	mb = 1.40 sigtm = -0.13 MPa k = 3.01 sigcm = 11.36 MPa	s = 0.0022 A = 0.50 phi = 30.12 degrees E = 6913.7 MPa	a = 0.5 B = 0.70 coh = 3.27 MPa
Tangent:	signt = 15.97 MPa	phit = 30.12 degrees	coht = 4.12 MPa

Calculation:

									Sums
sig3	1E-10	3.04	6.07	9.1	12.14	15.18	18.21	21.25	85.00
sig1	4.00	22.48	33.27	42.30	50.40	57.91	64.98	71.74	347.08
ds1ds3	15.89	4.07	3.19	2.80	2.56	2.40	2.27	2.18	35.35
sign	0.24	6.87	12.56	17.85	22.90	27.76	32.50	37.13	157.80
tau	0.94	7.74	11.59	14.62	17.20	19.48	21.54	23.44	116.55
x	-2.36	-1.08	-0.83	-0.67	-0.57	-0.48	-0.42	-0.36	-6.77
y	-1.95	-1.04	-0.87	-0.76	-0.69	-0.64	-0.60	-0.56	-7.11
xy	4.61	1.13	0.71	0.52	0.39	0.31	0.25	0.20	8.12
xsq	5.57	1.17	0.68	0.45	0.32	0.23	0.17	0.13	8.74
sig3sig1	0.00	68.23	202.01	385.23	612.01	878.92	1183.65	1524.51	4855
sig3sq	0.00	9.22	36.86	82.94	147.45	230.39	331.76	451.56	1290
taucalc	0.96	7.48	11.33	14.45	17.18	19.64	21.91	24.04	
sig1sig3fit	11.36	20.51	29.66	38.81	47.96	57.11	66.26	75.42	
signtaufit	3.41	7.26	10.56	13.63	16.55	19.38	22.12	24.81	
tangent	4.25309	8.10321	11.4032	14.4729	17.3991	20.2235	22.9702	25.655	

Cell formulae:

```

mb = mi*EXP((GSI-100)/28)
s = IF(GSI>25,EXP((GSI-100)/9),0)
a = IF(GSI>25,0.5,0.65-GSI/200)
sigtm = 0.5*sigci*(mb-SQRT(mb^2+4*s))
A = acalc = 10^(sumy/8 - bcalc*sumx/8)
B = bcalc = (sumxy - (sumx*sumy)/8)/(sumxsq - (sumx^2)/8)
k = (sumsig3sig1 - (sumsig3*sumsig1)/8)/(sumsig3sq-(sumsig3^2)/8)
phi = ASIN((k-1)/(k+1))*180/PI()
coh = (sigcm*(1-SIN(phi*PI()/180)))/(2*COS(phi*PI()/180))
sigcm = sumsig1/8 - k*sumsig3/8
E = IF(sigci>100,1000*10^((GSI-10)/40),SQRT(sigci/100)*1000*10^((GSI-10)/40))
phit = (ATAN(acalc*bcalc*((signt-sigtm)/sigci)^(bcalc-1)))*180/PI()
coht = acalc*sigci*((signt-sigtm)/sigci)^bcalc-signt*TAN(phit*PI()/180)
sig3 = Start at 1E-10 (to avoid zero errors) and increment in 7 steps of sigci/28 to 0.25*sigci
sig1 = sig3+sigci*((mb*sig3)/sigci)+s^a
ds1ds3 = IF(GSI>25,(1+(mb*sigci)/(2*(sig1-sig3))),1+(a*mb^a)*(sig3/sigci)^(a-1))
sign = sig3+(sig1-sig3)/(1+ds1ds3)
tau = (sign-sig3)*SQRT(ds1ds3)
x = LOG((sign-sigtm)/sigci)
y = LOG(tau/sigci)
xy = x*y      x sq = x^2      sig3sig1 = sig3*sig1      sig3sq = sig3^2
taucalc = acalc*sigci*((sign-sigtm)/sigci)^bcalc
s3sifit = sigcm+k*sig3
sntaufit = coh+sign*TAN(phi*PI()/180)
tangent = coht+sign*TAN(phit*PI()/180)

```

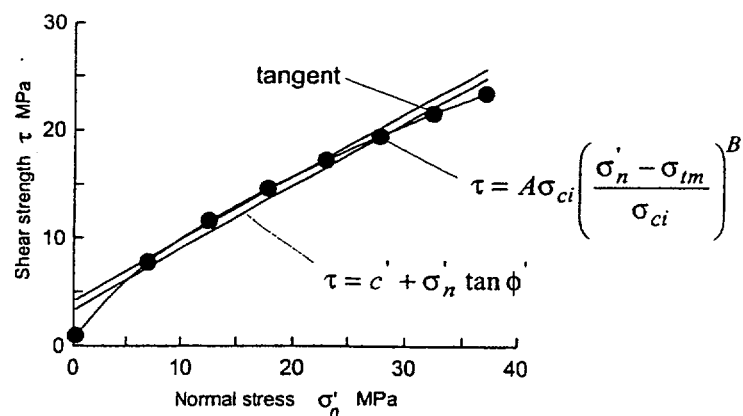
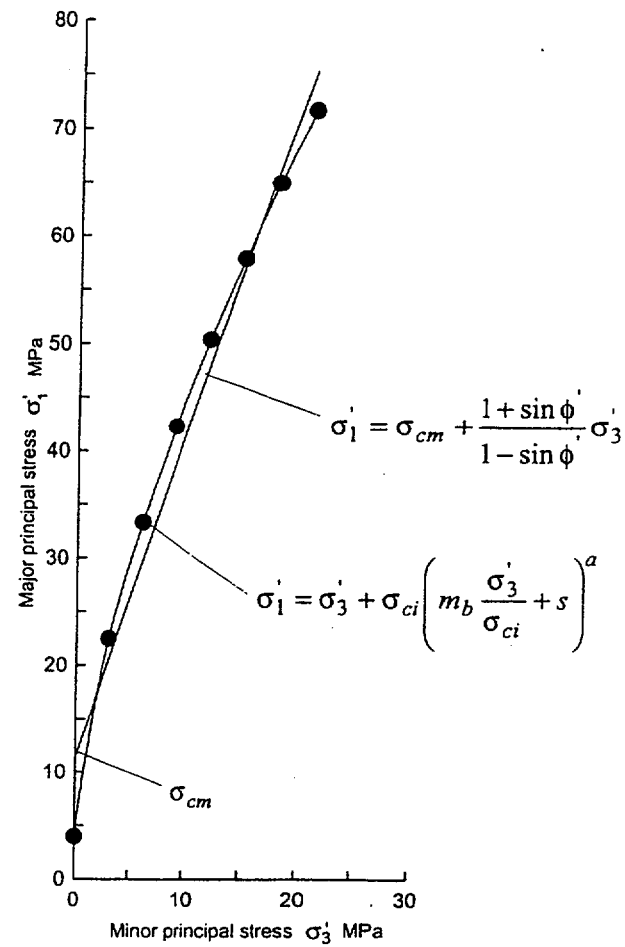
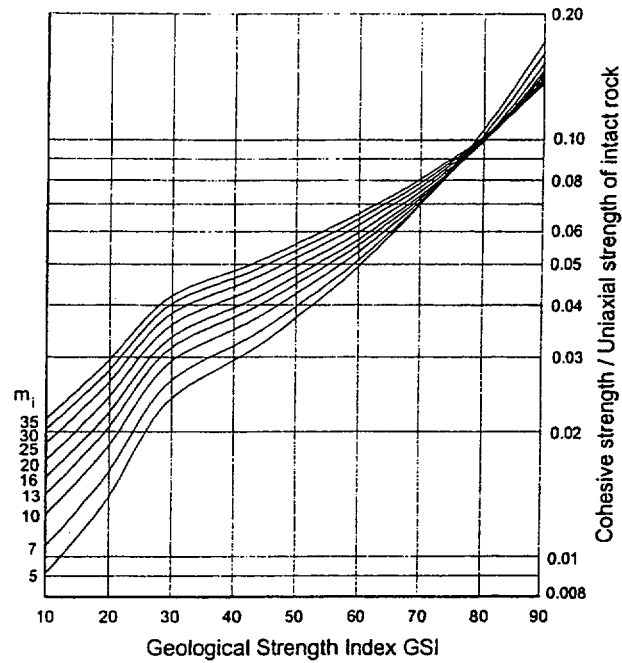
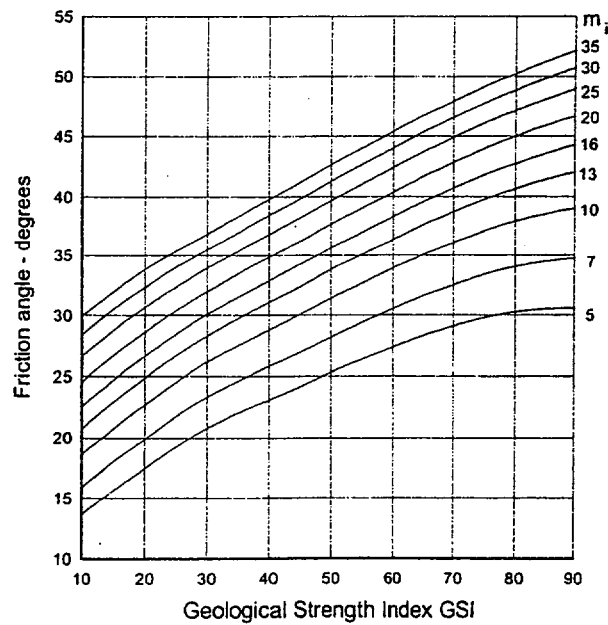


Figure 11.8: Plot of results from simulated full scale triaxial tests on a rock mass defined by a uniaxial compressive strength $\sigma_{ci} = 85$ MPa, a Hoek-Brown constant $m_i = 10$ and a Geological Strength Index GSI = 45.



a. Plot of ratio of cohesive strength c' to uniaxial compressive strength σ_{ci} .



b. Plot of friction angle ϕ'

Figure 11.9: Plots of cohesive strength and friction angles for different GSI and m_i values.

11.7 Deformation modulus

Serafim and Pereira (1983) proposed a relationship between the in situ modulus of deformation and Bieniawski's RMR classification. This relationship is based upon back analysis of dam foundation deformations and it has been found to work well for better quality rocks. However, for many of the poor quality rocks it appears to predict deformation modulus values which are too high. Based upon practical observations and back analysis of excavation behaviour in poor quality rock masses, the following modification to Serafim and Pereira's equation is proposed for $\sigma_{ci} < 100$:

$$E_m = \sqrt{\frac{\sigma_{ci}}{100}} 10^{\left(\frac{GSI-10}{40}\right)} \quad (11.30)$$

Note that GSI has been substituted for RMR in this equation and that the modulus E_m is reduced progressively as the value of σ_{ci} falls below 100. This reduction is based upon the reasoning that the deformation of better quality rock masses is controlled by the discontinuities while, for poorer quality rock masses, the deformation of the intact rock pieces contributes to the overall deformation process.

Based upon measured deformations, equation 11.30 appears to work reasonably well in those cases where it has been applied. However, as more field evidence is gathered it may be necessary to modify this relationship.

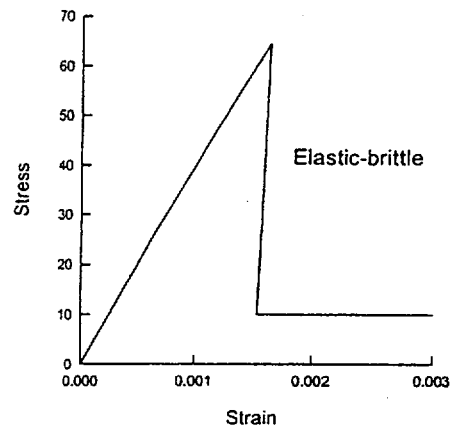
11.8 Post-failure behaviour

When using numerical models to study the progressive failure of rock masses, estimates of the post-peak or post-failure characteristics of the rock mass are required. In some of these models, the Hoek-Brown failure criterion is treated as a yield criterion and the analysis is carried out using plasticity theory (e.g. Pan and Hudson 1988). No definite rules for dealing with this problem can be given but, based upon experience in numerical analysis of a variety of practical problems, the post-failure characteristics illustrated in Figure 11.10 are suggested as a starting point.

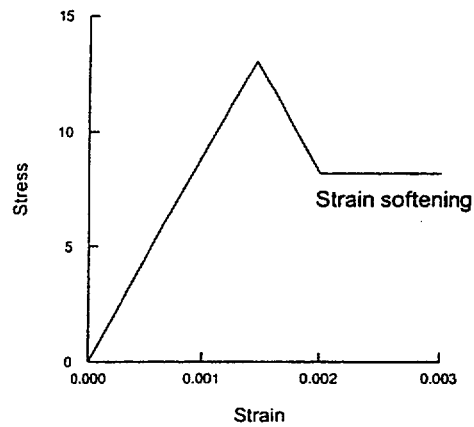
11.8.1 Very good quality hard rock masses

For very good quality hard rock masses, such as massive granites or quartzites, the analysis of spalling around highly stressed openings (Hoek, Kaiser and Bawden 1995) suggests that the rock mass behaves in an elastic brittle manner as shown in Figure 11.10(a). When the strength of the rock mass is exceeded, a sudden strength drop occurs. This is associated with significant dilation of the broken rock pieces. If this broken rock is confined, for example by rock support, then it can be assumed to behave as a rock fill with a friction angle of approximately $\phi' = 38^\circ$ and zero cohesive strength.

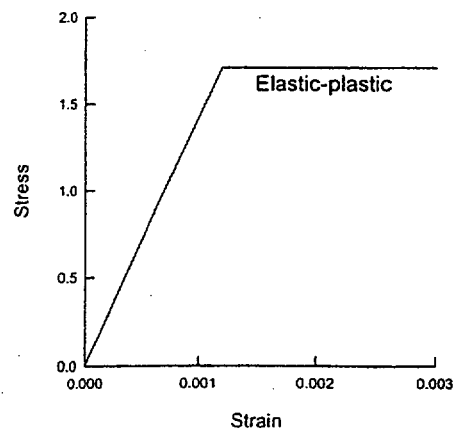
Typical properties for this very good quality hard rock mass may be as shown in Table 11.7. Note that, in some numerical analyses, it may be necessary to assign a very small cohesive strength in order to avoid numerical instability.



(a) Very good quality hard rock mass



(b) Average quality rock mass



(c) Very poor quality soft rock mass

Figure 11.10: Suggested post failure characteristics for different quality rock masses.

Table 11.7: Typical properties for a very good quality hard rock mass

Intact rock strength	σ_{ci}	150 MPa
Hoek-Brown constant	m_i	25
Geological Strength Index	GSI	75
Friction angle	ϕ'	46°
Cohesive strength	c'	13 MPa
Rock mass compressive strength	σ_{cm}	64.8 MPa
Rock mass tensile strength	σ_{tm}	-0.9 MPa
Deformation modulus	E_m	42000 MPa
Poisson's ratio	ν	0.2
Dilation angle	α	$\phi'/4 = 11.5^\circ$
<i>Post-peak characteristics</i>		
Friction angle	ϕ'_f	38°
Cohesive strength	c'_f	0
Deformation modulus	E_{fm}	10000 MPa

11.8.2 Average quality rock mass

In the case of an average quality rock mass it is reasonable to assume that the post-failure characteristics can be estimated by reducing the GSI value from the in situ value to a lower value which characterises the broken rock mass.

The reduction of the rock mass strength from the in situ to the broken state corresponds to the strain softening behaviour illustrated in Figure 11.10(b). In this figure it has been assumed that post failure deformation occurs at a constant stress level, defined by the compressive strength of the broken rock mass. The validity of this assumption is unknown.

Typical properties for this average quality rock mass may be as follows:

Table 10.8: Typical properties for an average rock mass.

Intact rock strength	σ_{ci}	80 MPa
Hoek-Brown constant	m_i	12
Geological Strength Index	GSI	50
Friction angle	ϕ'	33°
Cohesive strength	c'	3.5 MPa
Rock mass compressive strength	σ_{cm}	13 MPa
Rock mass tensile strength	σ_{tm}	-0.15
Deformation modulus	E_m	9000 MPa
Poisson's ratio	ν	0.25
Dilation angle	α	$\phi'/8 = 4^\circ$
<i>Post-peak characteristics</i>		
Broken rock mass strength	σ_{fcm}	8 MPa
Deformation modulus	E_{fm}	5000 MPa

11.8.3 Very poor quality rock mass

Analysis of the progressive failure of very poor quality rock masses surrounding tunnels suggests that the post-failure characteristics of the rock are adequately represented by assuming that it behaves perfectly plastically. This means that it

continues to deform at a constant stress level and that no volume change is associated with this ongoing failure. This type of behaviour is illustrated in Figure 10.10(c).

Typical properties for this very poor quality rock mass may be as follows:

Table 11.9: Typical properties for a very poor quality rock mass

Intact rock strength	σ_{ci}	20 MPa
Hoek-Brown constant	m_i	8
Geological Strength Index	GSI	30
Friction angle	ϕ'	24°
Cohesive strength	c'	0.55 MPa
Rock mass compressive strength	σ_{cm}	1.7 MPa
Rock mass tensile strength	σ_{tm}	-0.01 MPa
Deformation modulus	E_m	1400 MPa
Poisson's ratio	ν	0.3
Dilation angle	α	zero
<i>Post-peak characteristics</i>		
Broken rock mass strength	σ_{fcm}	1.7 MPa
Deformation modulus	E_{fm}	1400 MPa

11.9 Reliability of rock mass strength estimates

The techniques described in the preceding sections of this chapter can be used to estimate the strength and deformation characteristics of isotropic jointed rock masses. When applying this procedure to rock engineering design problems, most users consider only the 'average' or mean properties. In fact, all of these properties exhibit a distribution about the mean, even under the most ideal conditions, and these distributions can have a significant impact upon the design calculations.

In the text that follows, a slope stability calculation and a tunnel support design calculation are carried out in order to evaluate influence of these distributions. In each case the strength and deformation characteristics of the rock mass are estimated by means of the Hoek-Brown procedure, assuming that the three input parameters are defined by normal distributions.

11.9.1 Input parameters

Figure 11.11 has been used to estimate the value of the value of GSI from field observations of blockiness and discontinuity surface conditions. Included in this figure is a crosshatched circle representing the 90% confidence limits of a GSI value of 25 ± 5 (equivalent to a standard deviation of approximately 2.5). This represents the range of values that an experienced geologist would assign to a rock mass described as BLOCKY/DISTURBED or DISINTEGRATED and POOR. Typically, rocks such as flysch, schist and some phyllites may fall within this range of rock mass descriptions.

ATTACHMENT 2
Hoek-Brown Criterion Spreadsheet Verification Runs

VERIFICATION RUN CP19-V21

Input:	sig0 = 85 MPa	mi = 10	Unit m = 0.027 MN/m3
Output:	sig0 = 21.25 MPa	mi = 1.40 MPa	Unit m = 0.027 MN/m3
	a = 0.5	sigm = -0.1343 MPa	
	b = 0.6803	k = 3.01	
	c0h = 3.2710 MPa	sigm = 11.38 MPa	

Calculation:

sig3	1E-10	3.04	6.07	9.11	12.14	15.18	18.21	21.25	Sums
sig1	4.00	22.48	33.27	42.30	50.40	57.91	64.98	71.74	85.00
del683	15.89	4.07	3.19	2.60	2.56	2.40	2.27	2.16	347.08
sig4	0.24	6.87	12.58	17.85	22.90	27.76	32.50	37.13	35.35
tau	0.94	7.74	11.59	14.62	17.20	19.48	21.54	23.44	157.80
k	-2.36	-1.08	-0.83	-0.67	-0.57	-0.48	-0.42	-0.36	116.55
y	-1.95	-1.04	-0.87	-0.76	-0.69	-0.64	-0.60	-0.56	-0.77
xy	4.81	1.13	0.71	0.52	0.39	0.31	0.25	0.20	-7.11
tauq	3.57	1.17	0.88	0.45	0.32	0.23	0.17	0.13	8.12
sig6sig1	0.00	66.23	202.01	385.23	612.01	878.92	1183.65	1524.51	4855
sig3sig4	0.00	9.22	36.88	82.94	147.45	230.39	331.76	451.56	1290
taucaic	0.96	7.48	11.33	14.45	17.18	19.64	21.91	24.04	
sig1sig3sig1	11.38	20.51	28.66	36.81	47.98	57.11	66.26	75.42	
sigtau	3.41	7.26	10.56	13.63	16.55	19.38	22.12	24.81	

Verification Table 11.7: Typical properties for a very good quality hard rock mass

Run CP.19-VR2 input	Intact rock strength	σ_{ri} (A) 150 MPa	input
	Hoek-Brown constant	m_i (B) 25	
	Geological Strength Index	GSI (C) 75	
	Friction angle	ϕ' 46° (D)	Check values
	Cohesive strength	c' 13 MPa (E)	
	Rock mass compressive strength	σ_{cm} 64.8 MPa (F)	
	Rock mass tensile strength	σ_{tm} -0.9 MPa (G)	
	Deformation modulus	E_m 42000 MPa (H)	
	Poisson's ratio	ν 0.2	
	Dilation angle	α $\phi'/4 = 11.5^\circ$	
	Post-peak characteristics		
	Friction angle	ϕ'_r 38°	VR-2 INPUT
	Cohesive strength	c'_r 0	
	Deformation modulus	E_{rm} 10000 MPa	

11.8.2 Average quality rock mass

In the case of an average quality rock mass it is reasonable to assume that the post-failure characteristics can be estimated by reducing the GSI value from the in situ value to a lower value which characterises the broken rock mass.

The reduction of the rock mass strength from the in situ to the broken state corresponds to the strain softening behaviour illustrated in Figure 11.10(b). In this figure it has been assumed that post failure deformation occurs at a constant stress level, defined by the compressive strength of the broken rock mass. The validity of this assumption is unknown.

Typical properties for this average quality rock mass may be as follows:

Verification Run Table 10.8: Typical properties for an average rock mass.

CP.19-VR3 input	Intact rock strength	σ_{ri} 80 MPa (A)	input
	Hoek-Brown constant	m_i 12 (B)	
	Geological Strength Index	GSI 50 (C)	
	Friction angle	ϕ' 33° (D)	Check values
	Cohesive strength	c' 3.5 MPa (E)	
	Rock mass compressive strength	σ_{cm} 13 MPa (F)	
	Rock mass tensile strength	σ_{tm} -0.15 (G)	
	Deformation modulus	E_m 9000 MPa (H)	
	Poisson's ratio	ν 0.25	
	Dilation angle	α $\phi'/8 = 4^\circ$	
	Post-peak characteristics		
	Broken rock mass strength	σ_{fcm} 8 MPa	VR-3 INPUT
	Deformation modulus	E_{fm} 5000 MPa	

11.8.3 Very poor quality rock mass

Analysis of the progressive failure of very poor quality rock masses surrounding tunnels suggests that the post-failure characteristics of the rock are adequately represented by assuming that it behaves perfectly plastically. This means that it

Hoek, 2001

2

VERIFICATION RUN: TABLE 11.7 FROM CHAPT. 11, PAGE 184, HOEK (2000) - VERY GOOD ROCK MASS*

Input: slope = 150 MPa (5) m = 25 (5) GSI = 75 (5)
Depth of failure surface or tunnel below slope = 100 m Unit wt = 0.027 MN/m3

Output: stress = 37.50 MPa mb = 10.24 n = 0.0822
a = 0.5 siglm = -0.9105 MPa (5) A = 0.9894
B = 0.7202 k = 6.15 dh = 16.06
coh = 13.066 MPa (5) sigcm = 64.79 MPa (5) E = 42189.7 MPa (5)

Calculation:

sig3	1E+10	5.36	10.71	18.07	21.43	28.78	32.14	37.50	Sum	150.00
sig1	37.40	103.47	144.32	177.56	208.84	233.01	237.43	260.38		1440.20
da1da3	21.53	8.83	6.75	5.75	5.15	4.72	4.41	4.16		61.29
sign	1.66	15.34	27.96	39.88	51.57	62.82	73.80	84.55		357.59
lau	7.70	29.66	44.80	57.35	68.36	76.31	82.46	85.96		489.65
x	-1.77	-0.97	-0.72	-0.56	-0.46	-0.37	-0.30	-0.24		-5.39
y	-1.29	-0.70	-0.52	-0.42	-0.34	-0.28	-0.23	-0.19		-3.99
xy	2.28	0.68	0.38	0.24	0.16	0.10	0.07	0.05		3.95
xyq	3.12	0.93	0.51	0.32	0.21	0.14	0.09	0.06		5.38
sig3sig1	0.00	554.28	1546.32	2853.60	4428.04	6241.45	8274.89	10513.83		34412
sig3sig	0.00	28.70	114.80	258.29	459.18	717.47	1033.16	1408.25		4018
laucaic	7.77	28.34	44.38	57.02	68.25	76.50	82.02	86.97		4018
sig1sig3it	64.78	97.71	130.84	163.56	196.49	228.41	262.34	293.26		100.82
sigtauult	14.79	28.99	42.08	54.56	66.59	76.27	83.66	89.82		100.82

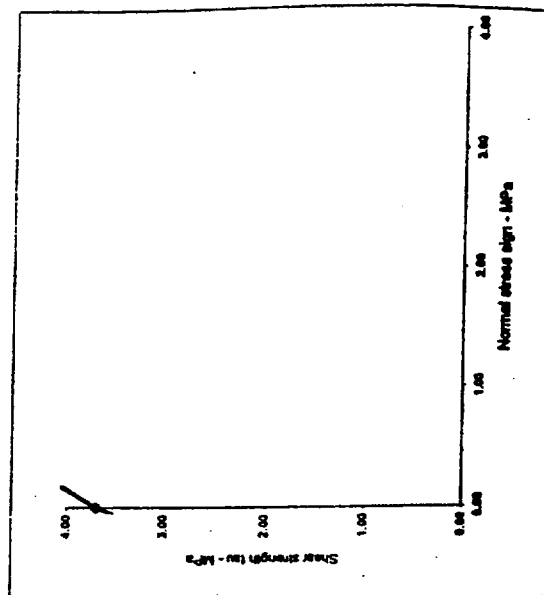
Cell formulas:

```

sigma3 = IF(depth>90, sigc*0.25, depth*unitwt)
mb = m*EXP((GSI-100)/28)
a = IF(GSI>25, EXP((GSI-100)/9), 0)
b = IF(GSI>25, 0.5-0.65*(GSI/200))
siglm = 0.5*sigc/(mb-SQRT((mb^2+4*a)))
sig3 = Start at 1E-10 (to avoid zero errors) and increment in 7 steps to stress
sig1 = sig3*sigc/((mb*sig3)/sigc+a)*a
da1da3 = IF(GSI>25, (1+(mb*sigc)/(2*(sig1-sig3))), 1+(a*mb*a)/(sig3*sigc)*(a-1))
lau = (sig1-sig3)/SQRT(da1da3)
x = LOG((lau-siglm)/sigc)
y = LOG((lau/sigc))
xy = x*y
xyq = x^2
A = scale = 10*(x+y)/8 - b*caic*sumx/8
B = b*caic = (sumxy - (sumx*sumy)/8)/(sumxq - (sumx^2)/8)
k = (sumsig3sig1 - (sumsig3*sumsig1)/8)/(sumsig3q - (sumsig3^2)/8)
phi = ASIN((k-1)/(k+1))^180/PI()
coh = sigcm/(2*SQRT(k))
sigcm = sumsig1/8 - k*sumsig3/8
E = IF(sigc>100, 1000*10^4*(GSI-10)/40, SQRT(sigc/100)*1000*10^4*(GSI-10)/40)
phiH = (ATAN((caic-b*caic)/(sig1-siglm)/sigc)/(b*caic-1))^180/PI()
cohH = caic*sigc/((sig1-siglm)/sigc)/(b*caic-sig1*TAN(phiH/PI/180))
sig3sig1 = sig3*sig1
laucaic = caic*sigc/((sig1-siglm)/sigc)/(b*caic-sig1*TAN(phiH/PI/180))
a3ult = sigcm+k*sig3
tauult = coh+sig1*TAN(phiH/PI/180)
tauq = coh+sig1*TAN(phiH/PI/180)

```

sig3 & sign	Principal stress plot	sig1	sig3	sign	sig3sig1	sign	laucaic	tauult
siglm	-0.91	0.00	-0.91	0.00	58.19	-0.91	0.00	12.12
siglm^3/4	-0.88	18.04	-0.88	0.00	60.59	-0.88	1.38	12.36
siglm^3/4	-0.48	28.00	-0.48	0.00	61.99	-0.48	2.23	12.59
0	-0.23	32.17	-0.23	0.00	63.39	-0.23	2.99	12.83
0	0.00	37.40	0.00	0.00	64.79	0.00	3.68	13.07
stress/10.5	3.28	83.30	3.28	0.00	64.83	3.28	11.02	16.45
stress/10	3.75	88.35	3.75	0.00	67.83	3.75	11.93	16.96
stress/9.5	3.95	90.32	3.95	0.00	69.05	3.95	12.29	17.16
stress/9	4.17	92.47	4.17	0.00	70.40	4.17	12.69	17.39
stress/8.5	4.41	94.82	4.41	0.00	71.80	4.41	13.13	17.65
stress/8	4.69	97.41	4.69	0.00	73.20	4.69	13.62	17.93
stress/7.5	5.00	100.27	5.00	0.00	74.62	5.00	14.16	18.26
stress/7	5.38	103.47	5.38	0.00	76.11	5.38	14.77	18.63
stress/6.5	5.77	107.05	5.77	0.00	77.71	5.77	15.46	19.05
stress/6	6.25	111.11	6.25	0.00	79.40	6.25	16.26	19.55
stress/5.5	6.82	115.78	6.82	0.00	81.18	6.82	17.18	20.14
stress/5	7.50	121.15	7.50	0.00	83.08	7.50	18.26	20.85
stress/4.5	8.33	127.48	8.33	0.00	85.11	8.33	19.54	21.72
stress/4	9.38	135.05	9.38	0.00	87.38	9.38	21.10	22.80
stress/3.5	10.71	144.32	10.71	0.00	90.00	10.71	23.05	24.19
stress/3	12.50	154.00	12.50	0.00	92.81	12.50	25.55	26.04
stress/2.5	15.00	171.31	15.00	0.00	95.88	15.00	28.89	28.63
stress/2	18.75	192.51	18.75	0.00	100.03	18.75	33.65	32.53
stress/1.5	23.00	224.47	23.00	0.00	106.44	23.00	41.05	39.01
stress	37.50	290.38	37.50	0.00	114.26	37.50	54.51	51.99
stress/0.5	75.00	416.42	75.00	0.00	125.74	75.00	89.03	90.91



VERIFICATION RUN, TABLE 11.8 FROM CHART 11, PAGE 184, HOEK (2000) - "AVERAGE ROCK MASS"
 Input: $\sigma_{ci} = 80$ MPa $\sigma_{ci} = 12$ MPa $GSI = 50$
 Depth of failure surface or tunnel below slope = 100 m Unit wt. = 0.027 MN/m³

Output: $\sigma_{ci} = 20.00$ MPa $\sigma_{ci} = 2.01$ MPa $\sigma_{ci} = 0.0039$ MPa
 $\sigma_{ci} = 0.5$ MPa $\sigma_{ci} = -0.1536$ MPa $\sigma_{ci} = 0.3715$ MPa
 $\sigma_{ci} = 0.7033$ MPa $\sigma_{ci} = 3.40$ MPa $\sigma_{ci} = 33.05$ MPa
 Coh = 3.339 MPa $\sigma_{ci} = 13.05$ MPa $\sigma_{ci} = 8944.3$ MPa

Calculation:																																																																																																																																																																																																																																																																																																																																																																																																																																																																																																																																																																																																																																																																																																																																																																																																																																																																																																																																																																																																																																																																																																																																																																																																																																																																																																																																																																																																																																																																						</
--------------	--	--	--	--	--	--	--	--	--	--	--	--	--	--	--	--	--	--	--	--	--	--	--	--	--	--	--	--	--	--	--	--	--	--	--	--	--	--	--	--	--	--	--	--	--	--	--	--	--	--	--	--	--	--	--	--	--	--	--	--	--	--	--	--	--	--	--	--	--	--	--	--	--	--	--	--	--	--	--	--	--	--	--	--	--	--	--	--	--	--	--	--	--	--	--	--	--	--	--	--	--	--	--	--	--	--	--	--	--	--	--	--	--	--	--	--	--	--	--	--	--	--	--	--	--	--	--	--	--	--	--	--	--	--	--	--	--	--	--	--	--	--	--	--	--	--	--	--	--	--	--	--	--	--	--	--	--	--	--	--	--	--	--	--	--	--	--	--	--	--	--	--	--	--	--	--	--	--	--	--	--	--	--	--	--	--	--	--	--	--	--	--	--	--	--	--	--	--	--	--	--	--	--	--	--	--	--	--	--	--	--	--	--	--	--	--	--	--	--	--	--	--	--	--	--	--	--	--	--	--	--	--	--	--	--	--	--	--	--	--	--	--	--	--	--	--	--	--	--	--	--	--	--	--	--	--	--	--	--	--	--	--	--	--	--	--	--	--	--	--	--	--	--	--	--	--	--	--	--	--	--	--	--	--	--	--	--	--	--	--	--	--	--	--	--	--	--	--	--	--	--	--	--	--	--	--	--	--	--	--	--	--	--	--	--	--	--	--	--	--	--	--	--	--	--	--	--	--	--	--	--	--	--	--	--	--	--	--	--	--	--	--	--	--	--	--	--	--	--	--	--	--	--	--	--	--	--	--	--	--	--	--	--	--	--	--	--	--	--	--	--	--	--	--	--	--	--	--	--	--	--	--	--	--	--	--	--	--	--	--	--	--	--	--	--	--	--	--	--	--	--	--	--	--	--	--	--	--	--	--	--	--	--	--	--	--	--	--	--	--	--	--	--	--	--	--	--	--	--	--	--	--	--	--	--	--	--	--	--	--	--	--	--	--	--	--	--	--	--	--	--	--	--	--	--	--	--	--	--	--	--	--	--	--	--	--	--	--	--	--	--	--	--	--	--	--	--	--	--	--	--	--	--	--	--	--	--	--	--	--	--	--	--	--	--	--	--	--	--	--	--	--	--	--	--	--	--	--	--	--	--	--	--	--	--	--	--	--	--	--	--	--	--	--	--	--	--	--	--	--	--	--	--	--	--	--	--	--	--	--	--	--	--	--	--	--	--	--	--	--	--	--	--	--	--	--	--	--	--	--	--	--	--	--	--	--	--	--	--	--	--	--	--	--	--	--	--	--	--	--	--	--	--	--	--	--	--	--	--	--	--	--	--	--	--	--	--	--	--	--	--	--	--	--	--	--	--	--	--	--	--	--	--	--	--	--	--	--	--	--	--	--	--	--	--	--	--	--	--	--	--	--	--	--	--	--	--	--	--	--	--	--	--	--	--	--	--	--	--	--	--	--	--	--	--	--	--	--	--	--	--	--	--	--	--	--	--	--	--	--	--	--	--	--	--	--	--	--	--	--	--	--	--	--	--	--	--	--	--	--	--	--	--	--	--	--	--	--	--	--	--	--	--	--	--	--	--	--	--	--	--	--	--	--	--	--	--	--	--	--	--	--	--	--	--	--	--	--	--	--	--	--	--	--	--	--	--	--	--	--	--	--	--	--	--	--	--	--	--	--	--	--	--	--	--	--	--	--	--	--	--	--	--	--	--	--	--	--	--	--	--	--	--	--	--	--	--	--	--	--	--	--	--	--	--	--	--	--	--	--	--	--	--	--	--	--	--	--	--	--	--	--	--	--	--	--	--	--	--	--	--	--	--	--	--	--	--	--	--	--	--	--	--	--	--	--	--	--	--	--	--	--	--	--	--	--	--	--	--	--	--	--	--	--	--	--	--	--	--	--	--	--	--	--	--	--	--	--	--	--	--	--	--	--	--	--	--	--	--	--	--	--	--	--	--	--	--	--	--	--	--	--	--	--	--	--	--	--	--	--	--	--	--	--	--	--	--	--	--	--	--	--	--	--	--	--	--	--	--	--	--	--	--	--	--	--	--	--	--	--	--	--	--	--	--	--	--	--	--	--	--	--	--	--	--	--	--	--	--	--	--	--	--	--	--	--	--	--	--	--	--	--	--	--	--	--	--	--	--	--	--	--	--	--	--	--	--	--	--	--	--	--	--	--	--	--	--	--	--	--	--	--	--	--	--	--	--	--	--	--	--	--	--	--	--	--	--	--	--	--	--	--	--	--	--	--	--	--	--	--	--	--	--	--	--	--	--	--	--	--	--	--	--	--	--	--	--	--	--	--	--	--	--	--	--	--	--	--	--	--	--	--	--	--	--	--	--	--	--	--	--	--	--	--	--	--	--	--	--	--	--	--	--	--	--	--	--	--	--	--	--	--	--	--	--	--	--	--	--	--	--	--	--	--	--	--	--	--	--	--	--	--	--	--	--	--	--	--	--	--	--	--	--	--	--	--	--	--	--	--	--	--	--	--	--	--	--	--	--	--	--	--	--	--	--	--	--	--	--	--	--	--	--	--	--	--	--	--	--	--	--	--	--	--	--	--	--	--	--	--	--	--	--	--	--	--	--	--	--	--	--	--	--	--	--	--	--	--	--	--	--	--	--	--	--	--	--	--	--	--	--	--	--	--	--	--	--	--	--	--	--	--	--	--	--	--	--	--	--	--	--	--	--	--	--	--	--	--	--	--	--	--	--	--	--	--	--	--	--	--	--	--	--	--	--	--	--	--	--	--	--	--	--	--	--	--	--	--	--	--	--	--	--	--	--	--	--	--	--	--	--	--	--	--	--	--	--	--	--	--	--	--	--	--	--	--	--	--	--	--	--	--	--	--	--	--	--	--	--	--	--	--	--	--	--	--	--	--	--	--	--	--	--	--	--	--	--	--	--	--	--	--	--	--	--	--	--	--	--	--	--	--	--	--	--	--	--	--	--	--	--	--	--	--	--	--	--	--	--	--	--	--	--	--	--	--	--	--	--	--	--	--	--	--	--	--	--	--	--	--	--	--	--	--	--	--	--	--	--	--	--	--	--	--	--	--	--	--	--	--	--	--	--	--	--	--	--	--	--	--	--	--	--	--	--	--	--	--	--	--	--	--	--	--	--	--	--	--	--	--	--	--	--	--	--	--	--	--	--	--	--	--	--	----

continues to deform at a constant stress level and that no volume change is associated with this ongoing failure. This type of behaviour is illustrated in Figure 10.10(c). Typical properties for this very poor quality rock mass may be as follows:

Table 11.9: Typical properties for a very poor quality rock mass

CP17-VR4 input	Intact rock strength	σ_{ri} (A) 20 MPa	input	VR-4 INPUT
	Hoek-Brown constant	m_i (B) 8		
	Geological Strength Index	GSI (C) 30		
	Friction angle	ϕ' 24° (D)	input	
	Cohesive strength	c' 0.55 MPa (E)		
	Rock mass compressive strength	σ_{cm} 1.7 MPa (F)		
	Rock mass tensile strength	σ_{tm} -0.01 MPa (G)	input	
	Deformation modulus	E_m 1400 MPa (H)		
	Poisson's ratio	ν 0.3		
	Dilation angle	α zero	input	
	Post-peak characteristics			
	Broken rock mass strength	σ_{brm} 1.7 MPa		
	Deformation modulus	E_{brm} 1400 MPa		

11.9 Reliability of rock mass strength estimates

The techniques described in the preceding sections of this chapter can be used to estimate the strength and deformation characteristics of isotropic jointed rock masses. When applying this procedure to rock engineering design problems, most users consider only the 'average' or mean properties. In fact, all of these properties exhibit a distribution about the mean, even under the most ideal conditions, and these distributions can have a significant impact upon the design calculations.

In the text that follows, a slope stability calculation and a tunnel support design calculation are carried out in order to evaluate influence of these distributions. In each case the strength and deformation characteristics of the rock mass are estimated by means of the Hoek-Brown procedure, assuming that the three input parameters are defined by normal distributions.

11.9.1 Input parameters

Figure 11.11 has been used to estimate the value of the value of GSI from field observations of blockiness and discontinuity surface conditions. Included in this figure is a crosshatched circle representing the 90% confidence limits of a GSI value of 25 ± 5 (equivalent to a standard deviation of approximately 2.5). This represents the range of values that an experienced geologist would assign to a rock mass described as BLOCKY/DISTURBED or DISINTEGRATED and POOR. Typically, rocks such as flysch, schist and some phyllites may fall within this range of rock mass descriptions.

Check input

VERIFICATION RUN: TABLE 11.9 FROM CHAPT. 11, PAGE 183, HOEK (2000) - VERY POOR ROCK MASS

Input: $\sigma_{3cd} = 20$ MPa $\sigma_1 = 8$ MPa $GSI = 30$ $\phi = 0.027$ $MFR = 3$
 Depth of failure surface of tunnel below slope = 100 m Unit wt. = 0.027 MPa/m

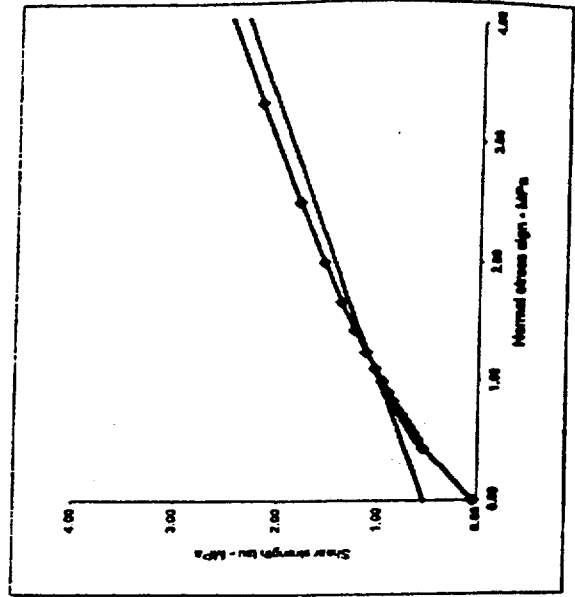
Output: stress = 5.00 MPa $m_b = 0.68$ $\sigma_{lim} = -0.0127$ MPa $\phi = 0.0004$
 $B = 0.8113$ $k = 2.41$ $pH = 24.39$ $\phi = 0.0004$
 $\phi_{cd} = 0.351$ $\mu_{cd} = 1.71$ $E = 1414.2$ MPa

Calculation:

	1E-10	0.71	1.43	2.14	2.86	3.57	4.29	5.00	Sums
σ_3	0.41	3.80	5.78	7.46	9.00	10.43	11.80	13.11	20.00
σ_1	17.04	3.13	2.51	2.23	2.07	1.96	1.87	1.81	61.00
σ_{lim}	0.02	1.46	2.87	3.79	4.86	5.89	6.90	7.89	32.92
τ	0.09	1.32	1.98	2.46	2.88	3.25	3.58	3.88	19.43
μ	-2.75	-1.13	-0.87	-0.72	-0.61	-0.53	-0.46	-0.40	-7.49
ν	-2.33	-1.18	-1.01	-0.91	-0.84	-0.79	-0.75	-0.71	-8.52
ν	6.41	1.33	0.88	0.66	0.52	0.42	0.34	0.29	10.85
σ_{3cd}	0.00	2.72	8.28	15.99	25.70	37.26	50.37	65.37	208
σ_{3cd}	0.00	0.51	2.04	4.59	8.16	12.76	18.37	25.00	71
τ_{cd}	0.10	1.26	1.90	2.42	2.88	3.29	3.67	4.02	13.74
σ_{1cd}	1.71	3.43	5.15	6.87	8.58	10.30	12.02	13.74	4.13
σ_{lim}	0.56	1.21	1.76	2.27	2.75	3.22	3.68	4.13	

Cell formulas:

$\sigma_3 = \text{IF}(\text{depth} > 90, \sigma_{3cd} \cdot 0.25, \text{depth} \cdot \text{unitwt})$
 $m_b = m \cdot \text{EXP}((GSI - 100)/28)$
 $a = \text{IF}(GSI > 25, \text{EXP}((GSI - 100)/9), 0)$
 $a = \text{IF}(GSI > 25, 0.5, 0.65 - GSI/200)$
 $\sigma_{lim} = 0.5 \cdot \sigma_{3cd} \cdot (m_b \cdot \text{SQRT}(m_b^2 + a^2))$
 $\sigma_3 = \sigma_3$ Start at 1E-10 (to avoid zero errors) and increment in 7 steps to stress
 $\sigma_1 = \sigma_3 + \sigma_{lim} \cdot ((m_b \cdot \sigma_3) / (\sigma_3 + a))$
 $\sigma_{1cd} = \text{IF}(GSI > 25, (1 + (m_b \cdot \sigma_{lim}) / (2 \cdot (\sigma_3 + a))) \cdot (a \cdot m_b \cdot a) \cdot (\sigma_3 + a) \cdot (e - 1))$
 $\sigma_{lim} = \sigma_3 + (\sigma_3 - \sigma_{lim}) / (1 + \sigma_{1cd})$
 $\tau = (\sigma_3 - \sigma_{lim}) \cdot \text{SQRT}(d \cdot \sigma_{1cd})$
 $\mu = \text{LOG}((\sigma_3 - \sigma_{lim}) / \sigma_{lim})$
 $\nu = \text{LOG}((\tau / \sigma_{lim}))$
 $\nu = \nu \cdot \nu$ $\nu = \nu \cdot \nu^2$
 $A = \text{scale} = 10 \cdot (\sum \nu^8 \cdot \text{scale} \cdot \sum \nu^8)$
 $B = \text{scale} = (\sum \nu^8 \cdot \text{scale} \cdot \sum \nu^8) / (\sum \nu^8 \cdot \text{scale} \cdot \sum \nu^8)$
 $k = (\sum \nu^8 \cdot \sigma_3 \cdot 1 - (\sum \nu^8 \cdot \sigma_3 \cdot \sum \nu^8) / (\sum \nu^8 \cdot \sigma_3 \cdot \sum \nu^8)) \cdot (\sum \nu^8 \cdot \sigma_3 \cdot 2) / 8$
 $pH = \text{ASIN}((k - 1) / (k + 1)) \cdot 180 / \pi$
 $\phi_{cd} = \phi_{lim} \cdot (1 - \text{SQRT}(1 - pH))$
 $\sigma_{lim} = \sum \nu^8 \cdot 1 / 8 \cdot k \cdot \sum \nu^8 / 8$
 $E = \text{IF}(\sigma_{lim} > 100, 1000 \cdot 10^{(GSI - 10)/40}, \text{SQRT}(\sigma_{lim} / 100) \cdot 1000 \cdot 10^{(GSI - 10)/40})$
 $pH = (\text{ATAN}(\text{scale} \cdot \text{scale} \cdot (\sigma_{lim} - \sigma_{lim}) / \sigma_{lim} \cdot \text{scale} \cdot 1)) \cdot 180 / \pi$
 $\phi_{cd} = \text{scale} \cdot \sigma_{lim} \cdot (\sigma_{lim} - \sigma_{lim}) / \sigma_{lim} \cdot \text{scale} \cdot \sigma_{lim} \cdot \text{TAN}(pH \cdot \pi / 180)$
 $\sigma_{3cd} = \sigma_3 + \sigma_1$ $\sigma_{3cd} = \sigma_3 + 2$
 $\tau_{cd} = \text{scale} \cdot \sigma_{lim} \cdot (\sigma_{lim} - \sigma_{lim}) / \sigma_{lim} \cdot \text{scale} \cdot \sigma_{lim} \cdot \text{TAN}(pH \cdot \pi / 180)$
 $\sigma_{1cd} = \text{scale} \cdot \sigma_{lim} \cdot (\sigma_{lim} - \sigma_{lim}) / \sigma_{lim} \cdot \text{scale} \cdot \sigma_{lim} \cdot \text{TAN}(pH \cdot \pi / 180)$
 $\sigma_{lim} = \text{scale} \cdot \sigma_{lim} \cdot (\sigma_{lim} - \sigma_{lim}) / \sigma_{lim} \cdot \text{scale} \cdot \sigma_{lim} \cdot \text{TAN}(pH \cdot \pi / 180)$



ATTACHMENT 3
ISFSI Site Hoek-Brown Criterion Shear Strength Calculation Runs

Calculation Package 0.19 - Hoek-Brown Rock Mass Strength Worksheet **DOLOMITE LOWER BOUND, HOEK-BROWN**

Input:	sigci = 18 MPa	mi = 13	GSI = 46
	Depth of failure surface or tunnel below slope = 50 m	Unit wt. = 0.022 MN/m3	
Output:	stress = 1.08 MPa	mb = 1.96	s = 0.0026
	a = 0.5	siglm = -0.0231 MPa	A = 0.6037
	B = 0.7176	k = 5.57	phi = 44.06 degrees
	coh = 0.341 MPa	sigcm = 1.61 MPa	E = 3400.3 MPa

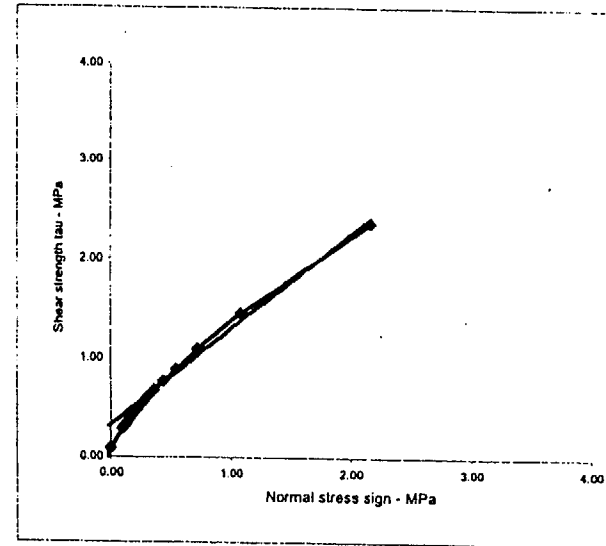
Calculation:

	sig3	sig1	ds1ds3	sign	tau	x	y	xy	xsq	sig3sig1	sig3sq	laucalc	sig1sig3fit	signtaufit	Sums
	1E-10	0.15	0.31	0.46	0.62	0.77	0.93	1.08	4.32						
	0.89	2.62	3.68	4.55	5.30	5.99	6.63	7.23	36.90						
	20.26	7.96	6.09	5.20	4.66	4.29	4.01	3.79	56.25						
	0.04	0.43	0.78	1.12	1.44	1.76	2.06	2.36	10.01						
	0.19	0.78	1.17	1.50	1.79	2.04	2.28	2.50	12.25						
	-2.43	-1.59	-1.34	-1.18	-1.08	-0.99	-0.92	-0.87	-10.39						
	-1.97	-1.35	-1.17	-1.07	-0.99	-0.93	-0.88	-0.85	-9.21						
	4.78	2.15	1.57	1.26	1.07	0.93	0.82	0.73	13.30						
	5.91	2.52	1.78	1.40	1.16	0.98	0.85	0.75	15.36						
	0.00	0.40	1.14	2.10	3.27	4.62	6.13	7.81	25						
	0.00	0.02	0.10	0.21	0.38	0.59	0.86	1.17	3						
	0.19	0.77	1.16	1.49	1.78	2.05	2.30	2.53							
	1.61	2.47	3.32	4.18	5.04	5.90	6.76	7.62							
	0.38	0.76	1.10	1.43	1.74	2.04	2.34	2.63							

Cell formulae:

σ_c	stress = if(depth>90, sigci*0.25,depth*unitwt)
m_b	mb = mi*EXP((GSI-100)/28)
s	s = IF(GSI>25,EXP((GSI-100)/9),0)
a	a = IF(GSI>25,0.5,0.65-GSI/200)
σ_{lm}	siglm = 0.5*sigci*(mb-SQRT(mb^2+4*s))
σ_3	sig3 = Start at 1E-10 (to avoid zero errors) and increment in 7 steps to stress
σ_1	sig1 = sig3+sigci*(((mb*sig3)/sigci)+s)^a
$\delta\sigma_1/\delta\sigma_3$	ds1ds3 = IF(GSI>25,(1+(mb*sigci)/(2*(sig1-sig3))),1+(a*mb*a)*(sig3/sigci)^(a-1))
σ_n	sign = sig3+(sig1-sig3)/(1+ds1ds3)
τ	tau = (sign-sig3)*SQRT(ds1ds3)
x	x = LOG((sign-siglm)/sigci)
y	y = LOG(tau/sigci)
	xy = x*y xsq = x^2
A	A = acalc = 10*(sumy/8 - bcalc*sumx/8)
B	B = bcalc = (sumxy - (sumx*sumy)/8)/(sumxsq - (sumx^2)/8)
k	k = (sumsig3sig1 - (sumsig3*sumsig1)/8)/(sumsig3sq - (sumsig3^2)/8)
ϕ	phi = ASIN((k-1)/(k+1))*180/PI()
c	coh = sigcm/(2*SQRT(k))
σ_{cm}	sigcm = sumsig1/8 - k*sumsig3/8
E	E = IF(sigci>100,1000*10^((GSI-10)/40),SQRT(sigci/100)*1000*10^((GSI-10)/40))
	phit = (ATAN(acalc*bcalc*((sign-siglm)/sigci)^(bcalc-1)))*180/PI()
	coht = acalc*sigci*((sign-siglm)/sigci)^bcalc-signt*TAN(phit*PI()/180)
	sig3sig1 = sig3*sig1 sig3sq = sig3^2
	laucalc = acalc*sigci*((sign-siglm)/sigci)^bcalc
	s3sifit = sigcm*k*sig3
	sntaufit = coh+sign*TAN(phi*PI()/180)
	tangent = coht+sign*TAN(phit*PI()/180)

sig3 & sign	Principal stress plot	sig1	s1s3fit	Mohr envelope	sign	laucalc	sntaufit
siglm	sig3	0.00	1.48	sign	-0.02	0.00	0.32
siglm^3/4	-0.02	0.43	1.51	laucalc	-0.02	0.03	0.32
siglm^2/4	-0.01	0.62	1.54		-0.01	0.06	0.33
siglm^1/4	-0.01	0.77	1.58		-0.01	0.07	0.33
0	0.00	0.89	1.61		0.00	0.09	0.34
stress/10.5	0.09	2.10	2.13		0.09	0.29	0.43
stress/10	0.11	2.23	2.21		0.11	0.32	0.45
stress/9.5	0.11	2.28	2.24		0.11	0.32	0.45
stress/9	0.12	2.34	2.27		0.12	0.34	0.46
stress/8.5	0.13	2.40	2.31		0.13	0.35	0.46
stress/8	0.13	2.46	2.36		0.13	0.36	0.47
stress/7.5	0.14	2.54	2.41		0.14	0.38	0.48
stress/7	0.15	2.62	2.47		0.15	0.39	0.49
stress/6.5	0.17	2.71	2.53		0.17	0.41	0.50
stress/6	0.18	2.82	2.61		0.18	0.43	0.51
stress/5.5	0.20	2.94	2.70		0.20	0.46	0.53
stress/5	0.22	3.08	2.81		0.22	0.48	0.55
stress/4.5	0.24	3.24	2.94		0.24	0.52	0.57
stress/4	0.27	3.44	3.11		0.27	0.56	0.60
stress/3.5	0.31	3.68	3.32		0.31	0.61	0.64
stress/3	0.36	3.99	3.61		0.36	0.68	0.69
stress/2.5	0.43	4.38	4.01		0.43	0.77	0.76
stress/2	0.54	4.93	4.61		0.54	0.90	0.86
stress/1.5	0.72	5.77	5.61		0.72	1.09	1.04
stress	1.08	7.23	7.62		1.08	1.45	1.39
stress/0.5	2.16	10.81	13.63		2.16	2.37	2.43



Calculation Package 0.19 - Hoek-Brown Rock Mass Strength Worksheet **DOLOMITE MEAN, HOEK-BROWN**

Input:	sigci = 32 MPa	mi = 15	GSI = 56
	Depth of failure surface or tunnel below slope* = 50 m	Unit wt. = 0.022 MN/m3	
Output:	stress = 1.08 MPa	mb = 3.14	s = 0.0073
	a = 0.5	sigtm = -0.0743 MPa	A = 0.7112
	B = 0.7243	k = 8.15	phi = 51.39 degrees
	coh = 0.628 MPa	sigcm = 3.58 MPa	E = 7866.0 MPa

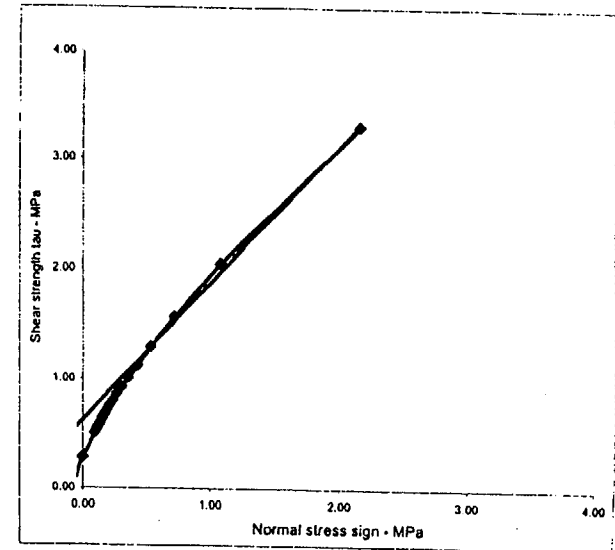
Calculation:

	sig3	sig1	ds1ds3	sign	tau	x	y	xy	xsq	sig3sig1	sig3sq	taucalc	sig1sig3fit	signtaufit
	1E-10	0.15	0.31	0.46	0.82	0.77	0.93	1.08	4.32					
	2.74	4.96	6.52	7.83	8.97	10.01	10.97	11.87	63.87					
	19.42	11.51	9.12	7.86	7.04	6.46	6.02	5.68	73.11					
	0.13	0.54	0.92	1.29	1.66	2.01	2.36	2.70	11.60					
	0.59	1.30	1.85	2.33	2.76	3.15	3.51	3.85	19.34					
	-2.19	-1.72	-1.51	-1.37	-1.27	-1.19	-1.12	-1.06	-11.43					
	-1.73	-1.39	-1.24	-1.14	-1.07	-1.01	-0.96	-0.92	-9.46					
	3.80	2.39	1.87	1.56	1.35	1.20	1.08	0.96	14.22					
	4.79	2.96	2.27	1.88	1.61	1.41	1.26	1.13	17.30					
	0.00	0.76	2.01	3.62	5.53	7.72	10.15	12.82	43					
	0.00	0.02	0.10	0.21	0.38	0.59	0.86	1.17	3					
	0.59	1.30	1.85	2.32	2.75	3.15	3.52	3.87						
	3.58	4.84	6.10	7.35	8.61	9.87	11.13	12.38						
	0.80	1.30	1.78	2.25	2.70	3.14	3.58	4.00						

Cell formulae:

σ_a	stress = if(depth>90, sigci*0.25,depth*unitwt)
m_b	mb = mi*EXP((GSI-100)/28)
s	s = IF(GSI>25,EXP((GSI-100)/9),0)
a	a = IF(GSI>25,0.5,0.65-GSI/200)
σ_{tm}	sigtm = 0.5*sigci*(mb-SQRT(mb*2+4*s))
σ_1	sig3 = Start at 1E-10 (to avoid zero errors) and increment in 7 steps to stress
σ_1	sig1 = sig3+sigci*((mb*sig3)/sigci)+s*a
$\delta\sigma_1/\delta\sigma_3$	ds1ds3 = IF(GSI>25,(1+(mb*sigci)/(2*(sig1-sig3))),1+(a*mb*a)*(sig3/sigci)^(a-1))
σ_a	sign = sig3+(sig1-sig3)/(1+ds1ds3)
τ	tau = (sign-sig3)*SQRT(ds1ds3)
x	x = LOG((sign-sigtm)/sigci)
y	y = LOG(tau/sigci)
	xy = x*y xsq = x^2
A	A = acalc = 10*(sumy/8 - bcalc*sumx/8)
B	B = bcalc = (sumxy - (sumx*sumy)/8)/(sumxsq - (sumx^2)/8)
k	k = (sumsig3sig1 - (sumsig3*sumsig1)/8)/(sumsig3sq - (sumsig3^2)/8)
ϕ	phi = ASIN((k-1)/(k+1))*180/PI()
c	coh = sigcm/(2*SQRT(k))
σ_{cm}	sigcm = sumsig1/8 - k*sumsig3/8
E	E = IF(sigci>100,1000*10*((GSI-10)/40),SQRT(sigci/100)*1000*10*((GSI-10)/40))
	phit = (ATAN(acalc*bcalc*((signt-sigtm)/sigci)*(bcalc-1)))*180/PI()
	coht = acalc*sigci*((signt-sigtm)/sigci)*bcalc-signt*TAN(phit*PI()/180)
	sig3sig1 = sig3*sig1 sig3sq = sig3^2
	taucalc = acalc*sigci*((sign-sigtm)/sigci)*bcalc
	s3sifit = sigcm+k*sig3
	sntaufit = coh+sign*TAN(phi*PI()/180)
	tangent = coh+sign*TAN(phi*PI()/180)

	Principal stress plot	Mohr envelope
sig3 & sign	sig3	sign
sigtm	sig1	taucalc
sigtm^3/4	s1s3fit	sntaufit
sigtm^2/4		
sigtm^1/4		
0		
strees/10.5		
strees/10		
strees/9.5		
strees/9		
strees/8.5		
strees/8		
strees/7.5		
strees/7		
strees/6.5		
strees/6		
strees/5.5		
strees/5		
strees/4.5		
strees/4		
strees/3.5		
strees/3		
strees/2.5		
strees/2		
strees/1.5		
strees		
strees/0.5		



Calculation Package 0.19 - Hoek-Brown Rock Mass Strength Worksheet **DOLOMITE UPPER BOUND, HOEK-BROWN**

Input:	sigci = 47 MPa	mi = 17	GSI = 65
	Depth of failure surface or tunnel below slope* = 50 m	Unit wt. = 0.022 MN/m3	
Output:	stress = 1.08 MPa	mb = 4.96	s = 0.0205
	a = 0.5	siglm = -0.1931 MPa	A = 0.8187
	B = 0.7281	k = 10.49	phi = 55.68 degrees
	coh = 1.153 MPa	sigcm = 7.47 MPa	E = 16222.7 MPa

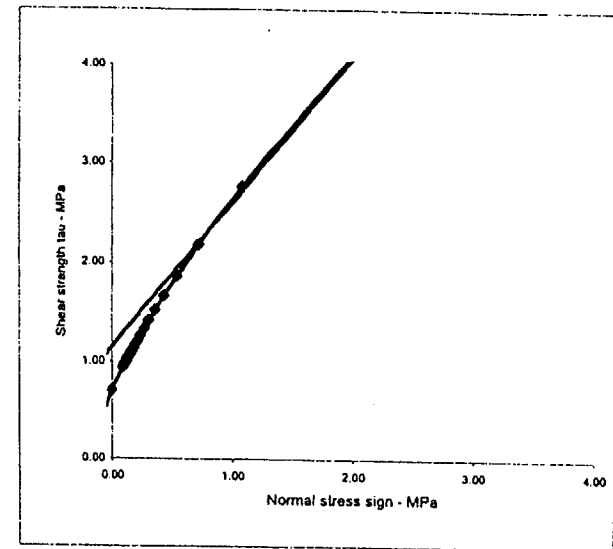
Calculation:

	sig3	1E-10	0.15	0.31	0.46	0.62	0.77	0.93	1.08	Sums
sig1	6.70	9.13	11.10	12.80	14.33	15.73	17.03	18.26	18.26	105.07
ds1ds3	18.32	13.92	11.75	10.40	9.46	8.75	8.20	7.75	7.75	88.56
sign	0.35	0.76	1.15	1.54	1.93	2.30	2.68	3.04	3.04	13.75
tau	1.48	2.25	2.90	3.49	4.03	4.54	5.01	5.47	5.47	29.17
x	-1.94	-1.69	-1.54	-1.43	-1.34	-1.27	-1.21	-1.16	-1.16	-11.59
y	-1.50	-1.32	-1.21	-1.13	-1.06	-1.01	-0.97	-0.93	-0.93	-9.13
xy	2.91	2.23	1.86	1.61	1.43	1.29	1.18	1.08	1.08	13.59
xsq	3.76	2.87	2.37	2.05	1.81	1.62	1.47	1.35	1.35	17.28
sig3sig1	0.00	1.41	3.42	5.92	8.84	12.13	15.76	19.71	19.71	67
sig3sq	0.00	0.02	0.10	0.21	0.38	0.59	0.86	1.17	1.17	3
laucalc	1.49	2.24	2.89	3.48	4.03	4.54	5.02	5.48	5.48	
sig1sig3fit	1.47	9.09	10.71	12.32	13.94	15.56	17.18	18.80	18.80	
signlaufit	1.66	2.26	2.84	3.42	3.98	4.53	5.07	5.61	5.61	

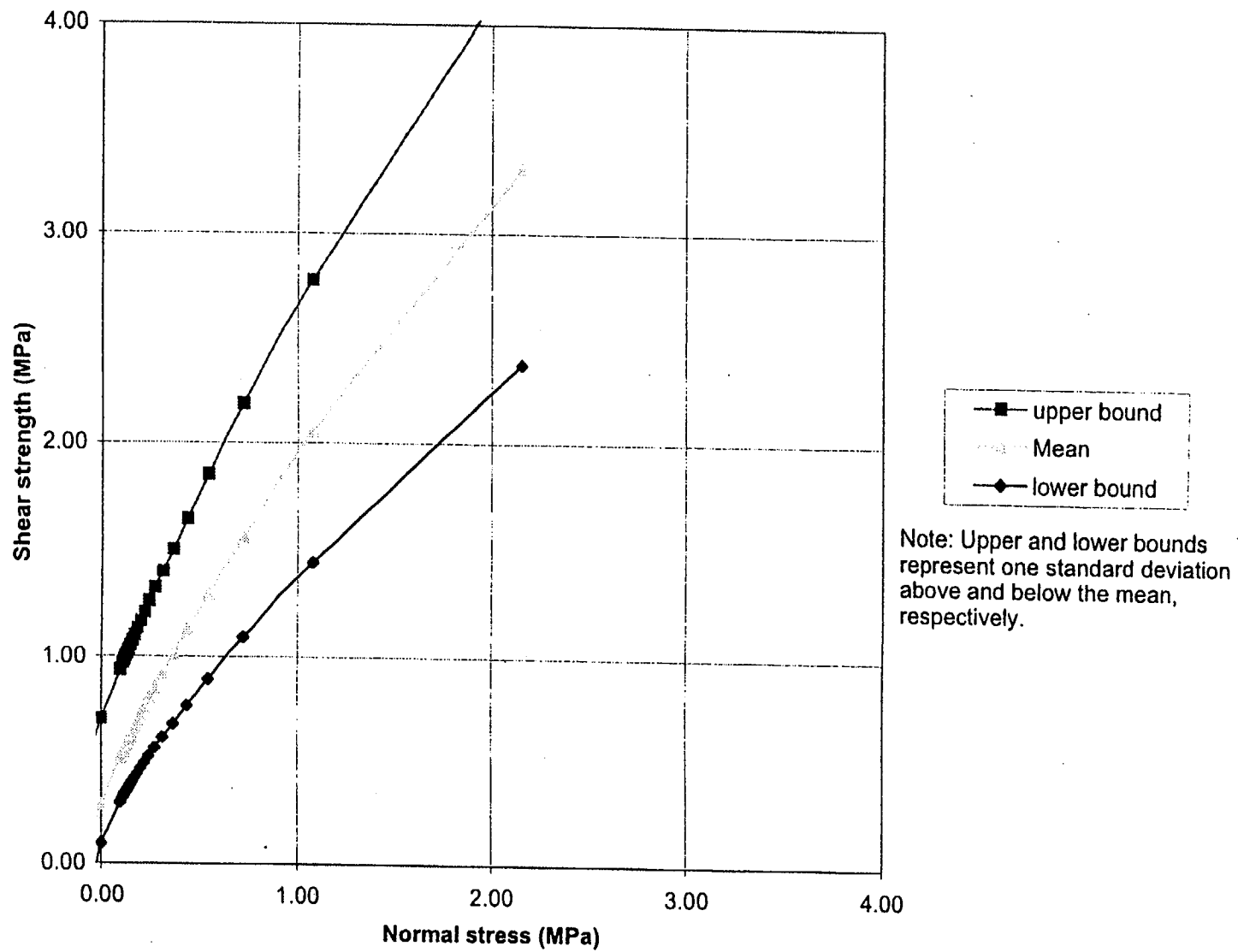
Cell formulae:

σ_n	stress = IF(depth>90, sigci*0.25, depth*unitwt)
m_b	mb = mi*EXP((GSI-100)/28)
s	s = IF(GSI>25, EXP((GSI-100)/9), 0)
a	a = IF(GSI>25, 0.5, 0.65-GSI/200)
σ_{lm}	siglm = 0.5*sigci*(mb-SQRT(mb^2+4*s))
σ_1	sig3 = Start at 1E-10 (to avoid zero errors) and increment in 7 steps to stress
σ_1	sig1 = sig3+sigci*((mb*sig3)/sigci)+s*a
$\delta\sigma_1/\delta\sigma_3$	ds1ds3 = IF(GSI>25, (1+(mb*sigci)/(2*(sig1-sig3))), 1+(a*mb*a)*(sig3/sigci)^(a-1))
σ_n	sign = sig3+(sig1-sig3)/(1+ds1ds3)
τ	tau = (sign-sig3)*SQRT(ds1ds3)
x	x = LOG((sign-siglm)/sigci)
y	y = LOG(tau/sigci)
xy	xy = x*y
A	A = acalc = 10*(sumxy/8 - bcalc*sumx/8)
B	B = bcalc = (sumxy - (sumx*sumy)/8)/(sumxsq - (sumx^2)/8)
k	k = (sumsig3sig1 - (sumsig3*sumsig1)/8)/(sumsig3sq - (sumsig3^2)/8)
ϕ	phi = ASIN((k-1)/(k+1))*180/PI()
c	coh = sigcm/(2*SQRT(k))
σ_{cm}	sigcm = sumsig1/8 - k*sumsig3/8
E	E = IF(sigci>100, 1000*10^((GSI-10)/40), SQRT(sigci/100)*1000*10^((GSI-10)/40))
	phit = (ATAN(acalc*bcalc*((sign-siglm)/sigci)*(bcalc-1)))*180/PI()
	cohl = acalc*sigci*((sign-siglm)/sigci)*bcalc-siglm*TAN(phit*PI()/180)
	sig3sig1 = sig3*sig1
	sig3sq = sig3^2
	laucalc = acalc*sigci*((sign-siglm)/sigci)*bcalc
	s3sfit = sigcm+k*sig3
	snlaufit = coh+sign*TAN(phit*PI()/180)
	langel = cohl+sign*TAN(phit*PI()/180)

sig3 & sign	sig3	sig1	s1s3fit	sign	laucalc	snlaufit
siglm	-0.19	0.00	5.45	-0.19	0.00	0.87
siglm^3/4	-0.14	3.21	5.95	-0.14	0.26	0.94
siglm^2/4	-0.10	4.64	6.46	-0.10	0.42	1.01
siglm^1/4	-0.05	5.75	6.97	-0.05	0.57	1.08
0	0.00	6.70	7.47	0.00	0.70	1.15
stress/10.5	0.09	8.26	8.46	0.09	0.94	1.29
stress/10	0.11	8.47	8.60	0.11	0.97	1.31
stress/9.5	0.11	8.55	8.66	0.11	0.99	1.32
stress/9	0.12	8.64	8.73	0.12	1.00	1.33
stress/8.5	0.13	8.75	8.80	0.13	1.02	1.34
stress/8	0.13	8.86	8.89	0.13	1.03	1.35
stress/7.5	0.14	8.99	8.98	0.14	1.06	1.36
stress/7	0.15	9.13	9.09	0.15	1.08	1.38
stress/6.5	0.17	9.30	9.21	0.17	1.11	1.40
stress/6	0.18	9.48	9.36	0.18	1.14	1.42
stress/5.5	0.20	9.70	9.53	0.20	1.17	1.44
stress/5	0.22	9.96	9.74	0.22	1.22	1.47
stress/4.5	0.24	10.26	9.99	0.24	1.27	1.50
stress/4	0.27	10.63	10.30	0.27	1.33	1.55
stress/3.5	0.31	11.10	10.71	0.31	1.41	1.61
stress/3	0.36	11.69	11.25	0.36	1.51	1.68
stress/2.5	0.43	12.47	12.00	0.43	1.65	1.79
stress/2	0.54	13.58	13.13	0.54	1.86	1.94
stress/1.5	0.72	15.27	15.02	0.72	2.18	2.21
stress	1.08	18.26	18.80	1.08	2.78	2.73
stress/0.5	2.16	25.52	30.12	2.16	4.34	4.32



Comparison of strength ranges - Dolomite (Tof_{b-1}), Hoek-Brown



Calculation Package 0.19 - Hoek-Brown Rock Mass Strength Worksheet **DOLOMITE UC LOW, HOEK-BROWN**

Input:	sigci = 18 MPa	mi = 15	GSI = 56
	Depth of failure surface or tunnel below slope = 50 m	Unit wt. = 0.022 MN/m3	
Output:	stress = 1.08 MPa	mb = 3.14	s = 0.0073
	a = 0.5	sigtm = -0.0405 MPa	A = 0.6992
	B = 0.7205	k = 6.58	phi = 47.39 degrees
	coh = 0.443 MPa	sigcm = 2.27 MPa	E = 5807.9 MPa

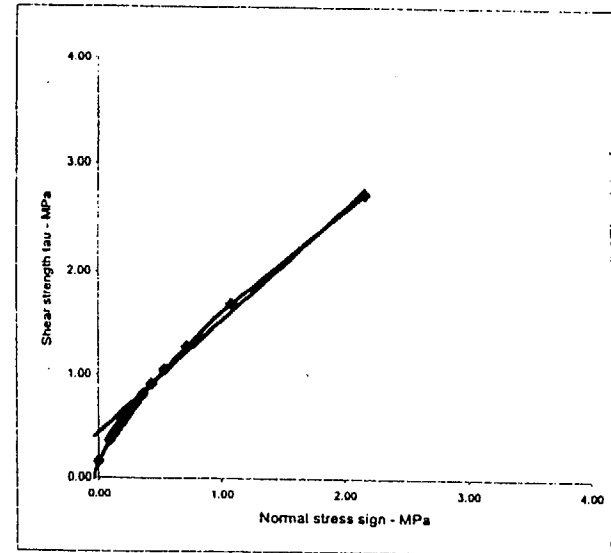
Calculation:

	sig3	sig1	ds1ds3	sign	tau	x	y	xy	xsq	sig3sig1	sig3sq	taucalc	sig1sig3fit	signtaufit
	1E-10	0.15	0.31	0.46	0.62	0.77	0.93	1.08	4.32					
	1.49	3.43	4.89	5.72	6.63	7.45	8.22	8.93	48.57					
	19.42	9.41	7.28	6.23	5.57	5.12	4.77	4.50	62.31					
	0.07	0.47	0.84	1.19	1.53	1.86	2.19	2.51	10.66					
	0.32	0.96	1.43	1.82	2.16	2.47	2.76	3.03	14.95					
	-2.19	-1.54	-1.30	-1.15	-1.05	-0.96	-0.90	-0.84	-9.92					
	-1.73	-1.26	-1.09	-0.98	-0.91	-0.85	-0.80	-0.76	-8.39					
	3.60	1.93	1.41	1.13	0.95	0.82	0.72	0.64	11.40					
	4.79	2.36	1.69	1.33	1.10	0.93	0.80	0.70	13.69					
	0.00	0.53	1.45	2.65	4.09	5.75	7.60	9.64	32					
	0.00	0.02	0.10	0.21	0.38	0.59	0.86	1.17	3					
	0.32	0.96	1.42	1.81	2.16	2.48	2.77	3.05						
	2.27	3.29	4.30	5.31	6.33	7.34	8.36	9.37						
	0.52	0.95	1.35	1.74	2.11	2.47	2.82	3.17						

Cell formulae:

σ_c	stress = if(depth>90, sigci*0.25,depth*unitwt)
m_b	mb = mi*EXP((GSI-100)/28)
s	s = IF(GSI>25,EXP((GSI-100)/9),0)
a	a = IF(GSI>25,0.5,0.65-GSI/200)
σ_{tm}	sigtm = 0.5*sigci*(mb*SQRT(mb*2+4*s))
σ_1	sig3 = Start at 1E-10 (to avoid zero errors) and increment in 7 steps to stress
σ_1	sig1 = sig3+sigci*(((mb*sig3)/sigci)+s)^a
$\delta\sigma_1/\delta\sigma_3$	ds1ds3 = IF(GSI>25,(1+(mb*sigci)/(2*(sig1-sig3))),1+(a*mb*a)*(sig3/sigci)^(a-1))
σ_1	sign = sig3+(sig1-sig3)/(1+ds1ds3)
τ	tau = (sign-sig3)*SQRT(ds1ds3)
x	x = LOG((sign-sigtm)/sigci)
y	y = LOG(tau/sigci)
	xy = x*y xsq = x^2
A	A = acalc = 10*(sumy/8 - bcalc*sumx/8)
B	B = bcalc = (sumxy - (sumx*sumy)/8)/(sumxsq - (sumx^2)/8)
k	k = (sumsig3sig1 - (sumsig3*sumsig1)/8)/(sumsig3sq - (sumsig3^2)/8)
ϕ	phi = ASIN((k-1)/(k+1))*180/PI()
c	coh = sigcm/(2*SQRT(k))
σ_{cm}	sigcm = sumsig1/8 - k*sumsig3/8
E	E = IF(sigci>100,1000*10^((GSI-10)/40),SQRT(sigci/100)*1000*10^((GSI-10)/40))
	phit = (ATAN(acalc*bcalc*((sign-sigtm)/sigci)^(bcalc-1)))*180/PI()
	cohl = acalc*sigci*((sign-sigtm)/sigci)^bcalc-signt*TAN(phit*PI()/180)
	sig3sig1 = sig3*sig1 sig3sq = sig3^2
	taucalc = acalc*sigci*((sign-sigtm)/sigci)^bcalc
	s3sifit = sigcm+k*sig3
	sntaufit = coh+sign*TAN(phit*PI()/180)
	tangent = cohl+sign*TAN(phit*PI()/180)

	Principal stress plot	Mohr envelope
sig3 & sign	sig3	sig1
sigtm	-0.04	0.00
sigtm^3/4	-0.03	0.72
sigtm^2/4	-0.02	1.04
sigtm^1/4	-0.01	1.28
0	0.00	1.49
stress/10.5	0.09	2.81
stress/10	0.11	2.97
stress/9.5	0.11	3.03
stress/9	0.12	3.09
stress/8.5	0.13	3.16
stress/8	0.13	3.24
stress/7.5	0.14	3.33
stress/7	0.15	3.43
stress/6.5	0.17	3.54
stress/6	0.18	3.66
stress/5.5	0.20	3.81
stress/5	0.22	3.97
stress/4.5	0.24	4.17
stress/4	0.27	4.40
stress/3.5	0.31	4.69
stress/3	0.36	5.05
stress/2.5	0.43	5.53
stress/2	0.54	6.19
stress/1.5	0.72	7.19
stress	1.08	8.93
stress/0.5	2.16	13.16
	s1s3fit	sign
	2.00	-0.04
	2.07	-0.03
	2.14	-0.02
	2.20	-0.01
	2.27	0.00
	2.89	0.09
	2.98	0.11
	3.02	0.11
	3.06	0.12
	3.11	0.13
	3.16	0.13
	3.22	0.14
	3.29	0.15
	3.36	0.17
	3.45	0.18
	3.56	0.20
	3.69	0.22
	3.85	0.24
	4.05	0.27
	4.30	0.31
	4.64	0.36
	5.11	0.43
	5.82	0.54
	7.00	0.72
	8.93	1.08
	16.47	2.16
	taucalc	sntaufit
	0.00	0.40
	0.06	0.41
	0.09	0.42
	0.13	0.43
	0.15	0.44
	0.37	0.54
	0.39	0.56
	0.40	0.57
	0.42	0.57
	0.43	0.58
	0.44	0.59
	0.46	0.60
	0.48	0.61
	0.50	0.62
	0.52	0.64
	0.55	0.66
	0.58	0.68
	0.62	0.70
	0.67	0.74
	0.73	0.78
	0.80	0.83
	0.91	0.91
	1.05	1.03
	1.28	1.23
	1.69	1.62
	2.75	2.79



Calculation Package 0.19 - Hoek-Brown Rock Mass Strength Worksheet **DOLOMITE UC HIGH, HOEK-BROWN**

Input:	sigci = 47 MPa	mi = 15	GSI = 56
	Depth of failure surface or tunnel below slope* = 50 m	Unit wt. = 0.022 MN/m ³	
Output:	stress = 1.08 MPa	mb = 3.14	s = 0.0073
	a = 0.5	siglm = -0.1083 MPa	A = 0.7179
	B = 0.7265	k = 9.26	phi = 53.61 degrees
	coh = 0.797 MPa	sigcm = 4.85 MPa	E = 9497.8 MPa

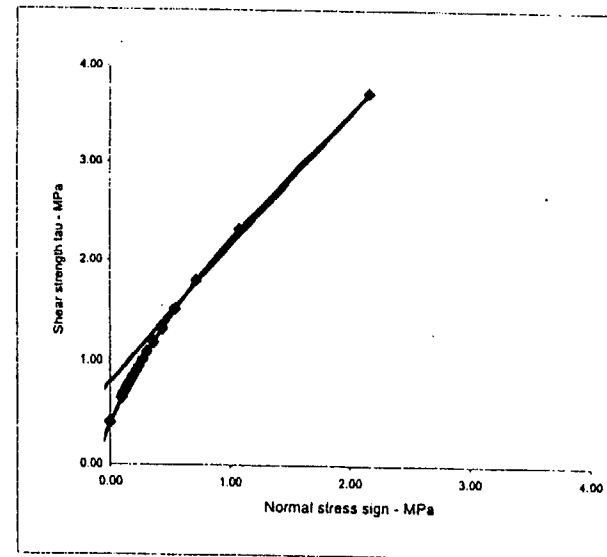
Calculation:

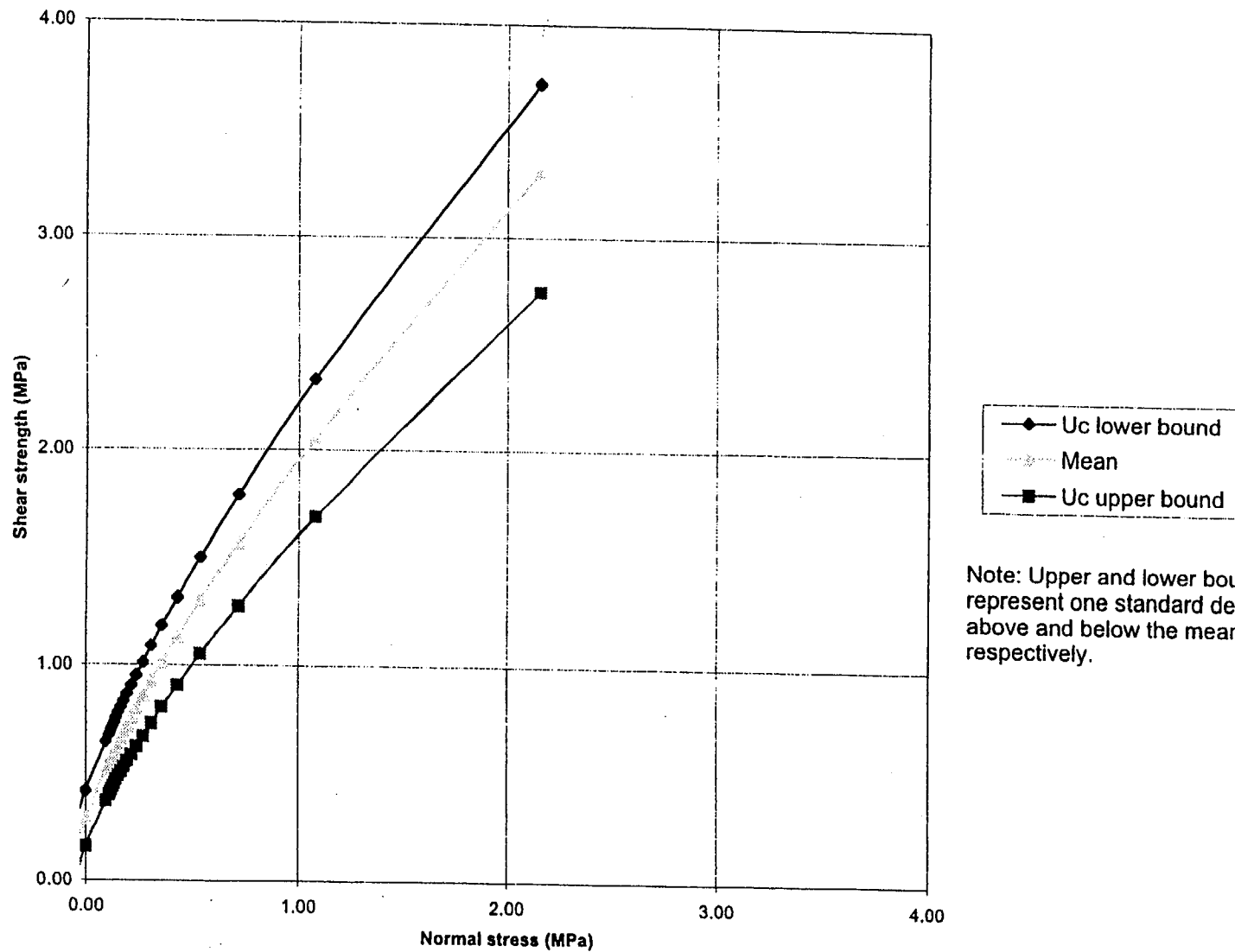
	sig3	sig1	ds1ds3	sign	lau	x	y	xy	xsq	sig3sig1	sig3sq	taucalc	sig1sig3fit	signtaufit
	1E-10	0.15	0.31	0.48	0.62	0.77	0.93	1.08	4.32					
	3.99	6.37	8.14	9.83	10.95	12.15	13.26	14.30	78.79					
	19.42	12.84	10.40	9.03	8.12	7.47	6.97	6.57	80.81					
	0.20	0.60	1.00	1.38	1.75	2.11	2.47	2.83	12.34					
	0.86	1.61	2.22	2.75	3.23	3.67	4.09	4.48	22.90					
	-2.19	-1.82	-1.63	-1.50	-1.40	-1.32	-1.26	-1.20	-12.32					
	-1.73	-1.46	-1.32	-1.23	-1.16	-1.11	-1.06	-1.02	-10.10					
	3.80	2.66	2.16	1.85	1.63	1.48	1.33	1.23	16.10					
	4.79	3.30	2.65	2.25	1.96	1.75	1.58	1.45	19.73					
	0.00	0.98	2.51	4.46	6.75	9.37	12.27	15.44	52					
	0.00	0.02	0.10	0.21	0.38	0.59	0.86	1.17	3					
	0.87	1.61	2.21	2.74	3.22	3.67	4.09	4.49						
	4.85	6.28	7.71	9.14	10.56	11.99	13.42	14.85						
	1.06	1.62	2.15	2.67	3.17	3.67	4.15	4.63						

Cell formulae:

σ_3	stress = if(depth>90, sigci*0.25*depth*unitwt)
m_b	mb = mi*EXP((GSI-100)/28)
s	s = IF(GSI>25,EXP((GSI-100)/9),0)
a	a = IF(GSI>25,0.5,0.65-GSI/200)
σ_{lm}	siglm = 0.5*sigci*(mb-SQRT(mb*2*4*s))
σ_1	sig3 = Start at 1E-10 (to avoid zero errors) and increment in 7 steps to stress
σ_1	sig1 = sig3+sigci*(((mb*sig3)/sigci)+s)*a
$\delta\sigma_1/\delta\sigma_3$	ds1ds3 = IF(GSI>25,(1+(mb*sigci)/(2*(sig1-sig3))),1+(a*mb*a)*(sig3/sigci)^(a-1))
σ_n	sign = sig3+(sig1-sig3)/(1+ds1ds3)
τ	lau = (sign-sig3)*SQRT(ds1ds3)
x	x = LOG((sign-siglm)/sigci)
y	y = LOG(lau/sigci)
	xy = x*y xsq = x^2
A	A = acalc = 10*(sumy/8 - bcalc*sumx/8)
B	B = bcalc = (sumxy - (sumx*sumy)/8)/(sumxsq - (sumx^2)/8)
k	k = (sumsig3sig1 - (sumsig3*sumsig1)/8)/(sumsig3sq - (sumsig3^2)/8)
ϕ	phi = ASIN((k-1)/(k+1))*180/PI()
c	coh = sigcm/(2*SQRT(k))
σ_{cm}	sigcm = sumsig1/8 - k*sumsig3/8
E	E = IF(sigci>100,1000*10^4*((GSI-10)/40),SQRT(sigci/100)*1000*10^4*((GSI-10)/40))
	phit = (ATAN(acalc*bcalc*((sign-siglm)/sigci)*(bcalc-1)))*180/PI()
	coht = acalc*sigci*((sign-siglm)/sigci)*bcalc-signt*TAN(phit*PI()/180)
	sig3sig1 = sig3*sig1 sig3sq = sig3^2
	taucalc = acalc*sigci*((sign-siglm)/sigci)*bcalc
	s3sift = sigcm*k*sig3
	sntaufit = coh+sign*TAN(phi*PI()/180)
	lagent = coht+sign*TAN(phit*PI()/180)

	sig3	sig1	s1s3fit	sign	taucalc	sntaufit
sig3 & sign	-0.11	0.00	3.85	-0.11	0.00	0.65
siglm	-0.08	1.92	4.10	-0.08	0.15	0.69
siglm^3/4	-0.05	2.77	4.35	-0.05	0.25	0.72
siglm^2/4	-0.03	3.43	4.60	-0.03	0.33	0.76
siglm^1/4	0.00	3.99	4.85	0.00	0.41	0.80
stress/10.5	0.09	5.55	5.72	0.09	0.64	0.92
stress/10	0.11	5.75	5.85	0.11	0.68	0.94
stress/9.5	0.11	5.83	5.90	0.11	0.69	0.95
stress/9	0.12	5.92	5.96	0.12	0.70	0.96
stress/8.5	0.13	6.01	6.03	0.13	0.72	0.97
stress/8	0.13	6.12	6.10	0.13	0.74	0.98
stress/7.5	0.14	6.24	6.18	0.14	0.76	0.99
stress/7	0.15	6.37	6.28	0.15	0.78	1.01
stress/6.5	0.17	6.52	6.39	0.17	0.80	1.02
stress/6	0.18	6.69	6.52	0.18	0.83	1.04
stress/5.5	0.20	6.89	6.67	0.20	0.87	1.06
stress/5	0.22	7.12	6.85	0.22	0.91	1.09
stress/4.5	0.24	7.40	7.07	0.24	0.96	1.12
stress/4	0.27	7.73	7.35	0.27	1.01	1.16
stress/3.5	0.31	8.14	7.71	0.31	1.09	1.22
stress/3	0.36	8.66	8.18	0.36	1.18	1.29
stress/2.5	0.43	9.35	8.85	0.43	1.31	1.38
stress/2	0.54	10.31	9.85	0.54	1.50	1.53
stress/1.5	0.72	11.76	11.51	0.72	1.79	1.77
stress	1.08	14.30	14.85	1.08	2.33	2.26
stress/0.5	2.16	20.43	24.84	2.16	3.73	3.73



Comparison of U_c ranges - Dolomite ($T_{of_{b-1}}$), HOEK-BROWN

Note: Upper and lower bounds represent one standard deviation above and below the mean, respectively.

Calculation Package 0.19 - Hoek-Brown Rock Mass Strength Worksheet **DOLOMITE MI LOW, HOEK-BROWN**

Input:	sigci = 32 MPa	mi = 13	GSI = 56
	Depth of failure surface or tunnel below slope* = 50 m	Unit wt. = 0.022 MN/m3	
Output:	stress = 1.08 MPa	mb = 2.73	s = 0.0073
	a = 0.5	sigtm = -0.0854 MPa	A = 0.6782
	B = 0.7219	k = 7.56	phi = 50.04 degrees
	coh = 0.633 MPa	sigcm = 3.48 MPa	E = 7866.0 MPa

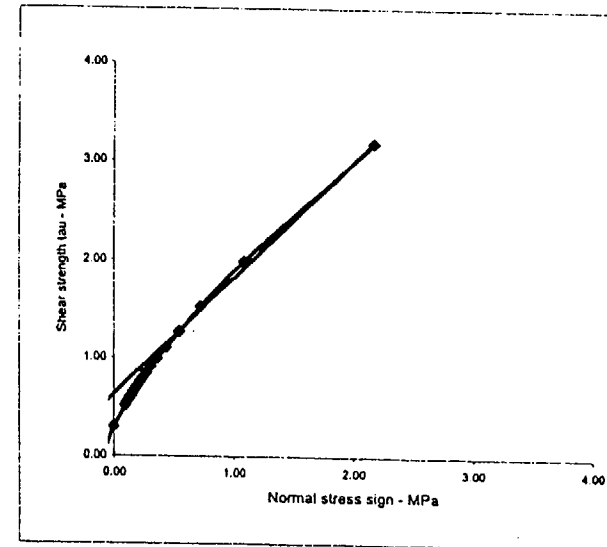
Calculation:

	sig3	1E-10	0.15	0.31	0.46	0.62	0.77	0.93	1.08	Sums
sig1	2.74	4.74	6.19	7.40	8.47	9.44	10.34	11.19	60.51	4.32
ds1ds3	17.02	10.57	8.46	7.33	6.59	6.06	5.66	5.34	67.02	4.32
sign	0.15	0.55	0.93	1.30	1.65	2.00	2.34	2.67	11.59	4.32
tau	0.63	1.29	1.81	2.25	2.66	3.02	3.36	3.69	18.71	4.32
x	-2.13	-1.70	-1.50	-1.37	-1.27	-1.19	-1.12	-1.07	-11.34	4.32
y	-1.71	-1.40	-1.25	-1.15	-1.08	-1.03	-0.98	-0.94	-9.54	4.32
xy	3.64	2.38	1.87	1.58	1.37	1.22	1.10	1.00	14.16	4.32
xsq	4.54	2.90	2.25	1.87	1.60	1.41	1.26	1.14	16.97	4.32
sig3sig1	0.00	0.73	1.91	3.42	5.22	7.28	9.57	12.08	40	4.32
sig3sq	0.00	0.02	0.10	0.21	0.38	0.59	0.86	1.17	3	4.32
taucalc	0.63	1.28	1.80	2.25	2.65	3.02	3.37	3.70	11.65	4.32
sig1sig3fit	3.48	4.65	5.81	6.98	8.15	9.31	10.48	11.65	3.42	4.32
signtaufit	0.81	1.29	1.74	2.18	2.60	3.02	3.42	3.82		4.32

Cell formulae:

σ_c	stress = if(depth>90, sigci*0.25, depth*unitwt)
m_b	mb = mi*EXP((GSI-100)/28)
s	s = IF(GSI>25, EXP((GSI-100)/9), 0)
a	a = IF(GSI>25, 0.5, 0.65-GSI/200)
σ_{tm}	sigtm = 0.5*sigci*(mb-SQRT(mb^2+4*s))
σ_1	sig3 = Start at 1E-10 (to avoid zero errors) and increment in 7 steps to stress
σ_1	sig1 = sig3+sigci*((mb*sig3)/sigci)*s
$\delta\sigma_1/\delta\sigma_3$	ds1ds3 = IF(GSI>25, (1+(mb*sigci)/(2*(sig1-sig3))), 1+(a*mb*a)*(sig3/sigci)^(a-1))
σ_2	sign = sig3*(sig1-sig3)/(1+ds1ds3)
t	tau = (sign-sig3)*SQRT(ds1ds3)
x	x = LOG((sign-sigtm)/sigci)
y	y = LOG((tau/sigci))
	xy = x*y xsq = x^2
A	A = acalc = 10*(sumy/8 - bcalc*sumx/8)
B	B = bcalc = (sumxy - (sumx*sumy)/8)/(sumxsq - (sumx^2)/8)
k	k = (sumsig3sig1 - (sumsig3*sumsig1)/8)/(sumsig3sq - (sumsig3^2)/8)
ϕ	phi = ASIN((k-1)/(k+1))*180/PI()
c	coh = sigcm/(2*SQRT(k))
σ_{cm}	sigcm = sumsig1/8 - k*sumsig3/8
E	E = IF(sigci>100, 1000*10^((GSI-10)/40), SQRT(sigci/100)*1000*10^((GSI-10)/40))
	phit = (ATAN(acalc*bcalc*((sign-sigtm)/sigci)*(bcalc-1)))*180/PI()
	coht = acalc*sigci*((sign-sigtm)/sigci)*bcalc-signt*TAN(phit*PI()/180)
	sig3sig1 = sig3*sig1 sig3sq = sig3^2
	taucalc = acalc*sigci*((sign-sigtm)/sigci)*bcalc
	s3sifit = sigcm+k*sig3
	signtaufit = coh+sign*TAN(phi*PI()/180)
	tangent = coht+sign*TAN(phit*PI()/180)

	Principal stress plot		Mohr envelope	
sig3 & sign	sig3	sig1	s1s3fit	sign
sigtm	-0.09	0.00	2.83	-0.09
sigtm^3/4	-0.06	1.31	3.00	-0.06
sigtm^2/4	-0.04	1.90	3.16	-0.04
sigtm^1/4	-0.02	2.35	3.32	-0.02
0	0.00	2.74	3.48	0.00
stress/10.5	0.09	4.06	4.19	0.09
stress/10	0.11	4.23	4.30	0.11
stress/9.5	0.11	4.29	4.34	0.11
stress/9	0.12	4.37	4.39	0.12
stress/8.5	0.13	4.45	4.44	0.13
stress/8	0.13	4.53	4.50	0.13
stress/7.5	0.14	4.63	4.57	0.14
stress/7	0.15	4.74	4.65	0.15
stress/6.5	0.17	4.86	4.74	0.17
stress/6	0.18	5.01	4.84	0.18
stress/5.5	0.20	5.17	4.97	0.20
stress/5	0.22	5.36	5.11	0.22
stress/4.5	0.24	5.58	5.30	0.24
stress/4	0.27	5.85	5.52	0.27
stress/3.5	0.31	6.19	5.81	0.31
stress/3	0.36	6.61	6.20	0.36
stress/2.5	0.43	7.17	6.75	0.43
stress/2	0.54	7.95	7.56	0.54
stress/1.5	0.72	9.13	8.92	0.72
stress	1.08	11.19	11.65	1.08
stress/0.5	2.16	16.19	19.81	2.16
				3.19
				3.21



Calculation Package 0.19 - Hoek-Brown Rock Mass Strength Worksheet **DOLOMITE MI HIGH, HOEK-BROWN**

Input:	sigci = 32 MPa	mi = 17	GSI = 56
	Depth of failure surface or tunnel below slope* = 50 m	Unit wt = 0.022 MN/m3	
Output:	stress = 1.08 MPa	mb = 3.56	s = 0.0073
	a = 0.5	siglm = -0.0657 MPa	A = 0.7408
	B = 0.7263	k = 6.70	phi = 52.54 degrees
	coh = 0.624 MPa	sigcm = 3.68 MPa	E = 7866.0 MPa

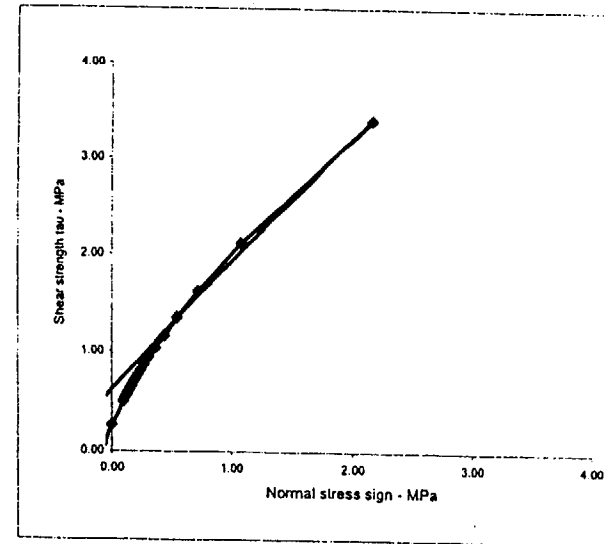
Calculation:

	sig3	1E-10	0.15	0.31	0.46	0.62	0.77	0.93	1.08	Sums
sig1	2.74	5.16	6.84	8.23	9.44	10.54	11.56	12.51	13.51	67.04
ds1ds3	21.83	12.39	9.73	8.35	7.47	6.84	6.37	5.99	5.62	78.97
sign	0.12	0.53	0.92	1.29	1.66	2.02	2.37	2.71	3.04	11.62
tau	0.56	1.32	1.90	2.40	2.85	3.26	3.64	4.00	4.32	19.93
x	-2.24	-1.73	-1.51	-1.37	-1.27	-1.19	-1.12	-1.06	-1.00	-11.50
y	-1.76	-1.39	-1.23	-1.13	-1.05	-0.99	-0.95	-0.90	-0.86	-9.39
xy	3.93	2.40	1.86	1.55	1.34	1.18	1.06	0.96	0.86	14.28
xsq	5.01	3.00	2.29	1.89	1.61	1.41	1.25	1.13	1.00	17.59
sig3sig1	0.00	0.80	2.11	3.81	5.83	8.13	10.70	13.51	16.51	45
sig3sq	0.00	0.02	0.10	0.21	0.38	0.59	0.86	1.17	1.51	3
taucalc	0.56	1.31	1.89	2.39	2.84	3.26	3.65	4.02	4.32	
sig1sig3fit	3.68	5.03	6.37	7.71	9.05	10.39	11.73	13.08	14.42	
signtaufit	0.78	1.31	1.82	2.31	2.79	3.26	3.72	4.17	4.62	

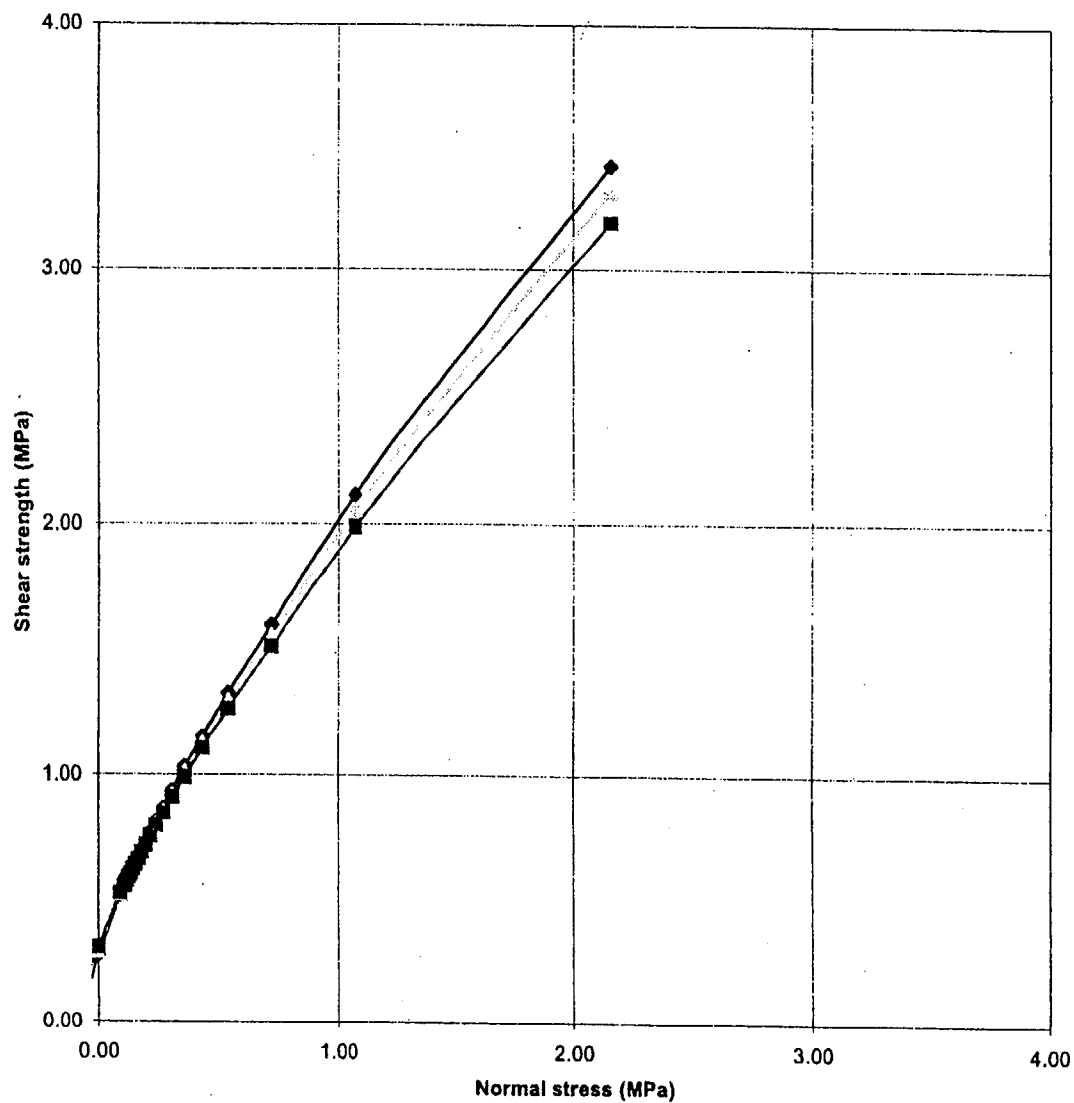
Cell formulae:

σ_c	stress = if(depth>90, sigci*0.25, depth*unitwt)
m_b	mb = mi*EXP((GSI-100)/28)
s	s = IF(GSI>25, EXP((GSI-100)/9), 0)
a	a = IF(GSI>25, 0.5, 0.65-GSI/200)
σ_{lm}	siglm = 0.5*sigci*(mb-SQRT(mb*2+4*s))
σ_1	sig3 = Start at 1E-10 (to avoid zero errors) and increment in 7 steps to stress
σ_1	sig1 = sig3+sigci*(((mb*sig3)/sigci)+s)*a
$\delta\sigma_1/\delta\sigma_3$	ds1ds3 = IF(GSI>25, (1+(mb*sigci)/(2*(sig1-sig3))), 1+(a*mb*a)*(sig3/sigci)*(a-1))
σ_n	sign = sig3*(sig1-sig3)/(1+ds1ds3)
τ	tau = (sign-sig3)*SQRT(ds1ds3)
x	x = LOG((sign-siglm)/sigci)
y	y = LOG(tau/sigci)
xy	xy = x*y
A	A = acalc = 10*(sumy/8 - bcalc*sumx/8)
B	B = bcalc = (sumxy - (sumx*sumy)/8)/(sumxsq - (sumx*2)/8)
k	k = (sumsig3sig1 - (sumsig3*sumsig1)/8)/(sumsig3sq - (sumsig3*2)/8)
ϕ	phi = ASIN((k-1)/(k+1))*180/PI()
c	coh = sigcm/(2*SQRT(k))
σ_{cm}	sigcm = sumsig1/8 - k*sumsig3/8
E	E = IF(sigci>100, 1000*10^((GSI-10)/40), SQRT(sigci/100)*1000*10^((GSI-10)/40))
	phit = (ATAN(acalc*bcalc*((signt-siglm)/sigci)*(bcalc-1)))*180/PI()
	coht = acalc*sigci*((signt-siglm)/sigci)*bcalc*signt*TAN(phit*PI()/180)
	sig3sig1 = sig3*sig1
	sig3sq = sig3*2
	taucalc = acalc*sigci*((sign-siglm)/sigci)*bcalc
	s3sifit = sigcm+k*sig3
	sntaufit = coh+sign*TAN(phi*PI()/180)
	tangent = coht+signt*TAN(phi*PI()/180)

	Principal stress plot	Mohr envelope	antaufit
sig3 & sign	sig3	sign	antaufit
siglm	-0.07	0.00	0.54
siglm*3/4	-0.05	1.32	0.58
siglm*2/4	-0.03	1.90	0.58
siglm*1/4	-0.02	2.36	0.60
0	0.00	2.74	0.62
stress/10.5	0.09	4.36	0.75
stress/10	0.11	4.56	0.77
stress/9.5	0.11	4.64	0.77
stress/9	0.12	4.72	0.78
stress/8.5	0.13	4.82	0.79
stress/8	0.13	4.92	0.80
stress/7.5	0.14	5.04	0.81
stress/7	0.15	5.16	0.83
stress/6.5	0.17	5.31	0.84
stress/6	0.18	5.48	0.86
stress/5.5	0.20	5.66	0.88
stress/5	0.22	5.89	0.91
stress/4.5	0.24	6.15	0.94
stress/4	0.27	6.46	0.98
stress/3.5	0.31	6.84	1.03
stress/3	0.36	7.33	1.09
stress/2.5	0.43	7.97	1.19
stress/2	0.54	8.85	1.33
stress/1.5	0.72	10.19	1.56
stress	1.08	12.51	2.03
stress/0.5	2.16	18.09	3.44



Comparison of mi ranges - Dolomite (Tof_{b-1}), HOEK-BROWN



Note: Upper and lower bounds represent one standard deviation above and below the mean, respectively.

Calculation Package 0.19 - Hoek-Brown Rock Mass Strength Worksheet **DOLOMITE GSI LOW, HOEK-BROWN**

Input:	sigci = 32 MPa	mi = 15	GSI = 46
	Depth of failure surface or tunnel below slope = 50 m	Unit wt. = 0.022 MN/m3	
Output:	stress = 1.08 MPa	mb = 2.26	s = 0.0026
	a = 0.5	siglm = -0.0369 MPa	A = 0.6468
	B = 0.7243	k = 7.44	phi = 49.74 degrees
	coh = 0.468 MPa	sigcm = 2.55 MPa	E = 4605.2 MPa

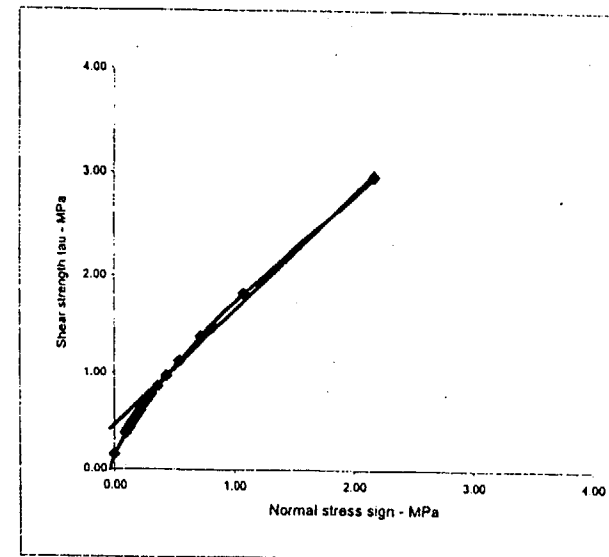
Calculation:

	sig3	sig1	ds1ds3	sign	tau	x	y	xy	xsq	sig3sig1	sig3sq	laucalc	sig1sig3fit	signtaufit
	1E-10	0.15	0.31	0.46	0.62	0.77	0.93	1.08	4.32					
	1.63	3.87	5.31	6.48	7.50	8.42	9.27	10.07	52.55					
	23.16	10.73	8.24	7.02	6.26	5.73	5.34	5.03	71.51					
	0.07	0.47	0.85	1.21	1.56	1.91	2.24	2.57	10.89					
	0.33	1.04	1.55	1.99	2.37	2.72	3.04	3.34	16.38					
	-2.49	-1.80	-1.56	-1.41	-1.30	-1.22	-1.15	-1.09	-12.02					
	-1.99	-1.49	-1.32	-1.21	-1.13	-1.07	-1.02	-0.98	-10.22					
	4.96	2.68	2.05	1.70	1.47	1.31	1.18	1.07	16.42					
	6.19	3.24	2.43	1.99	1.70	1.48	1.32	1.19	19.53					
	0.00	0.60	1.64	3.00	4.62	6.49	8.58	10.87	36					
	0.00	0.02	0.10	0.21	0.38	0.59	0.86	1.17	3					
	0.33	1.03	1.54	1.98	2.37	2.72	3.06	3.37						
	2.55	3.70	4.85	6.00	7.14	8.29	9.44	10.59						
	0.55	1.02	1.47	1.90	2.31	2.72	3.12	3.50						

Cell formulae:

σ_s	stress = if(depth>90, sigci*0.25,depth*unitwt)
m_b	mb = mi*EXP((GSI-100)/28)
s	s = IF(GSI>25,EXP((GSI-100)/9),0)
a	a = IF(GSI>25,0.5,0.65-GSI/200)
σ_{lm}	siglm = 0.5*sigci*(mb-SQRT(mb^2+4*s))
σ_3	sig3 = Start at 1E-10 (to avoid zero errors) and increment in 7 steps to stress
σ_1	sig1 = sig3+sigci*(((mb*sig3)/sigci)+s)^a
$\delta\sigma_1/\delta\sigma_3$	ds1ds3 = IF(GSI>25,(1+(mb*sigci)/(2*(sig1-sig3))),1+(a*mb*a)*(sig3/sigci)^(a-1))
σ_s	sign = sig3+(sig1-sig3)/(1+ds1ds3)
τ	tau = (sign-sig3)*SQRT(ds1ds3)
x	x = LOG((sign-siglm)/sigci)
y	y = LOG(tau/sigci)
	xy = x*y xsq = x^2
A	A = acalc = 10*(sumy/8 - bcalc*sumx/8)
B	B = bcalc = (sumxy - (sumx*sumy)/8)/(sumxsq - (sumx^2)/8)
k	k = (sumsig3sig1 - (sumsig3*sumsig1)/8)/(sumsig3sq - (sumsig3^2)/8)
ϕ	phi = ASIN((k-1)/(k+1))*180/PI()
c	coh = sigcm/(2*SQRT(k))
σ_{cm}	sigcm = sumsig1/8 - k*sumsig3/8
E	E = IF(sigci>100,1000*10^((GSI-10)/40),SQRT(sigci/100)*1000*10^((GSI-10)/40))
	phit = (ATAN(acalc*bcalc*((sign-siglm)/sigci)*(bcalc-1)))*180/PI()
	coht = acalc*sigci*((sign-siglm)/sigci)*bcalc-siglm*TAN(phit*PI()/180)
	sig3sig1 = sig3*sig1 sig3sq = sig3^2
	laucalc = acalc*sigci*((sign-siglm)/sigci)*bcalc
	s3sfit = sigcm+k*sig3
	sntaufit = coh+sign*TAN(phi*PI()/180)
	tangent = coht+sign*TAN(phi*PI()/180)

	Principal stress plot	Mohr envelope
sig3 & sign	sig3 sig1 s1s3fit	sign taucalc sntaufit
siglm	-0.04 0.00 2.28	-0.04 0.00 0.42
siglm^3/4	-0.03 0.79 2.35	-0.03 0.06 0.44
siglm^2/4	-0.02 1.14 2.42	-0.02 0.09 0.45
siglm^1/4	-0.01 1.41 2.48	-0.01 0.13 0.46
0	0.00 1.63 2.55	0.00 0.15 0.47
stress/10.5	0.09 3.17 3.25	0.09 0.39 0.58
stress/10	0.11 3.35 3.36	0.11 0.42 0.60
stress/9.5	0.11 3.41 3.40	0.11 0.43 0.60
stress/9	0.12 3.49 3.45	0.12 0.44 0.61
stress/8.5	0.13 3.57 3.50	0.13 0.45 0.62
stress/8	0.13 3.66 3.56	0.13 0.47 0.63
stress/7.5	0.14 3.76 3.62	0.14 0.49 0.64
stress/7	0.15 3.87 3.70	0.15 0.51 0.65
stress/6.5	0.17 4.00 3.79	0.17 0.53 0.66
stress/6	0.18 4.14 3.89	0.18 0.56 0.68
stress/5.5	0.20 4.31 4.01	0.20 0.59 0.70
stress/5	0.22 4.49 4.16	0.22 0.62 0.72
stress/4.5	0.24 4.72 4.34	0.24 0.66 0.75
stress/4	0.27 4.98 4.56	0.27 0.72 0.79
stress/3.5	0.31 5.31 4.85	0.31 0.78 0.83
stress/3	0.36 5.72 5.23	0.36 0.86 0.89
stress/2.5	0.43 6.26 5.77	0.43 0.97 0.98
stress/2	0.54 7.00 6.57	0.54 1.13 1.11
stress/1.5	0.72 8.12 7.91	0.72 1.38 1.32
stress	1.08 10.07 10.59	1.08 1.82 1.74
stress/0.5	2.16 14.77 18.62	2.16 2.98 3.02



Calculation Package 0.19 - Hoek-Brown Rock Mass Strength Worksheet **DOLOMITE GSI HIGH, HOEK-BROWN**

Input:	sigci = 32 MPa	mi = 15	GSI = 65
	Depth of failure surface or tunnel below slope = 50 m		Unit wt. = 0.022 MN/m3
Output:	stress = 1.08 MPa	mb = 4.38	s = 0.0205
	a = 0.5	siglm = -0.1497 MPa	A = 0.7806
	B = 0.7241	k = 8.71	phi = 52.56 degrees
	coh = 0.697 MPa	sigcm = 5.30 MPa	E = 13435.5 MPa

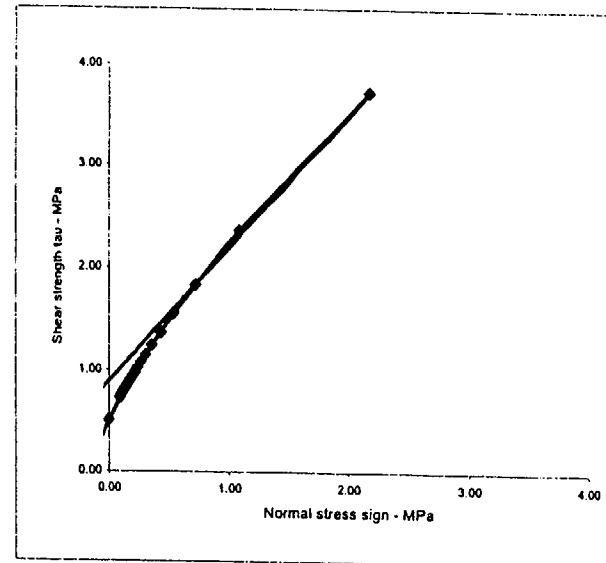
Calculation:

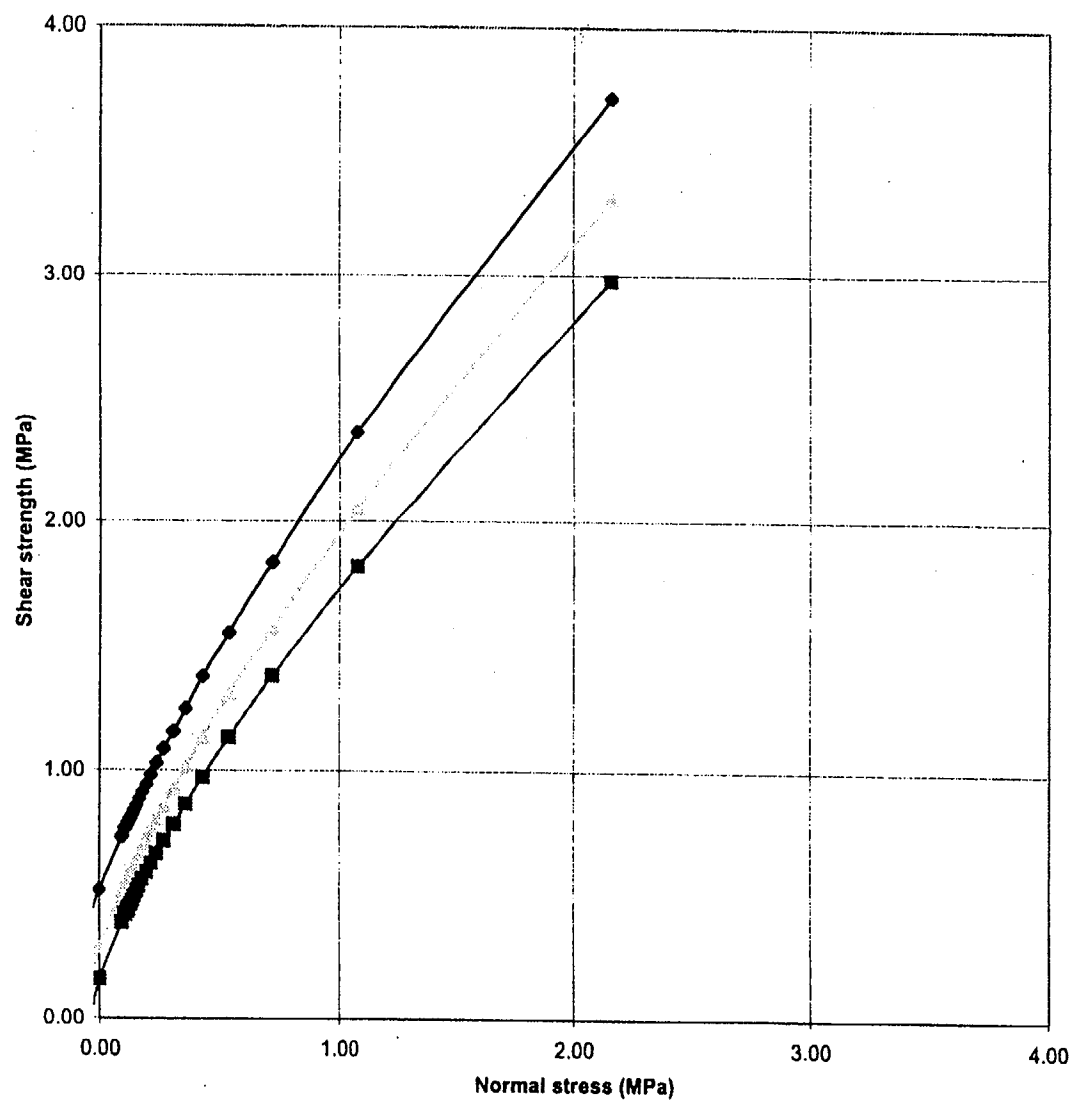
	sig3	1E-10	0.15	0.31	0.46	0.62	0.77	0.93	1.08	Sums
sig1	4.59	6.70	8.34	9.75	11.00	12.15	13.23	14.23	14.23	4.32
ds1ds3	16.32	11.76	9.76	8.58	7.77	7.18	6.72	6.35	74.44	79.99
sign	0.27	0.67	1.05	1.43	1.80	2.16	2.52	2.87	12.77	74.44
tau	1.07	1.76	2.33	2.84	3.30	3.73	4.13	4.51	23.67	12.77
x	-1.89	-1.59	-1.43	-1.31	-1.22	-1.14	-1.08	-1.03	-10.68	23.67
y	-1.48	-1.26	-1.14	-1.05	-0.99	-0.93	-0.89	-0.85	-8.60	11.91
xy	2.79	2.01	1.62	1.38	1.20	1.07	0.96	0.88	11.91	14.86
xsq	3.57	2.54	2.03	1.71	1.48	1.31	1.17	1.05	14.86	52
sig3sig1	0.00	1.03	2.57	4.51	6.79	9.37	12.24	15.36	52	3
sig3sq	0.00	0.02	0.10	0.21	0.38	0.59	0.86	1.17	1.17	3
laucalc	1.07	1.76	2.33	2.83	3.30	3.73	4.14	4.52		
sig1sig3fit	5.30	6.64	7.98	9.33	10.67	12.01	13.36	14.70		
signtaufit	1.24	1.77	2.28	2.77	3.25	3.72	4.19	4.65		

Cell formulae:

σ_c	stress = if(depth>90, sigci*0.25, depth*unitwt)
m_b	mb = mi*EXP((GSI-100)/28)
s	s = IF(GSI>25, EXP((GSI-100)/9), 0)
a	a = IF(GSI>25, 0.5, 0.65-GSI/200)
σ_{lm}	siglm = 0.5*sigci*(mb-SQRT(mb^2+4*s))
σ_1	sig3 = Start at 1E-10 (to avoid zero errors) and increment in 7 steps to stress
σ_1	sig1 = sig3+sigci*(((mb*sig3)/sigci)+s)^a
$\delta\sigma_1/\delta\sigma_3$	ds1ds3 = IF(GSI>25, (1+(mb*sigci)/(2*(sig1-sig3))), 1+(a*mb*a)*(sig3/sigci)^(a-1))
σ_c	sign = sig3+(sig1-sig3)/(1+ds1ds3)
τ	tau = (sign-sig3)*SQRT(ds1ds3)
x	x = LOG((sign-siglm)/sigci)
y	y = LOG(tau/sigci)
xy	xy = x*y
A	A = acalc = 10*(sumy/8 - bcalc*sumx/8)
B	B = bcalc = (sumxy - (sumx*sumy)/8)/(sumxsq - (sumx^2)/8)
k	k = (sumsig3sig1 - (sumsig3*sumsig1)/8)/(sumsig3sq - (sumsig3^2)/8)
ϕ	phi = ASIN((k-1)/(k+1))*180/PI()
c	coh = sigcm/(2*SQRT(k))
σ_{cm}	sigcm = sumsig1/8 - k*sumsig3/8
E	E = IF(sigci>100, 1000*10^((GSI-10)/40), SQRT(sigci/100)*1000*10^((GSI-10)/40))
	phit = (ATAN(acalc*bcalc*((sign-siglm)/sigci)*(bcalc-1)))*180/PI()
	coht = acalc*sigci*((sign-siglm)/sigci)*bcalc-signt*TAN(phit*PI()/180)
	sig3sig1 = sig3*sig1
	sig3sq = sig3^2
	laucalc = acalc*sigci*((sign-siglm)/sigci)*bcalc
	s3sfit = sigcm+k*sig3
	snlaufit = coh+sign*TAN(phit*PI()/180)
	tangent = coht+sign*TAN(phit*PI()/180)

	Principal stress plot		Mohr envelope		
sig3 & sign	sig3	sig1	s1s3fit	sign	taucalc
siglm	-0.15	0.00	3.99	-0.15	0.00
siglm^3/4	-0.11	2.19	4.32	-0.11	0.19
siglm^2/4	-0.07	3.17	4.65	-0.07	0.31
siglm^1/4	-0.04	3.94	4.97	-0.04	0.42
0	0.00	4.59	5.30	0.00	0.51
stress/10.5	0.09	5.95	6.12	0.09	0.73
stress/10	0.11	6.13	6.24	0.11	0.76
stress/9.5	0.11	6.20	6.29	0.11	0.77
stress/9	0.12	6.28	6.34	0.12	0.79
stress/8.5	0.13	6.37	6.40	0.13	0.80
stress/8	0.13	6.47	6.47	0.13	0.82
stress/7.5	0.14	6.57	6.55	0.14	0.84
stress/7	0.15	6.70	6.64	0.15	0.86
stress/6.5	0.17	6.83	6.74	0.17	0.88
stress/6	0.18	6.99	6.86	0.18	0.91
stress/5.5	0.20	7.18	7.01	0.20	0.94
stress/5	0.22	7.39	7.18	0.22	0.98
stress/4.5	0.24	7.65	7.39	0.24	1.03
stress/4	0.27	7.96	7.65	0.27	1.08
stress/3.5	0.31	8.34	7.98	0.31	1.15
stress/3	0.36	8.83	8.43	0.36	1.25
stress/2.5	0.43	9.48	9.06	0.43	1.37
stress/2	0.54	10.39	10.00	0.54	1.55
stress/1.5	0.72	11.78	11.57	0.72	1.84
stress	1.08	14.23	14.70	1.08	2.36
stress/0.5	2.16	20.18	24.10	2.16	3.72



Comparison of GSI ranges - Dolomite ($T_{of_{b-1}}$), HOEK-BROWN

Note: Upper and lower bounds represent one standard deviation above and below the mean, respectively.

Calculation Package 0.19 - Hoek-Brown Rock Mass Strength Worksheet SANDSTONE LOWER BOUND, HOEK-BROWN

Input:	sigci = 12 MPa	mi = 17	GSI = 62
	Depth of failure surface or tunnel below slope* = 50 m	Unit wt. = 0.022 MN/n3	
Output:	stress = 1.11 MPa	mb = 4.28	s = 0.0142
	a = 0.5	sigtm = -0.0408 MPa	A = 0.7600
	B = 0.7197	k = 6.39	phi = 46.82 degrees
	coh = 0.443 MPa	sigcm = 2.24 MPa	E = 6877.8 MPa

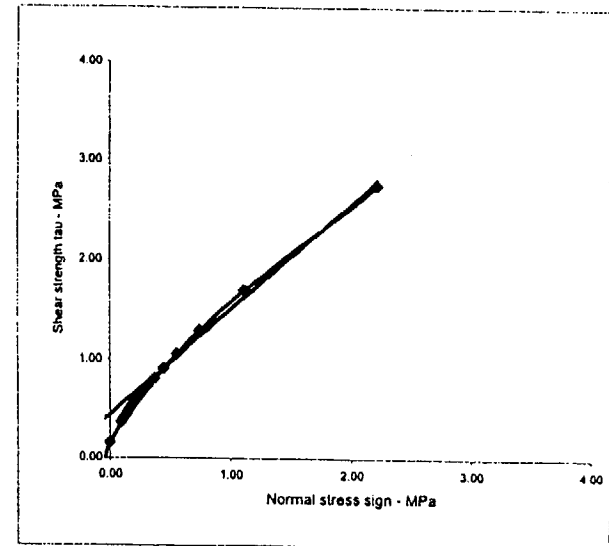
Calculation:

	sig3	1E-10	0.16	0.32	0.48	0.63	0.79	0.95	1.11	Suma
	sig1	1.46	3.40	4.66	5.69	6.59	7.42	8.18	8.89	46.29
	ds1ds3	18.96	9.12	7.06	6.05	5.41	4.97	4.64	4.38	60.60
	sign	0.07	0.46	0.86	1.22	1.56	1.90	2.23	2.56	10.88
	lau	0.32	0.97	1.43	1.82	2.16	2.47	2.76	3.03	14.96
	x	-2.03	-1.37	-1.14	-0.99	-0.88	-0.80	-0.73	-0.68	-8.63
	y	-1.59	-1.10	-0.93	-0.83	-0.76	-0.70	-0.65	-0.61	-7.16
	xy	3.22	1.52	1.06	0.82	0.67	0.56	0.48	0.41	8.74
	xsq	4.13	1.89	1.29	0.98	0.78	0.64	0.54	0.46	10.71
	sig3sig1	0.00	0.54	1.48	2.71	4.18	5.88	7.78	9.87	32
	sig3sq	0.00	0.03	0.10	0.23	0.40	0.63	0.91	1.23	4
	laucalc	0.32	0.96	1.42	1.81	2.16	2.48	2.77	3.05	
	sig1sig3fit	2.24	3.25	4.27	5.28	6.29	7.31	8.32	9.33	
	signtaufit	0.52	0.95	1.36	1.74	2.11	2.47	2.82	3.17	

Cell formulae:

σ_a	stress = IF(depth>90, sigci*0.25, depth*unitwt)
m_b	mb = mi*EXP((GSI-100)/28)
s	s = IF(GSI>25, EXP((GSI-100)/9), 0)
a	a = IF(GSI>25, 0.5, 0.65-GSI/200)
σ_{tm}	sigtm = 0.5*sigci*(mb*SQRT(mb^2+4*s))
σ_1	sig3 = Start at 1E-10 (to avoid zero errors) and increment in 7 steps to stress
σ_1	sig1 = sig3+sigci*(((mb*sig3)/sigci)+s)^a
$\delta\sigma_1/\delta\sigma_3$	ds1ds3 = IF(GSI>25, (1+(mb*sigci)/(2*(sig1-sig3))), 1+(a*mb*a)*(sig3/sigci)^(a-1))
σ_a	sign = sig3*(sig1-sig3)/(1+ds1ds3)
t	lau = (sign-sig3)*SQRT(ds1ds3)
x	x = LOG((sign-sigtm)/sigci)
y	y = LOG(lau/sigci)
xy	xy = x*y
A	A = acalc = 10*(sumy/8 - bcalc*sumx/8)
B	B = bcalc = (sumxy - (sumx*sumy)/8)/(sumxsq - (sumx^2)/8)
k	k = (sumsig3sig1 - (sumsig3*sumsig1)/8)/(sumsig3sq - (sumsig3^2)/8)
ϕ	phi = ASIN((k-1)/(k+1))*180/PI()
c	coh = sigcm/(2*SQRT(k))
σ_{cm}	sigcm = sumsig1/8 - k*sumsig3/8
E	E = IF(sigci>100, 1000*10^((GSI-10)/40), SQRT(sigci/100)*1000*10^((GSI-10)/40))
	phit = (ATAN(acalc*bcalc*((sign-sigtm)/sigci)*(bcalc-1)))*180/PI()
	coht = acalc*sigci*((sign-sigtm)/sigci)*bcalc-signl*TAN(phit*PI()/180)
	sig3sig1 = sig3*sig1
	sig3sq = sig3^2
	laucalc = acalc*sigci*((sign-sigtm)/sigci)*bcalc
	s3sfit = sigcm+k*sig3
	sntaufit = coh+sign*TAN(phi*PI()/180)
	tangent = coht+signl*TAN(phit*PI()/180)

sig3 & sign	sig3	sig1	s1s3fit	sign	laucalc	sntaufit
sigtm	-0.04	0.00	1.98	-0.04	0.00	0.40
sigtm^3/4	-0.03	0.70	2.05	-0.03	0.06	0.41
sigtm^2/4	-0.02	1.02	2.11	-0.02	0.09	0.42
sigtm^1/4	-0.01	1.26	2.18	-0.01	0.12	0.43
0	0.00	1.46	2.24	0.00	0.15	0.44
stress/10.5	0.10	2.78	2.86	0.10	0.37	0.55
stress/10	0.11	2.94	2.95	0.11	0.40	0.56
stress/9.5	0.12	3.00	2.99	0.12	0.41	0.57
stress/9	0.12	3.06	3.03	0.12	0.42	0.57
stress/8.5	0.13	3.13	3.08	0.13	0.43	0.58
stress/8	0.14	3.21	3.13	0.14	0.45	0.59
stress/7.5	0.15	3.30	3.19	0.15	0.46	0.60
stress/7	0.16	3.40	3.25	0.16	0.48	0.61
stress/6.5	0.17	3.51	3.33	0.17	0.50	0.63
stress/6	0.19	3.63	3.42	0.19	0.53	0.64
stress/5.5	0.20	3.77	3.53	0.20	0.55	0.66
stress/5	0.22	3.94	3.66	0.22	0.59	0.68
stress/4.5	0.25	4.14	3.82	0.25	0.63	0.71
stress/4	0.28	4.37	4.01	0.28	0.67	0.74
stress/3.5	0.32	4.66	4.27	0.32	0.73	0.78
stress/3	0.37	5.02	4.60	0.37	0.81	0.84
stress/2.5	0.44	5.49	5.08	0.44	0.91	0.92
stress/2	0.56	6.15	5.79	0.56	1.06	1.03
stress/1.5	0.74	7.15	6.97	0.74	1.29	1.23
stress	1.11	8.89	9.33	1.11	1.70	1.63
stress/0.5	2.22	13.13	16.42	2.22	2.76	2.81



Calculation Package 0.19 - Hoek-Brown Rock Mass Strength Worksheet SANDSTONE MEAN, HOEK-BROWN

Input:	sigci = 22 MPa	mi = 18	GSI = 65
	Depth of failure surface or tunnel below slope* = 50 m	Unit wt. = 0.022 MN/m3	
Output:	stress = 1.11 MPa	mb = 5.06	s = 0.0200
	a = 0.5	siglm = -0.0853 MPa	A = 0.8112
	B = 0.7243	k = 8.25	phi = 51.81 degrees
	coh = 0.680 MPa	sigcm = 3.91 MPa	E = 10895.0 MPa

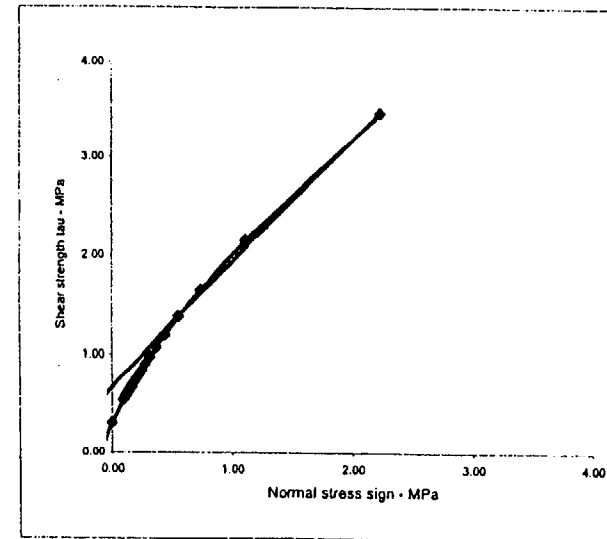
Calculation:

									Sums
sig3	1E-10	0.16	0.32	0.48	0.63	0.79	0.95	1.11	4.44
sig1	3.06	5.32	6.95	8.31	9.51	10.59	11.60	12.54	67.89
ds1ds3	18.89	11.59	9.24	7.98	7.16	6.58	6.14	5.78	73.36
sign	0.15	0.57	0.97	1.35	1.72	2.09	2.44	2.80	12.08
tau	0.67	1.40	1.97	2.46	2.91	3.32	3.70	4.05	20.47
x	-1.96	-1.52	-1.31	-1.18	-1.08	-1.00	-0.93	-0.87	-9.85
y	-1.51	-1.19	-1.04	-0.94	-0.87	-0.81	-0.77	-0.73	-7.86
xy	2.95	1.81	1.37	1.11	0.94	0.81	0.71	0.64	10.34
xsq	3.83	2.31	1.72	1.39	1.16	1.00	0.87	0.77	13.04
sig3sig1	0.00	0.84	2.20	3.95	6.03	8.40	11.04	13.92	46
sig3sq	0.00	0.03	0.10	0.23	0.40	0.63	0.91	1.23	4
taucalc	0.67	1.39	1.96	2.46	2.90	3.32	3.71	4.07	
sig1sig3fit	3.91	5.21	6.52	7.83	9.14	10.45	11.76	13.07	
signtaufit	0.87	1.40	1.90	2.38	2.85	3.31	3.76	4.21	

Cell formulas:

σ_c	stress = if(depth>90, sigci*0.25, depth*unitwt)
m_b	mb = mi*EXP((GSI-100)/28)
s	s = IF(GSI>25, EXP((GSI-100)/9), 0)
a	a = IF(GSI>25, 0.5, 0.65-GSI/200)
σ_{lm}	siglm = 0.5*sigci*(mb-SQRT(mb^2+4*s))
σ_3	sig3 = Start at 1E-10 (to avoid zero errors) and increment in 7 steps to stress
σ_1	sig1 = sig3+sigci*(((mb*sig3)/sigci)+s)^a
$\delta\sigma_1/\delta\sigma_3$	ds1ds3 = IF(GSI>25, (1+(mb*sigci)/((2*(sig1-sig3))), 1+(a*mb*a)*(sig3/sigci)^(a-1))
σ_c	sign = sig3*(sig1-sig3)/(1+ds1ds3)
τ	tau = (sign-sig3)*SQRT(ds1ds3)
x	x = LOG((sign-siglm)/sigci)
y	y = LOG(tau/sigci)
	xy = x*y xsq = x^2
A	A = acalc = 10*(sumy/8 - bcalc*sumx/8)
B	B = bcalc = (sumxy - (sumx*sumy)/8)/(sumxsq - (sumx^2)/8)
k	k = (sumsig3sig1 - (sumsig3*sumsig1)/8)/(sumsig3sq - (sumsig3^2)/8)
ϕ	phi = ASIN((k-1)/(k+1))*180/PI()
c	coh = sigcm/(2*SQRT(k))
σ_{cm}	sigcm = sumsig1/8 - k*sumsig3/8
E	E = IF(sigci>100, 1000*10^((GSI-10)/40), SQRT(sigci/100)*1000*10^((GSI-10)/40))
	phit = (ATAN(acalc*bcalc*((sign-siglm)/sigci)*(bcalc-1)))*180/PI()
	coht = acalc*sigci*((sign-siglm)/sigci)*bcalc-siglm*TAN(phit*PI()/180)
	sig3sig1 = sig3*sig1 sig3sq = sig3^2
	taucalc = acalc*sigci*((sign-siglm)/sigci)*bcalc
	s3sfit = sigcm+k*sig3
	snlaufit = coh+sign*TAN(phit*PI()/180)
	tangent = coht+sign*TAN(phit*PI()/180)

	Principal stress plot			Mohr envelope		
	sig3	sig1	s1s3fit	sign	taucalc	snlaufit
sig3 & sign	-0.09	0.00	3.20	-0.09	0.00	0.57
siglm	-0.06	1.47	3.38	-0.06	0.12	0.60
siglm^3/4	-0.04	2.12	3.55	-0.04	0.19	0.63
siglm^2/4	-0.02	2.63	3.73	-0.02	0.26	0.65
siglm^1/4	0.00	3.06	3.91	0.00	0.32	0.68
0	0.10	4.56	4.70	0.10	0.55	0.80
stress/10.5	0.11	4.75	4.82	0.11	0.58	0.82
stress/10	0.12	4.82	4.87	0.12	0.59	0.83
stress/9.5	0.12	4.90	4.92	0.12	0.61	0.84
stress/9	0.13	4.99	4.98	0.13	0.62	0.84
stress/8.5	0.14	5.09	5.05	0.14	0.64	0.85
stress/8	0.15	5.20	5.13	0.15	0.66	0.87
stress/7.5	0.16	5.32	5.21	0.16	0.68	0.88
stress/7	0.17	5.46	5.32	0.17	0.71	0.90
stress/6.5	0.19	5.62	5.43	0.19	0.73	0.91
stress/6	0.20	5.81	5.57	0.20	0.77	0.93
stress/5.5	0.22	6.02	5.74	0.22	0.81	0.96
stress/5	0.25	6.27	5.94	0.25	0.85	0.99
stress/4.5	0.28	6.58	6.20	0.28	0.91	1.03
stress/4	0.32	6.95	6.52	0.32	0.98	1.08
stress/3.5	0.37	7.43	6.96	0.37	1.07	1.15
stress/3	0.44	8.05	7.57	0.44	1.19	1.24
stress/2.5	0.56	8.92	8.49	0.56	1.37	1.38
stress/2	0.74	10.24	10.01	0.74	1.65	1.61
stress/1.5	1.11	12.54	13.07	1.11	2.15	2.06
stress	2.22	18.10	22.23	2.22	3.47	3.48



Calculation Package 0.19 - Hoek-Brown Rock Mass Strength Worksheet SANDSTONE UPPER BOUND, HOEK-BROWN

Input:	sigci = 31 MPa	mi = 19	GSI = 68
	Depth of failure surface or tunnel below slope* = 50 m	Unit wt. = 0.022 MN/m3	
Output:	stress = 1.11 MPa	mb = 5.97	s = 0.0282
	a = 0.5	siglm = -0.1460 MPa	A = 0.8580
	B = 0.7271	k = 9.78	phi = 54.54 degrees
	coh = 0.965 MPa	sigcm = 6.04 MPa	E = 15576.8 MPa

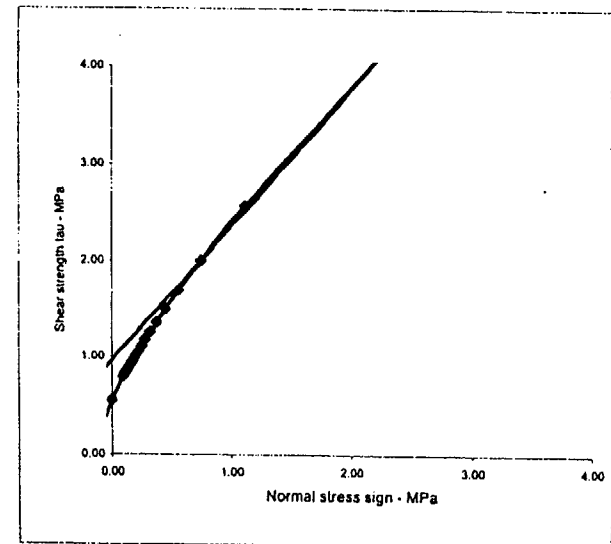
Calculation:

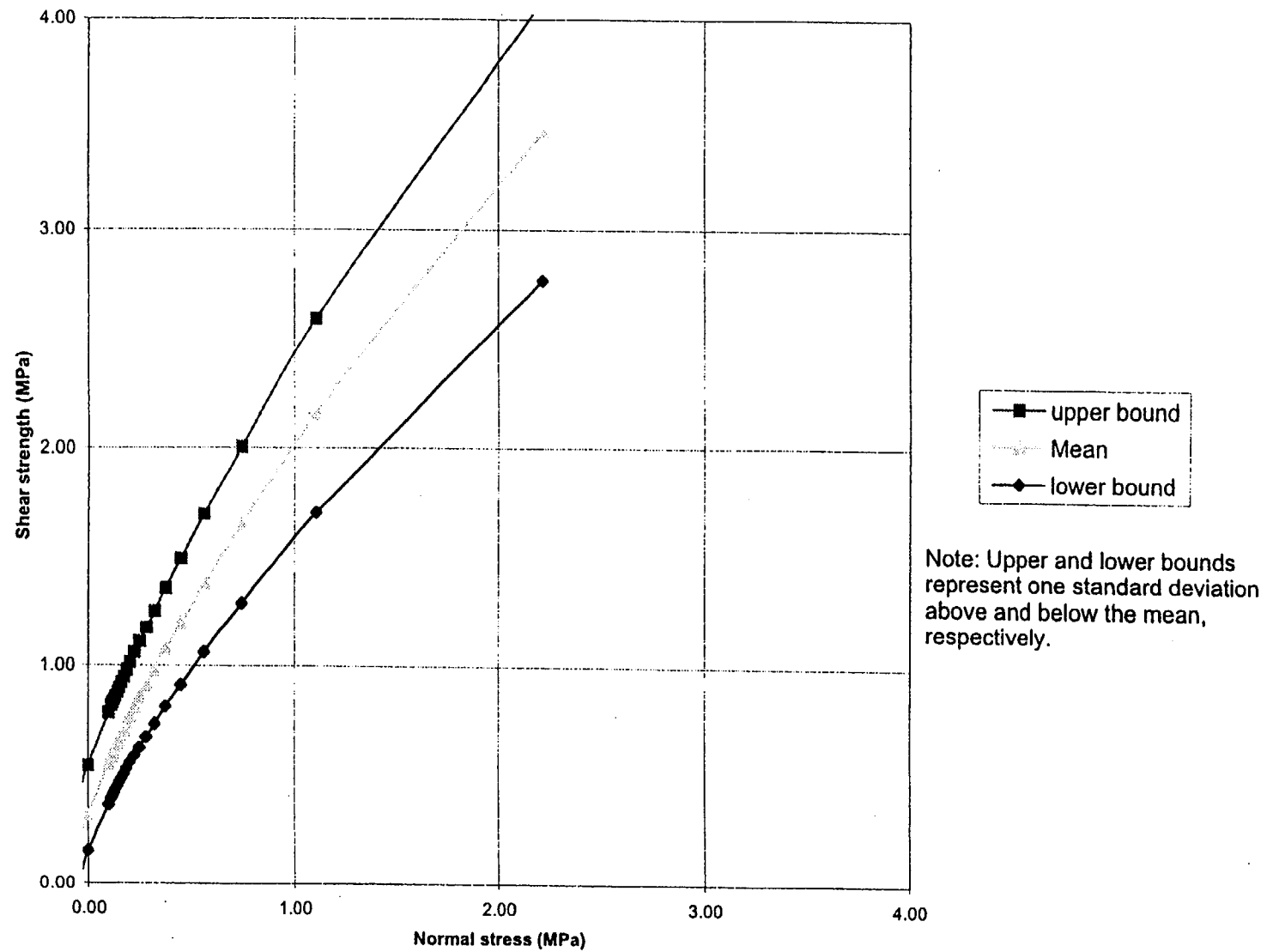
	sig3	1E-10	0.16	0.32	0.48	0.63	0.79	0.95	1.11	Sums
sig1	5.19	7.66	9.56	11.19	12.64	13.96	15.19	16.34	17.72	4.44
ds1ds3	18.77	13.31	10.98	9.61	8.69	8.01	7.48	7.06	6.34	91.72
sign	0.26	0.68	1.09	1.49	1.87	2.25	2.63	3.00	3.27	83.92
lau	1.14	1.91	2.56	3.13	3.65	4.14	4.59	5.02	5.26	13.27
x	-1.88	-1.57	-1.40	-1.28	-1.18	-1.11	-1.05	-0.99	-0.96	26.13
y	-1.43	-1.21	-1.08	-0.99	-0.93	-0.87	-0.83	-0.79	-0.74	-10.46
xy	2.69	1.90	1.51	1.27	1.10	0.97	0.87	0.78	0.71	-8.14
xsq	3.53	2.47	1.96	1.63	1.40	1.23	1.10	0.98	0.91	11.09
sig3sig1	0.00	1.21	3.03	5.32	8.02	11.07	14.45	18.13	21.61	14.30
sig3sq	0.00	0.03	0.10	0.23	0.40	0.63	0.91	1.23	1.61	61
laucalc	1.14	1.91	2.55	3.12	3.65	4.14	4.60	5.03	5.26	4
sig1sig3fit	6.04	7.59	9.14	10.69	12.24	13.79	15.34	16.89	18.44	
signtaufit	1.33	1.92	2.49	3.05	3.59	4.13	4.66	5.18	5.69	

Cell formulae:

σ_n	stress = IF(depth>90, sigci*0.25, depth*unitwt)
m_b	mb = mi*EXP((GSI-100)/28)
s	s = IF(GSI>25, EXP((GSI-100)/9), 0)
a	a = IF(GSI>25, 0.5, 0.65-GSI/200)
σ_{lm}	siglm = 0.5*sigci*(mb-SQRT(mb*2+4*s))
σ_1	sig3 = Start at 1E-10 (to avoid zero errors) and increment in 7 steps to stress
σ_1	sig1 = sig3+sigci*((mb*sig3)/sigci)+s*a
$\delta\sigma_1/\delta\sigma_3$	ds1ds3 = IF(GSI>25, (1+(mb*sigci)/(2*(sig1-sig3))), 1+(a*mb*a)*(sig3/sigci)^(a-1))
σ_n	sign = sig3+(sig1-sig3)/(1+ds1ds3)
τ	lau = (sign-sig3)*SQRT(ds1ds3)
x	x = LOG((sign-siglm)/sigci)
y	y = LOG(lau/sigci)
xy	xy = x*y
A	acalc = 10*(sumy/8 - bcalc*sumx/8)
B	B = (sumxy - (sumx*sumy)/8)/(sumxsq - (sumx^2)/8)
k	k = (sumsig3sig1 - (sumsig3*sumsig1)/8)/(sumsig3sq - (sumsig3^2)/8)
ϕ	phi = ASIN((k-1)/(k+1))*180/PI()
c	coh = sigcm/(2*SQRT(k))
σ_{cm}	sigcm = sumsig1/8 - k*sumsig3/8
E	E = IF(sigci>100, 1000*10^((GSI-10)/40), SQRT(sigci/100)*1000*10^((GSI-10)/40))
	phit = (ATAN(acalc*bcalc*((sign-siglm)/sigci)^(bcalc-1)))*180/PI()
	coht = acalc*sigci*((sign-siglm)/sigci)*bcalc-signt*TAN(phit*PI()/180)
	sig3sig1 = sig3*sig1
	sig3sq = sig3^2
	laucalc = acalc*sigci*((sign-siglm)/sigci)*bcalc
	s3sfit = sigcm+k*sig3
	snlaufit = coh+sign*TAN(phi*PI()/180)
	lagent = coht+sign*TAN(phi*PI()/180)

	Principal stress plot	Mohr envelope
sig3 & sign	sig3	sign
siglm	-0.15	0.00
siglm^3/4	-0.11	2.49
siglm^2/4	-0.07	3.60
siglm^1/4	-0.04	4.46
0	0.00	5.19
stress/10.5	0.10	6.79
stress/10	0.11	7.00
stress/9.5	0.12	7.08
stress/9	0.12	7.18
stress/8.5	0.13	7.28
stress/8	0.14	7.39
stress/7.5	0.15	7.52
stress/7	0.16	7.66
stress/6.5	0.17	7.82
stress/6	0.19	8.00
stress/5.5	0.20	8.22
stress/5	0.22	8.47
stress/4.5	0.25	8.76
stress/4	0.28	9.12
stress/3.5	0.32	9.56
stress/3	0.37	10.13
stress/2.5	0.44	10.88
stress/2	0.56	11.93
stress/1.5	0.74	13.53
stress	1.11	16.34
stress/0.5	2.22	23.12
		27.75
		2.22
		4.09
		4.08



Comparison of strength ranges - Sandstone (Tof_{b-2}), HOEK-BROWN

Calculation Package 0.19 - Hoek-Brown Rock Mass Strength Worksheet SANDSTONE UC LOW, HOEK-BROWN

Input:	sigci = 12 MPa	mi = 18	GSI = 65
	Depth of failure surface of tunnel below slope* = 50 m		Unit wt. = 0.022 MN/m3
Output:	stress = 1.11 MPa	mb = 5.06	s = 0.0200
	a = 0.5	sigtm = -0.0486 MPa	A = 0.8002
	B = 0.7208	k = 6.78	phi = 47.98 degrees
	coh = 0.487 MPa	sigcm = 2.54 MPa	E = 8221.5 MPa

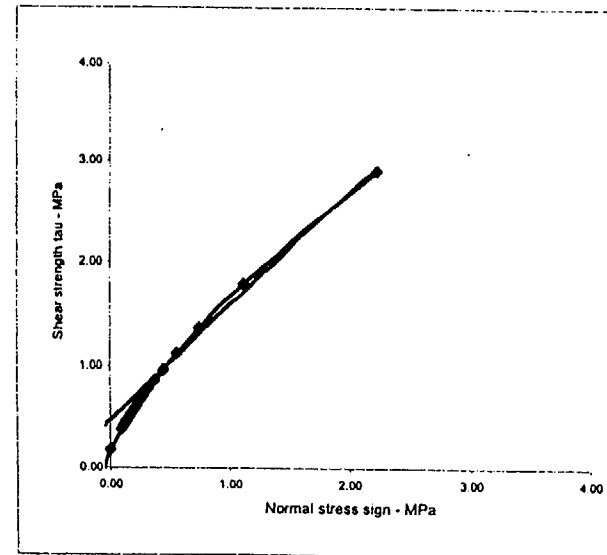
Calculation:

	sig3	1E-10	0.16	0.32	0.48	0.63	0.79	0.95	1.11	Sums
sig1	1.74	3.75	5.09	6.19	7.16	8.03	8.84	9.60	10.41	50.41
ds1ds3	18.89	9.67	7.52	6.45	5.77	5.30	4.95	4.67	4.44	63.22
sign	0.09	0.50	0.88	1.24	1.60	1.94	2.28	2.61	2.95	11.13
lau	0.38	1.05	1.54	1.95	2.31	2.65	2.95	3.24	3.54	16.06
x	-1.96	-1.35	-1.12	-0.98	-0.87	-0.79	-0.72	-0.67	-0.62	-8.47
y	-1.51	-1.07	-0.90	-0.80	-0.73	-0.67	-0.62	-0.58	-0.54	-6.88
xy	2.95	1.45	1.02	0.78	0.63	0.53	0.45	0.39	0.34	8.20
xsq	3.83	1.83	1.26	0.96	0.76	0.63	0.52	0.44	0.38	10.24
sig3sig1	0.00	0.59	1.61	2.94	4.54	6.37	8.41	10.66	13.11	35
sig3sq	0.00	0.03	0.10	0.23	0.40	0.63	0.91	1.23	1.61	4
laucalc	0.38	1.04	1.53	1.94	2.31	2.65	2.96	3.26	3.56	
sig1sig3fit	2.54	3.61	4.69	5.76	6.84	7.91	8.99	10.06	11.13	
signtaufit	0.58	1.04	1.46	1.87	2.26	2.64	3.02	3.38	3.75	

Cell formulae:

σ_c	stress = IF(depth>90, sigci*0.25, depth*unitwt)
m_b	mb = mi*EXP((GSI-100)/28)
s	s = IF(GSI>25, EXP((GSI-100)/9), 0)
a	a = IF(GSI>25, 0.5, 0.65-GSI/200)
σ_{tm}	sigtm = 0.5*sigci*(mb-SQRT(mb*2*4*s))
σ_1	sig3 = Start at 1E-10 (to avoid zero errors) and increment in 7 steps to stress
σ_1	sig1 = sig3+sigci*((mb*sig3)/sigci+s)*a
$\delta\sigma_1/\delta\sigma_3$	ds1ds3 = IF(GSI>25, (1+(mb*sigci)/(2*(sig1-sig3))), 1+(a*mb*a)*(sig3/sigci)^(a-1))
σ_c	sign = sig3+(sig1-sig3)/(1+ds1ds3)
τ	lau = (sign-sig3)*SQRT(ds1ds3)
x	x = LOG((sign-sigtm)/sigci)
y	y = LOG(lau/sigci)
xy	xy = x*y
A	A = acalc = 10^(sumy/8 - bcalc*sumx/8)
B	B = bcalc = (sumxy - (sumx*sumy)/8)/(sumxsq - (sumx*2)/8)
k	k = (sumsig3sig1 - (sumsig3*sumsig1)/8)/(sumsig3sq - (sumsig3*2)/8)
ϕ	phi = ASIN((k-1)/(k+1))*180/PI()
c	coh = sigcm/(2*SQRT(k))
σ_{cm}	sigcm = sumsig1/8 - k*sumsig3/8
E	E = IF(sigci>100, 1000*10^((GSI-10)/40), SQRT(sigci/100)*1000*10^((GSI-10)/40))
	phil = (ATAN(acalc*bcalc*((sign-sigtm)/sigci)+(bcalc-1)))*180/PI()
	coht = acalc*sigci*((sign-sigtm)/sigci)*bcalc-sigtm*TAN(phil*PI()/180)
	sig3sig1 = sig3*sig1
	sig3sq = sig3*2
	laucalc = acalc*sigci*((sign-sigtm)/sigci)*bcalc
	s3sifit = sigcm+k*sig3
	sntaufit = coh+sign*TAN(phil*PI()/180)
	tangent = coht+sign*TAN(phil*PI()/180)

sig3 & sign	sig3	sig1	s1s3fit	sign	laucalc	sntaufit
sigtm	-0.05	0.00	2.21	-0.05	0.00	0.43
sigtm*3/4	-0.04	0.83	2.29	-0.04	0.07	0.45
sigtm*2/4	-0.02	1.21	2.37	-0.02	0.11	0.46
sigtm*1/4	-0.01	1.50	2.46	-0.01	0.15	0.47
0	0.00	1.74	2.54	0.00	0.18	0.49
stress/10.5	0.10	3.10	3.19	0.10	0.40	0.59
stress/10	0.11	3.26	3.29	0.11	0.43	0.61
stress/9.5	0.12	3.33	3.33	0.12	0.44	0.62
stress/9	0.12	3.40	3.37	0.12	0.45	0.62
stress/8.5	0.13	3.47	3.42	0.13	0.47	0.63
stress/8	0.14	3.55	3.48	0.14	0.48	0.64
stress/7.5	0.15	3.65	3.54	0.15	0.50	0.65
stress/7	0.16	3.75	3.61	0.16	0.52	0.66
stress/6.5	0.17	3.87	3.70	0.17	0.54	0.68
stress/6	0.19	4.00	3.79	0.19	0.57	0.69
stress/5.5	0.20	4.15	3.91	0.20	0.59	0.71
stress/5	0.22	4.33	4.04	0.22	0.63	0.73
stress/4.5	0.25	4.54	4.21	0.25	0.67	0.76
stress/4	0.28	4.78	4.42	0.28	0.72	0.80
stress/3.5	0.32	5.09	4.69	0.32	0.78	0.84
stress/3	0.37	5.48	5.05	0.37	0.86	0.90
stress/2.5	0.44	5.98	5.55	0.44	0.97	0.98
stress/2	0.56	6.69	6.30	0.56	1.12	1.10
stress/1.5	0.74	7.75	7.56	0.74	1.36	1.31
stress	1.11	9.60	10.06	1.11	1.79	1.72
stress/0.5	2.22	14.11	17.59	2.22	2.91	2.95



Calculation Package 0.19 - Hoek-Brown Rock Mass Strength Worksheet SANDSTONE UC HIGH, HOEK-BROWN

Input:	sigci = 31 MPa	mi = 18	GSI = 65
	Depth of failure surface or tunnel below slope* = 50 m	Unit wt. = 0.022 MN/m3	
Output:	stress = 1.11 MPa	mb = 5.06	s = 0.0200
	a = 0.5	sigtm = -0.1221 MPa	A = 0.8176
	B = 0.7263	k = 9.29	phi = 53.68 degrees
	coh = 0.857 MPa	sigcm = 5.23 MPa	E = 13031.0 MPa

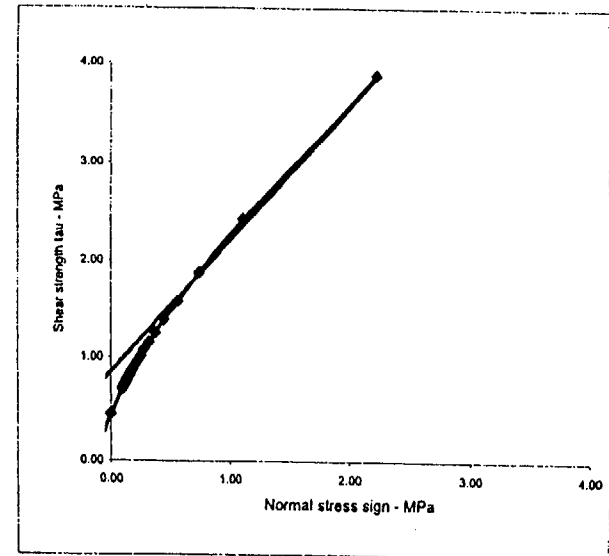
Calculation:

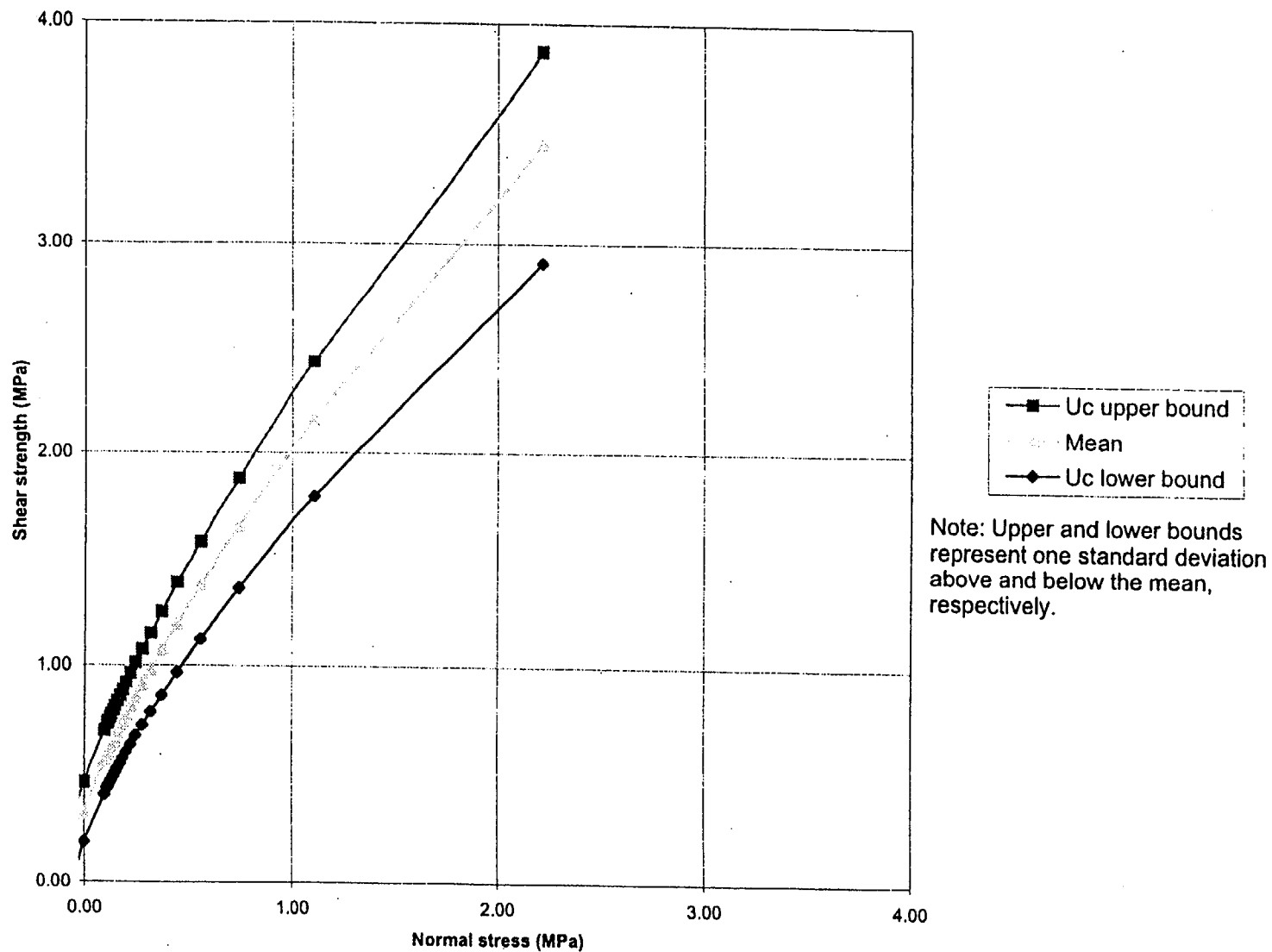
	sig3	1E-10	0.16	0.32	0.48	0.63	0.79	0.95	1.11	Sums
sig1	4.37	6.79	8.61	10.15	11.51	12.76	13.91	14.99	15.99	83.09
ds1ds3	18.89	12.80	10.44	9.09	8.19	7.54	7.04	6.63	6.32	80.62
sign	0.22	0.64	1.04	1.43	1.82	2.19	2.56	2.93	3.29	12.84
tau	0.96	1.72	2.34	2.89	3.39	3.85	4.28	4.68	5.04	24.10
x	-1.96	-1.61	-1.42	-1.30	-1.20	-1.13	-1.06	-1.01	-0.96	-10.68
y	-1.51	-1.25	-1.12	-1.03	-0.96	-0.90	-0.86	-0.82	-0.78	-8.46
xy	2.95	2.02	1.60	1.34	1.15	1.02	0.91	0.82	0.75	11.81
xsq	3.83	2.59	2.03	1.68	1.45	1.27	1.13	1.01	0.92	14.97
sig3sig1	0.00	1.08	2.73	4.83	7.30	10.12	13.24	16.64	20.40	56
sig3sq	0.00	0.03	0.10	0.23	0.40	0.63	0.91	1.23	1.60	4
laucalc	0.96	1.71	2.33	2.88	3.38	3.85	4.29	4.70	5.06	
sig1sig3fit	5.23	6.70	8.18	9.65	11.12	12.60	14.07	15.55	17.02	
signtaufit	1.16	1.73	2.28	2.81	3.33	3.84	4.35	4.84	5.32	

Cell formulae:

σ_a	stress = if(depth>90, sigci*0.25, depth*unitwt)
m_b	mb = mi*EXP((GSI-100)/28)
s	s = IF(GSI>25, EXP((GSI-100)/9), 0)
a	a = IF(GSI>25, 0.5, 0.65-GSI/200)
σ_{tm}	sigtm = 0.5*sigci*(mb-SQRT(mb*2+4*s))
σ_3	sig3 = Start at 1E-10 (to avoid zero errors) and increment in 7 steps to stress
σ_1	sig1 = sig3+sigci*(((mb*sig3)/sigci)+s)^a
$\delta\sigma_1/\delta\sigma_3$	ds1ds3 = IF(GSI>25, (1+(mb*sigci)/(2*(sig1-sig3))), 1+(a*mb*a)*(sig3/sigci)^(a-1))
σ_a	sign = sig3+(sig1-sig3)/(1+ds1ds3)
τ	tau = (sign-sig3)*SQRT(ds1ds3)
x	x = LOG((sign-sigtm)/sigci)
y	y = LOG(tau/sigci)
xy	xy = x*y
A	A = acalc = 10*(sumy/8 - bcalc*sumx/8)
B	B = bcalc = (sumxy - (sumx*sumy)/8)/(sumxsq - (sumx*2)/8)
k	k = (sumsig3sig1 - (sumsig3*sumsig1)/8)/(sumsig3sq - (sumsig3*2)/8)
ϕ	phi = ASIN((k-1)/(k+1))*180/PI()
c	coh = sigcm/(2*SQRT(k))
σ_{cm}	sigcm = sumsig1/8 - k*sumsig3/8
E	E = IF(sigci>100, 1000*10^((GSI-10)/40), SQRT(sigci/100)*1000*10^((GSI-10)/40))
	phit = (ATAN(acalc*bcalc*((sign-sigtm)/sigci)+(bcalc-1))) * 180/PI()
	coht = acalc*sigci*((sign-sigtm)/sigci)*bcalc-sigtm*TAN(phit*PI()/180)
	sig3sig1 = sig3*sig1
	sig3sq = sig3^2
	laucalc = acalc*sigci*((sign-sigtm)/sigci)*bcalc
	s3sfit = sigcm+k*sig3
	snlaufit = coh+sign*TAN(phi*PI()/180)
	tangent = coht+sign*TAN(phit*PI()/180)

	Principal stress plot	Mohr envelope
sig3 & sign	sig3	sign
sigtm	-0.12	0.00
sigtm^3/4	-0.09	2.10
sigtm^2/4	-0.06	3.03
sigtm^1/4	-0.03	3.76
0	0.00	4.37
stress/10.5	0.10	5.95
stress/10	0.11	6.15
stress/9.5	0.12	6.23
stress/9	0.12	6.32
stress/8.5	0.13	6.42
stress/8	0.14	6.53
stress/7.5	0.15	6.65
stress/7	0.16	6.79
stress/6.5	0.17	6.94
stress/6	0.19	7.12
stress/5.5	0.20	7.32
stress/5	0.22	7.56
stress/4.5	0.25	7.84
stress/4	0.28	8.19
stress/3.5	0.32	8.61
stress/3	0.37	9.15
stress/2.5	0.44	9.86
stress/2	0.56	10.85
stress/1.5	0.74	12.35
stress	1.11	14.99
stress/0.5	2.22	21.36
	laucalc	sign
	0.00	-0.12
	0.17	-0.09
	0.27	-0.06
	0.37	-0.03
	0.45	0.00
	0.69	0.10
	0.73	0.11
	0.77	0.12
	0.82	0.12
	0.88	0.12
	0.99	0.12
	1.01	0.12
	1.04	0.12
	1.05	0.12
	1.06	0.12
	1.07	0.12
	1.09	0.12
	1.11	0.12
	1.13	0.12
	1.16	0.12
	1.19	0.12
	1.23	0.12
	1.29	0.12
	1.36	0.12
	1.46	0.12
	1.61	0.12
	1.86	0.12
	2.37	0.12



Comparison of U_c ranges - Sandstone (Tof_{b-2}), HOEK-BROWN

Calculation Package 0.19 - Hoek-Brown Rock Mass Strength Worksheet SANDSTONE MI LOW, HOEK-BROWN

Input:	sigci = 22 MPa	mi = 17	GSI = 65
	Depth of failure surface or tunnel below slope* = 50 m	Unit wt. = 0.022 MN/m3	
Output:	stress = 1.11 MPa	mb = 4.78	s = 0.0200
	a = 0.5	siglm = -0.0904 MPa	A = 0.7960
	B = 0.7233	k = 8.00	phi = 51.06 degrees
	coh = 0.683 MPa	sigcm = 3.86 MPa	E = 10895.0 MPa

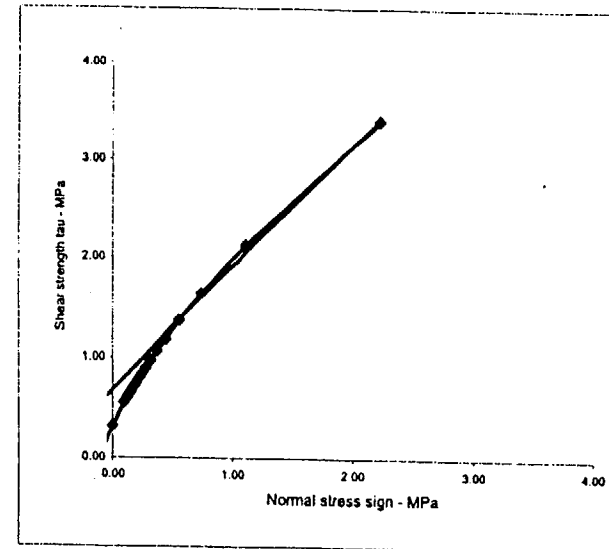
Calculation:

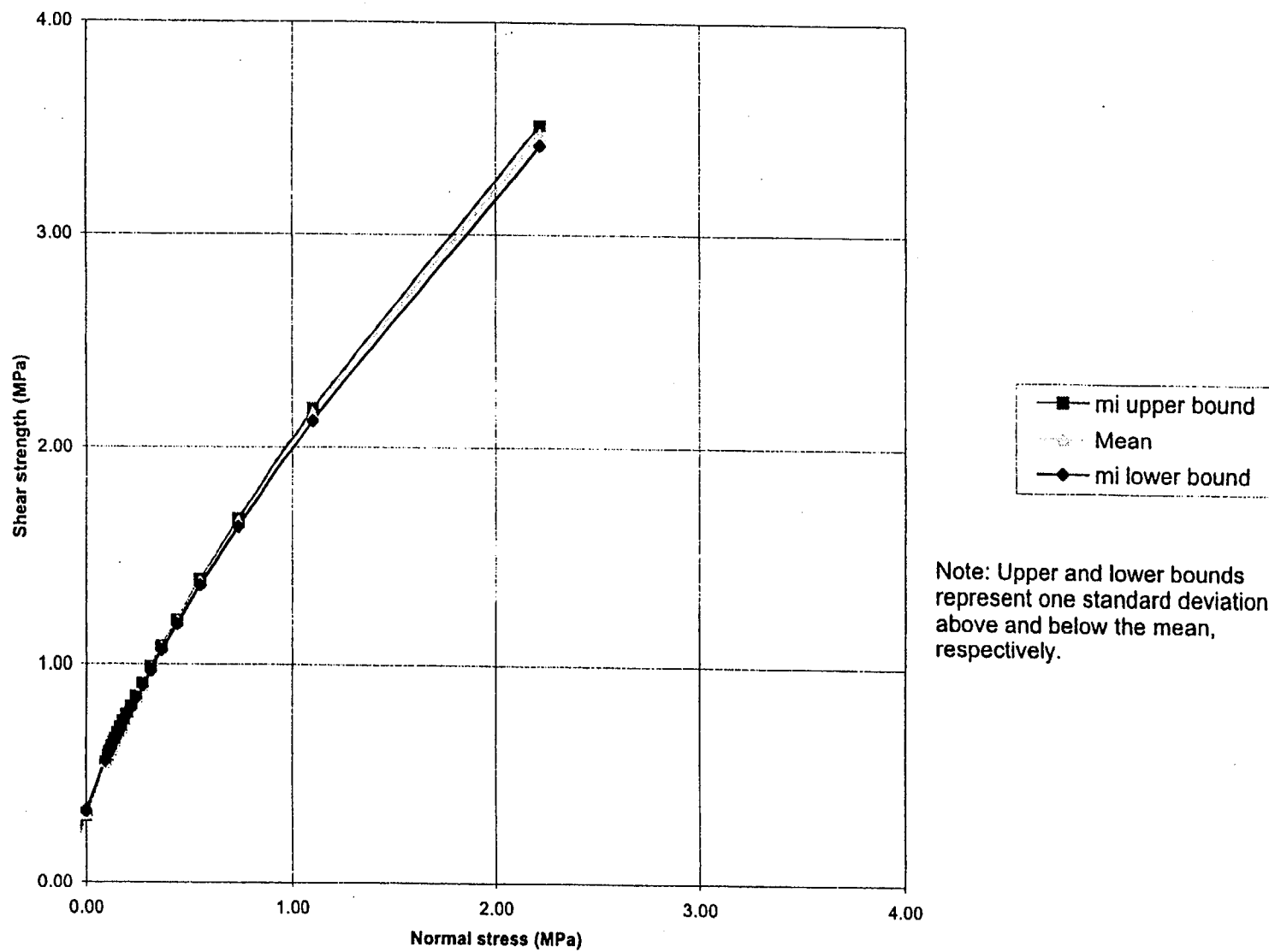
	sig3	1E-10	0.16	0.32	0.48	0.63	0.79	0.95	1.11	Sums
sig1	3.06	5.23	6.80	8.12	9.28	10.34	11.32	12.24	13.14	66.40
ds1ds3	17.89	11.18	8.96	7.75	6.97	6.41	5.98	5.64	5.34	70.76
sign	0.16	0.57	0.97	1.35	1.72	2.08	2.44	2.79	3.14	12.08
tau	0.68	1.39	1.95	2.43	2.87	3.26	3.63	3.98	4.34	20.20
x	-1.93	-1.51	-1.31	-1.18	-1.08	-1.00	-0.93	-0.88	-0.81	-7.89
y	-1.50	-1.19	-1.04	-0.95	-0.88	-0.82	-0.77	-0.73	-0.69	-7.89
xy	2.90	1.80	1.37	1.12	0.94	0.82	0.72	0.64	0.58	10.31
xsq	3.74	2.28	1.71	1.38	1.16	0.99	0.87	0.77	0.69	12.91
sig3sig1	0.00	0.83	2.16	3.86	5.89	8.20	10.77	13.59	16.59	45
sig3sq	0.00	0.03	0.10	0.23	0.40	0.63	0.91	1.23	1.60	4
laucalc	0.69	1.39	1.94	2.42	2.86	3.27	3.64	4.00	4.34	
sig1sig3fit	3.86	5.13	6.40	7.67	8.93	10.20	11.47	12.74	14.01	
signtaufit	0.88	1.39	1.88	2.35	2.81	3.26	3.70	4.13	4.57	

Cell formulae:

σ_c	stress = if(depth>90, sigci*0.25, depth*unitwt)
m_b	mb = mi*EXP((GSI-100)/28)
s	s = IF(GSI>25, EXP((GSI-100)/9), 0)
a	a = IF(GSI>25, 0.5, 0.65-GSI/200)
σ_{lm}	siglm = 0.5*sigci*(mb-SQRT(mb*2+4*s))
σ_1	sig3 = Start at 1E-10 (to avoid zero errors) and increment in 7 steps to stress
σ_1	sig1 = sig3+sigci*(((mb*sig3)/sigci)+s)^a
$\delta\sigma_1/\delta\sigma_3$	ds1ds3 = IF(GSI>25, (1+(mb*sigci)/(2*(sig1-sig3))), 1+(a*mb*a)*(sig3/sigci)^(a-1))
σ_n	sign = sig3+(sig1-sig3)/(1+ds1ds3)
τ	tau = (sign-sig3)*SQRT(ds1ds3)
x	x = LOG((sign-siglm)/sigci)
y	y = LOG(tau/sigci)
A	xy = x*y xsq = x^2
B	A = acalc = 10*(sumy/8 - bcalc*sumx/8)
k	B = bcalc = (sumxy - (sumx*sumy)/8)/(sumxsq - (sumx^2)/8)
ϕ	k = (sumsig3sig1 - (sumsig3*sumsig1)/8)/(sumsig3sq - (sumsig3^2)/8)
c	phi = ASIN((k-1)/(k+1))*180/PI()
σ_{cm}	coh = sigcm/(2*SQRT(k))
E	sigcm = sumsig1/8 - k*sumsig3/8
	E = IF(sigci>100, 1000*10^((GSI-10)/40), SQRT(sigci/100)*1000*10^((GSI-10)/40))
	phi1 = (ATAN(acalc*bcalc*((signt-siglm)/sigci)*(bcalc-1)))*180/PI()
	coht = acalc*sigci*((signt-siglm)/sigci)*bcalc-signt*TAN(phi1*PI()/180)
	sig3sig1 = sig3*sig1 sig3sq = sig3^2
	laucalc = acalc*sigci*((sign-siglm)/sigci)*bcalc
	s3sift = sigcm+k*sig3
	sntaufit = coh+sign*TAN(phi*PI()/180)
	langent = coht+signt*TAN(phi1*PI()/180)

	Principal stress plot	Mohr envelope	
sig3 & sign	sig3	sig1	s1s3fit
siglm	-0.09	0.00	3.14
siglm^3/4	-0.07	1.46	3.32
siglm^2/4	-0.05	2.12	3.50
siglm^1/4	-0.02	2.62	3.68
0	0.00	3.06	3.86
stress/10.5	0.10	4.49	4.63
stress/10	0.11	4.67	4.75
stress/9.5	0.12	4.74	4.80
stress/9	0.12	4.82	4.85
stress/8.5	0.13	4.91	4.91
stress/8	0.14	5.00	4.97
stress/7.5	0.15	5.11	5.04
stress/7	0.16	5.23	5.13
stress/6.5	0.17	5.36	5.23
stress/6	0.19	5.52	5.34
stress/5.5	0.20	5.69	5.47
stress/5	0.22	5.90	5.64
stress/4.5	0.25	6.15	5.83
stress/4	0.28	6.44	6.08
stress/3.5	0.32	6.80	6.40
stress/3	0.37	7.26	6.82
stress/2.5	0.44	7.87	7.41
stress/2	0.56	8.72	8.30
stress/1.5	0.74	10.00	9.78
stress	1.11	12.24	12.74
stress/0.5	2.22	17.66	21.62
	sign	laucalc	sntaufit
	-0.09	0.00	0.57
	-0.07	0.12	0.60
	-0.05	0.20	0.63
	-0.02	0.27	0.65
	0.00	0.33	0.68
	0.10	0.55	0.80
	0.11	0.58	0.82
	0.12	0.60	0.83
	0.12	0.61	0.84
	0.13	0.63	0.84
	0.14	0.64	0.85
	0.15	0.66	0.87
	0.16	0.68	0.88
	0.17	0.71	0.89
	0.19	0.73	0.91
	0.20	0.76	0.93
	0.22	0.80	0.96
	0.25	0.85	0.99
	0.28	0.90	1.03
	0.32	0.97	1.07
	0.37	1.06	1.14
	0.44	1.18	1.23
	0.56	1.36	1.37
	0.74	1.63	1.60
	1.11	2.13	2.06
		3.41	3.43



Comparison of mi ranges - Sandstone (Tof_{b.2}), HOEK-BROWN

Calculation Package 0.19 - Hoek-Brown Rock Mass Strength Worksheet SANDSTONE GSI LOW, HOEK-BROWN

Input:	sigci = 22 MPa	mi = 18	GSI = 62
	Depth of failure surface or tunnel below slope* = 50 m	Unit wt = 0.022 MN/m3	
Output:	stress = 1.11 MPa	mb = 4.53	s = 0.0142
	a = 0.5	siglm = -0.0675 MPa	A = 0.7862
	B = 0.7243	k = 8.03	phi = 51.13 degrees
	coh = 0.610 MPa	sigcm = 3.46 MPa	E = 9114.4 MPa

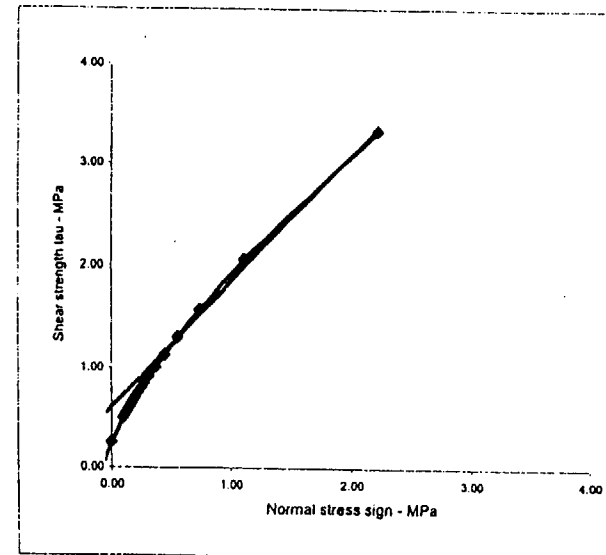
Calculation:

	sig3	1E-10	0.16	0.32	0.48	0.63	0.79	0.95	1.11	Sums
sig1	2.57	4.86	6.45	7.77	8.92	9.97	10.94	11.85	12.38	4.44
ds1ds3	20.03	11.40	8.98	7.71	6.91	6.33	5.90	5.56	5.22	83.34
sign	0.12	0.54	0.93	1.31	1.68	2.04	2.40	2.75	3.09	72.82
tau	0.55	1.28	1.84	2.32	2.76	3.15	3.52	3.86	4.19	11.78
x	-2.06	-1.55	-1.33	-1.19	-1.09	-1.01	-0.94	-0.89	-0.85	19.28
y	-1.60	-1.23	-1.07	-0.97	-0.89	-0.84	-0.79	-0.75	-0.71	-10.07
xy	3.28	1.90	1.43	1.16	0.98	0.84	0.74	0.66	0.60	-8.13
xsq	4.23	2.41	1.78	1.43	1.19	1.02	0.89	0.78	0.70	10.99
sig3sig1	0.00	0.77	2.05	3.70	5.66	7.91	10.41	13.15	16.11	13.73
sig3sq	0.00	0.03	0.10	0.23	0.40	0.63	0.91	1.23	1.61	44
taucalc	0.55	1.28	1.83	2.32	2.75	3.15	3.53	3.88	4.19	4
sig1sig3fit	3.46	4.73	6.01	7.28	8.55	9.83	11.10	12.38	13.66	
signtaufit	0.76	1.28	1.77	2.24	2.70	3.15	3.59	4.02	4.44	

Cell formulae:

σ_a	stress = IF(depth>90, sigci*0.25, depth*unitwt)
m_b	mb = mi*EXP((GSI-100)/28)
s	s = IF(GSI>25, EXP((GSI-100)/9), 0)
a	a = IF(GSI>25, 0.5, 0.65-GSI/200)
σ_{lm}	siglm = 0.5*sigci*(mb-SQRT(mb^2+4*s))
σ_1	sig3 = Start at 1E-10 (to avoid zero errors) and increment in 7 steps to stress
σ_1	sig1 = sig3+sigci*((mb*sig3)/sigci+s)*a
$\delta\sigma_1/\delta\sigma_3$	ds1ds3 = IF(GSI>25, (1+(mb*sigci)/(2*(sig1-sig3))), 1+(a*mb*a)*(sig3/sigci)^(a-1))
σ_a	sign = sig3+(sig1-sig3)/(1+ds1ds3)
τ	tau = (sign-sig3)*SQRT(ds1ds3)
x	x = LOG((sign-siglm)/sigci)
y	y = LOG(tau/sigci)
	xy = x*y xsq = x^2
A	A = acalc = 10*(sumy/8 - bcalc*sumx/8)
B	B = bcalc = (sumxy - (sumx*sumy)/8)/(sumxsq - (sumx^2)/8)
k	k = (sumsig3sig1 - (sumsig3*sumsig1)/8)/(sumsig3sq - (sumsig3^2)/8)
ϕ	phi = ASIN((k-1)/(k+1))*180/PI()
c	coh = sigcm/(2*SQRT(k))
σ_{cm}	sigcm = sumsig1/8 - k*sumsig3/8
E	E = IF(sigci>100, 1000*10^4*((GSI-10)/40), SQRT(sigci/100)*1000*10^4*((GSI-10)/40))
	phit = (ATAN(acalc*bcalc)/((sign-siglm)/sigci)^(bcalc-1))*180/PI()
	coht = acalc*sigci*((sign-siglm)/sigci)^bcalc-signt*TAN(phit*PI()/180)
	sig3sig1 = sig3*sig1 sig3sq = sig3^2
	taucalc = acalc*sigci*((sign-siglm)/sigci)^bcalc
	s3sfit = sigcm+k*sig3
	signtaufit = coh+sign*TAN(phit*PI()/180)
	tangent = coht+sign*TAN(phit*PI()/180)

sig3 & sign	Principal stress plot	Mohr envelope
sig3	sig3	sign
siglm	sig1	taucalc
siglm^3/4	s1s3fit	signtaufit
siglm^2/4		
siglm^1/4		
0		
stress/10.5		
stress/10		
stress/9.5		
stress/9		
stress/8.5		
stress/8		
stress/7.5		
stress/7		
stress/6.5		
stress/6		
stress/5.5		
stress/5		
stress/4.5		
stress/4		
stress/3.5		
stress/3		
stress/2.5		
stress/2		
stress/1.5		
stress		
stress/0.5		



Calculation Package 0.19 - Hoek-Brown Rock Mass Strength Worksheet **SANDSTONE GSI HIGH, HOEK-BROWN**

Input:	sigci = 22 MPa	mi = 18	GSI = 68
	Depth of failure surface or tunnel below slope* = 50 m	Unit wt. = 0.022 MN/m ³	
Output:	stress = 1.11 MPa	mb = 5.66	s = 0.0282
	a = 0.5	siglm = -0.1078 MPa	A = 0.8369
	B = 0.7243	k = 8.45	phi = 52.04 degrees
	coh = 0.783 MPa	sigcm = 4.44 MPa	E = 13023.5 MPa

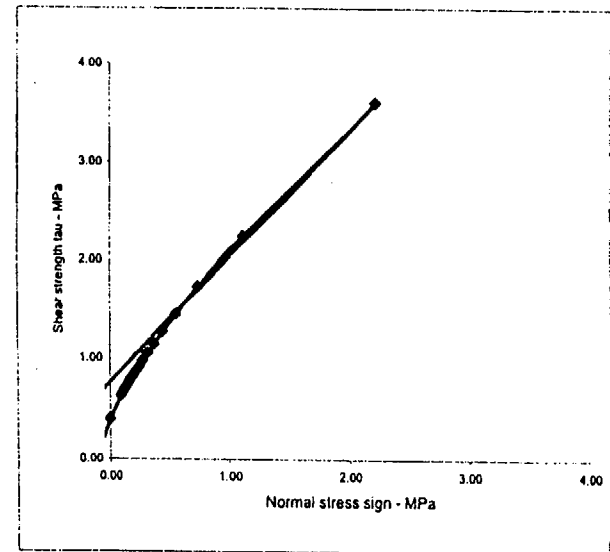
Calculation:

	sig3	1E-10	0.16	0.32	0.48	0.63	0.79	0.95	1.11	Sums
sig1	3.63	5.86	7.52	8.92	10.16	11.28	12.33	13.31	13.31	73.01
ds1ds3	17.83	11.71	9.48	8.23	7.42	6.82	6.37	6.01	73.86	
sign	0.19	0.61	1.00	1.39	1.77	2.13	2.50	2.85	12.44	
lau	0.81	1.54	2.12	2.62	3.08	3.50	3.90	4.27	21.84	
x	-1.86	-1.48	-1.29	-1.16	-1.06	-0.98	-0.92	-0.86	-9.61	
y	-1.42	-1.15	-1.01	-0.92	-0.85	-0.79	-0.74	-0.70	-7.58	
xy	2.64	1.70	1.30	1.06	0.90	0.78	0.68	0.61	9.67	
xsq	3.45	2.19	1.66	1.34	1.13	0.97	0.84	0.75	12.32	
sig3sig1	0.00	0.93	2.39	4.24	6.44	8.95	11.73	14.77	49	
sig3sq	0.00	0.03	0.10	0.23	0.40	0.63	0.91	1.23	4	
taucalc	0.82	1.53	2.11	2.62	3.08	3.50	3.90	4.28		
sig1sig3fit	4.44	5.78	7.12	8.46	9.80	11.14	12.48	13.82		
sigtaufit	1.01	1.54	2.05	2.54	3.03	3.50	3.96	4.42		

Cell formulae:

σ_n	stress = if(depth>90, sigci*0.25, depth*unitwt)
m_b	mb = mi*EXP((GSI-100)/28)
s	s = IF(GSI>25, EXP((GSI-100)/9), 0)
a	a = IF(GSI>25, 0.5, 0.65-GSI/200)
σ_{lm}	siglm = 0.5*sigci*(mb-SQRT(mb^2+4*s))
σ_1	sig3 = Start at 1E-10 (to avoid zero errors) and increment in 7 steps to stress
σ_2	sig1 = sig3+sigci*(((mb*sig3)/sigci)+s)^a
$\delta\sigma_1/\delta\sigma_3$	ds1ds3 = IF(GSI>25, (1+(mb*sigci)/(2*(sig1-sig3))), 1+(a*mb*a)*(sig3/sigci)^(a-1))
σ_n	sign = sig3*(sig1-sig3)/(1+ds1ds3)
τ	lau = (sign-sig3)*SQRT(ds1ds3)
x	x = LOG((sign-siglm)/sigci)
y	y = LOG(lau/sigci)
	xy = x*y xsq = x^2
A	A = acalc = 10*(sumy/8 - bcalc*sumx/8)
B	B = bcalc = (sumxy - (sumx*sumy)/8)/(sumxsq - (sumx^2)/8)
k	k = (sumsig3sig1 - (sumsig3*sumsig1)/8)/(sumsig3sq - (sumsig3^2)/8)
ϕ	phi = ASIN((k-1)/(k+1))*180/PI()
c	coh = sigcm/(2*SQRT(k))
σ_{cm}	sigcm = sumsig1/8 - k*sumsig3/8
E	E = IF(sigci>100, 1000*10^((GSI-10)/40), SQRT(sigci/100)*1000*10^((GSI-10)/40))
	phit = (ATAN(acalc*bcalc*((signt-siglm)/sigci)^(bcalc-1)))*180/PI()
	cohl = acalc*sigci*((signt-siglm)/sigci)^bcalc-signt*TAN(phit*PI()/180)
	sig3sig1 = sig3*sig1 sig3sq = sig3^2
	taucalc = acalc*sigci*((sign-siglm)/sigci)^bcalc
	s3sifit = sigcm*k*sig3
	sntaufit = coh+sign*TAN(phi*PI()/180)
	tangent = cohl+sign*TAN(phi*PI()/180)

	Principal stress plot			Mohr envelope		
sig3 & sign	sig3	sig1	s1s3fit	sign	taucalc	sntaufit
siglm	-0.11	0.00	3.52	-0.11	0.00	0.82
siglm^3/4	-0.08	1.74	3.75	-0.08	0.14	0.66
siglm^2/4	-0.05	2.51	3.98	-0.05	0.24	0.69
siglm^1/4	-0.03	3.12	4.21	-0.03	0.32	0.73
0	0.00	3.63	4.44	0.00	0.39	0.76
stress/10.5	0.10	5.09	5.25	0.10	0.62	0.89
stress/10	0.11	5.28	5.37	0.11	0.65	0.91
stress/9.5	0.12	5.36	5.42	0.12	0.66	0.91
stress/9	0.12	5.44	5.48	0.12	0.68	0.92
stress/8.5	0.13	5.53	5.54	0.13	0.69	0.93
stress/8	0.14	5.63	5.61	0.14	0.71	0.94
stress/7.5	0.15	5.74	5.69	0.15	0.73	0.95
stress/7	0.16	5.86	5.78	0.16	0.75	0.97
stress/6.5	0.17	6.01	5.88	0.17	0.77	0.98
stress/6	0.19	6.17	6.00	0.19	0.80	1.00
stress/5.5	0.20	6.35	6.14	0.20	0.84	1.02
stress/5	0.22	6.57	6.31	0.22	0.87	1.05
stress/4.5	0.25	6.83	6.52	0.25	0.92	1.08
stress/4	0.28	7.14	6.78	0.28	0.98	1.12
stress/3.5	0.32	7.52	7.12	0.32	1.05	1.17
stress/3	0.37	8.01	7.56	0.37	1.14	1.24
stress/2.5	0.44	8.66	8.19	0.44	1.27	1.33
stress/2	0.56	9.55	9.13	0.56	1.45	1.47
stress/1.5	0.74	10.82	10.69	0.74	1.73	1.71
stress	1.11	13.31	13.82	1.11	2.25	2.19
stress/0.5	2.22	19.08	23.20	2.22	3.60	3.61



Comparison of GSI ranges - Sandstone (T_{f-b-2}), HOEK-BROWN